ISTANBUL TECHNICAL UNIVERSITY ★ GRADUATE SCHOOL OF SCIENCE ENGINEERING AND TECHNOLOGY

INFLUENCES OF ATMOSPHERIC BLOCKING OVER TURKEY: CLIMATOLOGICAL ANALYSIS

Ph. D. THESIS

Bahtiyar EFE

Department of Meteorological Engineering

Atmospheric Sciences Graduate Programme

JUNE 2019

ISTANBUL TECHNICAL UNIVERSITY ★ GRADUATE SCHOOL OF SCIENCE ENGINEERING AND TECHNOLOGY

INFLUENCES OF ATMOSPHERIC BLOCKING OVER TURKEY: CLIMATOLOGICAL ANALYSIS

Ph. D. THESIS

Bahtiyar EFE
(511122001)

Department of Meteorological Engineering

Atmospheric Sciences Graduate Programme

Thesis Advisor: Prof. Dr. Ali DENİZ

JUNE 2019

İSTANBUL TEKNİK ÜNİVERSİTESİ ★ FEN BİLİMLERİ ENSTİTÜSÜ

ATMOSFERİK ENGELLEMENİN TÜRKİYE ÜZERİNE ETKİLERİ: KLİMATOLOJİK ANALİZ

DOKTORA TEZİ

Bahtiyar EFE
(511122001)

Meteoroloji Mühendisliği Anabilim Dalı

Atmosfer Bilimleri Lisansüstü Programı

Tez Danışmanı: Prof. Dr. Ali DENİZ

HAZİRAN 2019

Bahtiyar EFE, a Ph.D. student of İTÜ Graduate School of Science Engineering and Technology student ID 511122001, successfully defended the dissertation entitled "INFLUENCES OF ATMOSPHERİC BLOCKING OVER TURKEY: CLIMATOLOGICAL ANALYSIS", which he prepared after fulfilling the requirements specified in the associated legislations, before the jury whose signatures are below.

Thesis Advisor :	**Prof. Dr. Ali DENİZ** İstanbul Technical University	.....
Jury Members :	**Prof. Dr. Kasım KOÇAK** Istanbul Technical University	.....
	Assoc. Prof. Dr. Haldun KARAN TÜBİTAK MAM Research Center	.....
	Prof. Dr. Anthony R. LUPO University of Missouri- Columbia	.....
	Prof. Dr. Ş. Sibel MENTEŞ İstanbul Technical University	.....

Date of Submission : 28 May 2019
Date of Defense : 27 June 2019

To my family,

FOREWORD

First of all, I would like to thank my supervisors.

The first person I would like to thank Dr. Ali DENİZ my supervisor for his support and guidance to study atmospheric blocking. I also would like to thank Dr. Anthony LUPO for his exceptional supervising my research, encouraging me to write the research papers, making my visit in USA enjoyable and providing opportunities for me in the USA. My committee members Dr. Kasim KOÇAK, Dr. Haldun KARAN and Dr. Ş. Sibel MENTEŞ are also acknowledged for helping me to make my dissertation stronger.

Secondly, I would thank my family. Special thanks to my parent who have been loving me without any response and have encouraged my beliefs and life goals; my wife who made my life meaningful and happy and my studies possible; my sons Ali and Hasan who makes my life as life; and my brother and sister for making my life enjoyable.

Thirdly, I would like to thank my friends. Thanks also to valuable friends (in no particular order): İsmail SEZEN for everything in particular encouraging me to write my own codes for my dissertation; Tuncay ÖZDEMİR encouraging me to get my graduate and publish papers; Sarah BALKISSOON and Katherine ROJAS MURILLO for valuable supports and making my University of Missouri visiting easy and enjoyable; Burak ÖZTANER, Seda OCAKLI, Ekrem OCAKLI, İbrahim Halil CİHAN, Mowaffak İBRAHİM, Gökay ÖZTÜRK, and other friends who made my research succeed.

Lastly, I would like to thank my government and other contributors. I would like to thank my government for supporting my education at every stage. I graduated from the best schools during my education and taught by excellent teachers. I would also thank Turkish State Meteorological Service for providing meteorological data; Istanbul Technical University for providing me a working and studying environment, University of Columbia – Missouri, USA for providing me a study environment, NCEP –NCAR for upper-level data.

This research has been supported by TÜBİTAK 2214, İTÜ BAP and SU VAKFI programs.

June 2019

Bahtiyar EFE
(M. Sc. Meterological Engineer)

TABLE OF CONTENTS

Page

ABBREVIATIONS

BF : Blocking Frequency

BI : Blocking Intensity

CC : Correlation Coefficient

EN : El Nino

ENSO : El Nino Southern Oscillation

GEV : Generalized Extreme Value Theory

GHGS : Geopotential Height Gradient in the Southern part of φ_0

GHGN : Geopotential Height Gradient in the Northern part of φ_0

Gpm : Geopotential Meter

LN : La Nina

LO83 : Lejenäs and Økland (1983)

LS95 : Lupo and Smith (1995)

NSS : Not Scientifically Significant

MPF : Mean Precipitation Frequency

NAO : North Atlantic Oscillation

NCEP : National Centers for Environmental Prediction

NCAR : National Center for Atmospheric Research

NEU : Neutral

NSS : Not statistically significant

OYS : Ortalama Yağış Frekansı

P1b : First Pattern for Blocked Days

P2b : Second Pattern for Blocked Days

P3b : Third Pattern for Blocked Days

P4b : Fourth Pattern for Blocked Days

P1d : First Pattern for Difference Between Blocked and Non-Blocked Days

P2d : Second Pattern for Difference Between Blocked and Non-Blocked Days

P3d : Third Pattern for Difference Between Blocked and Non-Blocked Days

P4d : Fourth Pattern for Difference Between Blocked and Non-Blocked Days

P1n **:** First Pattern for Non-blocked Days

P2n **:** Second Pattern for Non-blocked Days

P3n **:** Third Pattern for Non-blocked Days

P4n **:** Fourth Pattern for Non-blocked Days

R90p **:** Index that uses the 90^{th} percentile as a threshold

S1 **:** Sector 1 (sector covers 20^{o} W – 0^{o} E)

S2 **:** Sector 2 (sector covers 0^{o} E – 30^{o} E)

S3 **:** Sector 3 (sector covers 30^{o} E – 60^{o} E)

S4 **:** Sector 4 (sector covers 60^{o} E – 90^{o} E)

TM90 **:** Tibaldi and Molteni (1990)

Tmax **:** Maximum temperature

Tmin **:** Minimum temperature

Tn **:** Extreme Cold Temperature

Tx **:** Extreme Hot Temperature

USA **:** United States of America

UTC **:** Coordinated Universal Time

WI02 **:** Wiedenmann et al. (2002)

SYMBOLS

^{o} C	**:** Celcius degrees
^{o} E	**:** Degrees East
hPa	**:** hecto Pascal
^{o} N	**:** Degrees North
^{o} W	**:** Degrees West
Z	**:** Geopotential Height
$Z_{\lambda,\varphi}$	**:** Geopotential Height at longitude λ and latitude φ
λ	**:** Longitude
φ	**:** Latitude
σ	**:** Standart deviation of the temperature anomaly
μ	**:** Seasonal-mean of the temperature anomaly

LIST OF TABLES

Page

LIST OF FIGURES

Page

EFFECTS OF ATMOSPHERIC BLOCKING OVER TURKEY: CLIMATOLOGICAL ANALYSIS

SUMMARY

The relationship between atmospheric blocking and meteorological parameters has not been studied in depth for Turkey. The scope of this dissertation is to put forth the relationship between atmospheric blocking and temperature anomalies, mean precipitation frequency and extreme temperatures for Turkey. In this dissertation, these relationships are investigated for the period 1977 – 2016 using 77 stations that have complete meteorological data for the aforementioned period from Turkish State Meteorological Service. The 500 hPa geopotential height data from National Center for Environmental Protection (NCEP) – National Center for Atmospheric Research (NCAR) Reanalysis 1 data set was used in order to detect blocking and compute blocking characteristics.

The statistical characteristics of atmospheric blocking events with respect to seasons in the study domain are calculated. The maximum value for mean block duration occurs during the winter and spring seasons at 9.2 days. The fall season has the minimum block duration at 8.1 days, while the overall value for the mean duration is 8.8 days.

The mean occurrence for atmospheric blocking events is nearly the same during winter, summer and fall at 2.7, 2.5 and 2.6 events, respectively. In contrast, spring has more blocking occurrences than any other season (3.9 events).

The mean seasonal values for blocking intensity (BI) range between 1.91 and 2.65 in the study area. The most intense blocking events are observed in winter (2.65), while the weakest blocking events are observed in summer (1.91). Spring and fall have nearly the same values for BI, 2.31 and 2.36, respectively. The overall mean BI is 2.41 in the study domain.

The last blocking characteristic examined here is the longitudinal extent as measured by degrees longitude. The seasonal longitudinal extent fluctuates between 25 and 29 degrees longitude. The longitudinal extent of atmospheric blocking is the largest in winter (29 degrees longitude), while spring (27 degrees longitude) had the second largest extent, and summer and fall had a nearly the same longitudinal extent (25 degrees longitude).

The first meteorological parameter, the temperature is investigated according to its relationship with atmospheric blocking in terms of anomalies. The temperature anomalies of any station were calculated by using the seasonal mean temperature observations. The seasonal mean temperature anomalies at all stations during blocked days varies between -2.1^{o} C and 0.8^{o} C. There are four main patterns representing the mean seasonal anomaly curve of all stations. The anomaly difference between blocked and non-blocked days' curve follows the anomaly during blocked days' curve in almost all instances. This indicates the impact of blocking on observed temperature, since blocked days comprised 30% of the study period. When focusing on the spatial

distribution of mean seasonal anomalies, winter (DJF) and fall (SON), almost all stations show negative temperature anomalies although anomalies are close to zero during warm seasons. The composite analysis shows that the western part of the country is strongly affected by cold air advection during cold blocking events and the eastern part of the country is affected by warm temperature advection during warm blocking events. There is a statistically significant (95% confidence level) negative correlation between blocking intensity and temperature anomalies in all seasons except spring (MAM). There is no relationship between both blocking duration and the longitudinal extent and the seasonal mean temperature anomaly except during winter, which has a negative correlation. The temperature anomaly distribution stratified by season shows that strong positive anomalies are rarely observed in all seasons. Even the summer and fall had no stations in which a very strong positive anomaly was observed. The analysis of coldest and warmest blocking event shows that Rex-type atmospheric blocking events are observed during the period of not only the maximum temperature anomaly but also for minimum anomalies. However, the location of the blocking differs.

The second meteorological parameter investigated according to its relationship with atmospheric blocking is precipitation. It was investigated in terms of mean precipitation frequency (MPF). Precipitation frequency of an event is the ratio of rainy days during the event to the total duration of the event. The overall MPF for the examined stations during blocked days (non-blocked days) fluctuated between 0.15 and 0.43 (0.12 and 0.38). The ratio of MPF during the blocked days to non-blocked days ranges between 12% and 38%. During the winter season, the country has higher MPF values during blocked days. The greatest ratio of MPF values during blocked days to non-blocked days are observed in summer due to smaller values of MPF occurring during this season overall. Higher MPF occurs when the event center was located between 0^o – 30^o E (mean: 0.27, range: 0.17 – 0.51). There is no relationship between blocking duration and MPF for all seasons. There is a positive relationship between BI and MPF during the summer (Correlation Coefficient (CC) = 0.35, significant at 95% level) and fall (CC = 0.43, significant at 95% level). The relationship between blocking longitudinal extent and MPF is significant at the 95% confidence level during the summer and fall season with the CC of 0.29 and 0.25, respectively. A composite of the 10 blocking events associated with the largest MPF demonstrated there is moist advection via westerly flow into Turkey in all seasons. For the blocking case study (31 October to 5 November 2009) associated with the largest MPF, the mean value across the country was 0.73. The mean total precipitation during this period was 63.4 mm.

Lastly, extreme maximum (Tx) and extreme minimum temperature (Tn) frequency distributions during summer and winter for blocked conditions were analyzed for Turkey for the period from 1977 to 2016 by using observational data. Both Tx and Tn are defined by using threshold value. Tx is the maximum temperature that is greater than the 99^{th} percentile. Similarly, Tn is the minimum temperature that is smaller than the 1^{st} percentile. The Tx (0.5 - 0.8 percent) and Tn (0.4 - 2.0 percent) frequency vary between these values for the entire period during summer. However, Tx varies between 0.0 and 1.0 whilst Tn varies between 0.8 and 2.4 during winter. It is quite clear that atmospheric blocking has a greater cooling effect during winter. The maximum values for Tx and Tn are observed when the block center located within the easternmost sector for summer. The maximum Tx frequency is observed in association with blocking in the westernmost sector and the maximum Tn frequency is observed with blocking in

the easternmost sector during the winter season. BI has almost no impact on Tx frequency although it has an enhancing effect on Tn frequency during the summer. For winter, BI has a decreasing effect on maximum Tn and decreasing effect on maximum Tx. The maximum Tx and Tn values increase with the blocking longitudinal extent for the summer. During the winter, the maximum Tx frequency decreases with the increase in the blocking longitudinal extent however, the greatest Tn frequency is observed within the second sector and lowest within the third sector. The block duration has an enhancing influence on the maximum Tx value whilst maximum Tn is observed during short duration events and a minimum is observed during moderate duration events during the summer season. For the winter season, the block duration has a decreasing effect for Tx frequencies and increasing effect for Tn.

ATMOSFERİK ENGELLEMENİN TÜRKİYE ÜZERİNE ETKİLERİ: KLİMATOLOJİK ANALİZ

ÖZET

Bir bölgede görülen meteorolojik koşulların belirli bir süreden daha fazla gözlemlenmesine sebep olan olaya engelleme denir. Atmosferik engelleme eğer kış aylarında meydana gelirse, çok düşük sıcaklıklara, kuvvetli kar yağışına sebep olurken ilkbahar ya da yaz aylarında görülürse yüksek sıcaklıklara ve kuraklığa sebep olabilir.

Engelleme olayına bu ismin verilmesinin sebebi yukarı seviyede oluşan jeti engellemesidir. 300 mb. ve daha yukarı seviyedeki 60 knot veya daha fazla şiddete sahip rüzgârlara jet denir. Jetler kuzey yarımkürede ve güney yarımkürede batıdan doğuya doğru eserler kısaca yukarı seviye rüzgârları batılıdır. Fakat herhangi bir bölgede, yer seviyesinde bir yüksek basınç merkezinin bulunması durumunda yukarı seviyedeki rüzgarlar yüksek basınç merkezinin bulunduğu bu bölgeye girememekte, zonal (batı doğu doğrultusunda) olan yukarı seviye rüzgarları meridyonel (kuzey – güney doğrultusunda) hale gelmekte bazen de doğudan batıya doğru (retrograt hareket) esmektedirler. Yüksek basınç sisteminin belirli bir yerde uzun süre (5 gün ve daha fazla) kalması durumuna engelleme olayı denilmektedir. Engelleme olayının seçilmesinin sebebi, olayın hem hava şartlarına hem de insanlar, canlılar ve çevre üzerine etkilerinin kuvvetli olmasıdır. Örnek vermek gerekirse 2010 yılı Haziran ve Ağustos ayları arasında Rusya'yı etkileyen engelleme olayında, orman yangınları artmış, hava kalitesinin düşmesinden ve yüksek sıcaklıklardan dolayı Moskova'da ölüm oranları 700 kişi/gün ile ortalama değerinin iki katına çıkmıştır Yine aynı dönemde, Moskova'da son 130 yılın en yüksek sıcaklık değeri (37.8 ^{o}C) ölçülmüştür.

Engelleme ile ilgili ilk çalışma, 1900lü yılların başında yapılmış olup, 1940'lı yıllarda engellemenin bölgesel iklimler üzerine etkileri ile ilgili birkaç çalışma yapılmıştır. İkinci Dünya Savaşı sonrasında yukarı seviye verilerinin temininin artması ile yukarı seviye haritaları çizilmeye başlamıştır ve engelleme ile ilgili çalışmaların sayısı artmıştır. İlk çalışmalarda, öznel olarak yapılan engelleme tanımları, sonraları engelleme tespitini bilgisayarlar ile kolaylıkla yapabilmek için daha nesnel hale getirilmeye çalışılmıştır.

Engelleme olayı, araştırmacılar tarafından farklı yaklaşımlarla (dinamik, klimatolojik) hem oluştuğu bölgedeki etkilerini hem de uzaktaki bölgelerdeki etkilerini gözönünde bulunduracak şekilde incelenmiştir. Bu çalışmalardan bir kısmı engellemenin klimatolojik özellikleri, engelleme tespit yöntemleri, engellemenin tahmin edilmesi gibi konulara yoğunlaşırken bir kısmı da engellemenin meteorolojik değişkenler üzerine etkisi üzerine araştırmalar yapmıştır.

Atmosferik engelleme ile meteorolojik değişkenler arasındaki ilişki Türkiye için şimdiye kadar detaylı bir şekilde incelenmemiştir. Bu çalışmanın amacı atmosferik engelleme olayı ile sıcaklık anomalisi, ortalama yağış sıklığı ve uç sıcaklık değişkenleri arasındaki ilişkiyi ortaya koymaktır. Bu çalışmada 1977 ve 2016 yılları

arasındaki dönem için atmosferik engelleme olayı ile meteorolojik değişkenler arasındaki ilişki incelenmiştir. Kullanılan sıcaklık, yağış, maksimum ve minimum sıcaklık verileri Meteoroloji Genel Müdürlüğü'nden belirtilen periyot için alınmıştır. Çalışmada sadece belirtilen aralık için tam veri sayısına sahip olan 77 istasyon kullanılmıştır.

Atmosferik engelleme olayının tespit edilmesi için gerekli olan 500 hPa jeopotansiyel yükseklik verisi ise National Center for Environmental Protection (NCEP) – National Center for Atmospheric Research (NCAR) Reanalysis 1 veri setinden alınmıştır. Bu veri seti 2.5^o x 2.5^o mekansal (enlem - boylam) çözünürlüğe sahiptir. NCEP – NCAR Reanalysis 1 veri seti hem yer seviyesi için hem de çeşitli basınç seviyeleri için çok sayıda değişkeni içermektedir. NCEP – NCAR 500 hPa verisi araştırmacılar tarafından engelleme tespitinde sıklıkla kullanılan bir veri setidir. Engelleme tespiti için kullanılan bölge 20^o Batı - 90^o Doğu boylamları ve 30^o Kuzey - 90^o Kuzey enlemleri arasında kalan bölgedir. Bu bölgede oluşan engelleme olayları Türkiye'yi etkileyebileceği için bu bölge seçilmiştir.

İncelenen zaman diliminde atmosferik engellemenin özellikleri çalışma alanı için hesaplanmıştır. Buna göre ortalama engelleme şiddeti mevsimlere göre ayrı ayrı değerlendirildiğinde minimum değer 1.91 ile yaz mevsimine ait iken, maksimum değer 2.65 ile kış mevsimine aittir. İlkbahar ve sonbahar için ortalama engelleme şiddeti değerleri ise sırası ile 2.31 ve 2.36'dır. Bütün engelleme olaylarının ortalama şiddeti ise, 2.41'dir. Engelleme olaylarının ortalama süresinin en yüksek olduğu mevsimler 9.2 gün ile kış ve ilkbahar mevsimleridir. Yaz ve sonbahar mevsimlerinde gözlemlenen engelleme olaylarının ortalama süresi ise sırasıyla 8.4 ve 8.1 olup, bu değer tüm veri için 8.8 gündür. Çalışma bölgesindeki ortalama engelleme sayısı 3.9 ile en yüksek ilkbahar mevsiminde iken kış, yaz ve sonbahar mevsimlerindeki ortalama engelleme sayısı, sırasıyla 2.7, 2.5 ve 2.6'dır. Yıllık ortalama engelleme sayısı ise 11.7 olarak hesaplanmıştır. Engelleme olaylarının boylamsal uzunluğu incelendiğinde kış mevsiminin ortalama 29 boylam ile en yüksek değere sahip olduğu görülmüştür. En küçük değer ise 25 boylam ile yaz ve sonbaharda görülmüştür. İlkbahar mevsimindeki engelleme olaylarının ortalama boylamsal uzunluğu 27 boylam olup, bu değer tüm veri için 28 gündür.

Sıcaklık anomalisi incelenen ilk parametre olup, her bir istasyon için kendisine ait verilerden, bulunduğu mevsimdeki verilerin ortalaması çıkarılacak hesaplanmıştır. Mevsimsel ortalama sıcaklık anomalisi değerleri bütün istasyonlar göz önüne alındığında, -2.1^o C ile 0.8^o C değerleri arasında değişmektedir.

Bütün istasyonların mevsimsel değişimi incelendiğinde 4 tane temel örüntü görülmektedir. Birinci örüntü, kış mevsiminde minimum anomali değeri (negatif değerlerde), ilkbaharda artarak 0'a yaklaşan anomali, yazın ilkbahara göre hafifçe artan ya da azalan anomali değeri ve son olarak ani bir şekilde negatif değerlere düşen anomali olarak tanımlanabilir. Bu örüntü daha çok Karadeniz, Marmara ve Ege kıyılarında görülmüştür. İkinci örüntü, soğuk mevsimlerde neredeyse aynı negatif anomali değerleri, sıcak mevsimlerde ise 0 ^{o}C civarında anomali ile ifade edilebilir. Bu örüntü, İç Anadolu Bölgesi'nde ve Karadeniz Bölgesi'nin iç kesimlerinde daha çok görülmektedir. Üçüncü örüntü, kış mevsiminde negatif anomali, ilkbaharda +0.5 ^{o}C'ye yükselen pozitif anomali ve yaz ile sonbaharda tekrar negatife düşen anomali değerleri ile tarif edilebilir. Bu örüntü, daha çok Güneydoğu Anadolu Bölgesi'nin güneyindeki şehirlerde görülmektedir. Son örüntü ise ilkbaharda 0 ^{o}C civarında pozitif anomali, diğer mevsimlerde ise aynı büyüklüğe sahip negatif anomali değerleri ile ifade

edilebilir. Bu örüntü ise daha çok Marmara Bölgesi'nde ve Ege Bölgesi'nin güneyinde görülmektedir.

Engelleme olan günler ile engelleme olmayan günlerdeki sıcaklık anomalisi değerleri arasındaki fark eğrisi bütün durumlarda engellemeli günlere ait eğriye benzer bir durum sergilemektedir. Bu ise engelleme olaylarının incelenen dönemin sadece %30'unda görülmesine rağmen yüzey sıcaklıkları üzerindeki etkisini göstermektedir.

Ortalama mevsimsel anomalilerin engelleme olan günlerdeki yersel dağılımını incelediğimiz zaman kış (Aralık, Ocak ve Şubat ayları) ve sonbahar (Eylül, Ekim ve Kasım ayları) mevsiminde nerede ise bütün istasyonların negatif anomali değerlerine sahip olduğu görülmektedir. İlkbahar (Mart, Nisan ve Mayıs ayları) ve yaz (Haziran, Temmuz ve Ağustos ayları) mevsimlerinde engellemeli günlerdeki ortalama mevsimsel anomali değerleri ise $^{o}0$ civarındadır. Kuvvetli anomali olan günlerdeki birleşik (kompozit) 500 hPa ve 850 hPa haritaları incelendiğinde, negatif anomaliye sahip engelleme olaylarında Türkiye'nin batı bölgelerinin kuvvetli soğuk hava adveksiyonundan etkilendiği görülürken, pozitif anomaliye sahip engelleme olaylarında Türkiye'nin doğu bölgelerinin kuvvetli sıcak hava adveksiyonundan etkilendiği görülmektedir.

Engelleme olayının çeşitli özellikleri ile Türkiye için ortalama sıcaklık anomalisi arasındaki ilişki de incelenmiştir. Engelleme şiddeti ile ortalama sıcaklık anomalisi arasında ilkbahar hariç %95 anlamlılık seviyesinde negatif ilişki bulunmuştur. Engelleme süresi ve engellemenin boylamsal genişliği ile ortalama sıcaklık arasında kış mevsimi hariç anlamlı bir ilişki bulunamamıştır. Kış aylarında bu iki parametre ile ortalama sıcaklık anomalisi arasında %95 anlamlılık seviyesinde zayıf negatif bir ilişki bulunmuştur.

İstasyonların engelleme olan günlerdeki ortalama sıcaklık anomalisi mevsimsel olarak incelendiğinde, çok kuvvetli pozitif sıcaklık anomalilerinin çok nadir gözlendiği görülmüştür. Hatta yaz ve sonbahar mevsimlerinde hiç bir istasyonda çok kuvvetli pozitif anomaliler gözlemlenmemiştir. Türkiye'nin kuzey bölgelerinde kuvvetli ve çok kuvvetli negatif sıcaklık anomalileri bütün mevsimlerde gözlenmiştir. Bu bölge engellemenin antisiklonik kısmının sağ kanadında bulunmakta olup soğuk hava adveksiyonundan en çok etkilenen bölgedir. Ülkenin batı bölgelerinde, çok kuvvetli, kuvvetli ve mutedil negatif sıcaklık anomalileri gözlemlenirken, orta kesimlerde daha çok mutedil negatif anomaliler gözlemlenmektedir. Ülkenin doğu bölümünde ise mutedil sıcaklık anomalileri gözlemlenmektedir.

Çok kuvvetli pozitif ve negatif anomaliye sahip engelleme olaylarının 500 hPa haritalarının analizi sonucu, her iki olayda da Rex tipi engelleme olayının gözlemlendiği görülmüştür. Bununla birlikte iki engelleme olayının konumları birbirinden farklıdır.

İncelenen ikinci meteorolojik parametre ise yağıştır. Yağış ile atmosferik engelleme arasındaki ilişki, ortalama yağış sıklığı ile ifade edilmiştir. Yağış sıklığı belirtilen bir olayın kapsadığı zamanda, yağışlı günlerin toplam günlere olan oranı şeklinde tanımlanmıştır. Ortalama yağış sıklığı ise, yağış sıklığının belirtilen dönem için ortalaması alınarak elde edilmiştir.

Ortalama yağış sıklığı bütün veri için engelleme olan günlerde 0.15 ile 0.43 arasında değişirken, engelleme olmayan günlerde 0.12 ile 0.38 arasında değişmektedir. Bütün veri için engelleme olan günlerdeki ortalama yağış sıklığı, engelleme olmayan günlerdeki yağış sıklığına göre %12 ile %38 arasındaki değerlerde artış

göstermektedir. Ortalama yağış sıklığı mevsimsel olarak incelendiğinde, kış mevsiminde, engellemeli günlerde ülkemizdeki istasyonların daha büyük ortalama yağış sıklığı değerlerine sahip olduğu görülmüştür. Engelleme olan günlerdeki ortalama yağış sıklığı, engelleme olmayan günlerdeki yağış sıklığına göre her mevsimde artış göstermektedir. Bu artış en fazla yaz mevsiminde olmaktadır. Bunun sebebi ise yaz mevsiminde hem engelleme olan günlerdeki hem de olmayan günlerdeki ortalama yağış sıklığı değerlerinin küçük olmasıdır.

Engelleme olayının özellikleri ile ortalama yağış sıklığı arasındaki ilişki incelendiğinde, en büyük ortalama yağış sıklığı değerlerinin, engelleme olayı 0^o – 30^o Doğu boylamları arasındaki bölgede gerçekleştiği zaman elde edildiği sonucuna varılmıştır. Engelleme olayının bu bölgede gerçekleştiği durumlarda ortalama yağış sıklığı değerinin ortalaması 0.27 olup en küçük ve en büyük değerler sırası ile 0.17 ve 0.51'dir. Engelleme şiddeti ile ortalama yağış sıklığı arasında yaz ve sonbahar mevsimlerinde pozitif bir ilişki vardır. Her iki mevsimdeki ilişki %95 anlamlılık seviyesinde olup yaz için korelasyon katsayısı 0.35, sonbahar için ise 0.43'tür. Engellemenin boylamsal uzunluğu ile ortalama yağış sıklığı arasında yine yaz ve sonbahar mevsimlerinde %95 seviyesinde pozitif bir ilişki olup korelasyon katsayısı değerleri sırası ile 0.29 ve 0.25'tir. Engelleme süresi ile ortalama yağış sıklığı arasında hiç bir mevsimde bir ilişki bulunamamıştır.

Her bir mevsimdeki en yüksek ve en düşük ortalama yağış sıklığına sahip engelleme olayları incelendiğinde, en yüksek ortalama yağış sıklığına sahip olaylarda batılı akışlar sayesinde Türkiye'ye nem adveksiyonu olduğu görülmektedir. Yağış sıklığı için son olarak bir durum çalışması yapılmış ve en yüksek ortalama yağış sıklığına sahip olan olay incelenmiştir. Bu engelleme olayı 31 Ekim ile 5 Kasım 2009 tarihleri arasında gerçekleşmiş ve bu zaman diliminde ortalama yağış sıklığı 0.73 olarak hesaplanmış, ortalama toplam yağış ise 63.4 mm. olarak ölçülmüştür.

İncelelenen son parametre ise uç sıcaklık değerleri olmuştur. Her iki uç sıcaklık değeri yaz ve kış mevsimi için değelendirilmiştir. Uç sıcaklıklar hesaplanırken, eşik değeri yaklaşımı kullanılmıştır. Buna göre bir maksimum sıcaklık değerinin uç maksimum sıcaklık (Tx) olabilmesi için, 99. persentildeki maksimum sıcaklık değerinden büyük olması gerekir. Benzer yaklaşımla, bir minimum sıcaklık değerinin uç minimum sıcaklık (Tn) olabilmesi için, 1. persentile karşılık gelen minimum sıcaklık değerinden küçük olması gerekir.

Yaz aylarında bütün istasyonlar için Tx görülme sıklığı %0.5 ile %0.8 arasında değişirken Tn görülme sıklığı %0.4 ile %2.0 arasında değişim göstermektedir. Kış aylarında ise, Tx görülme sıklığı %0.0 ile %1.0 arasında değişirken Tn görülme sıklığı %0.8 ile %2.4 arasında değişim göstermektedir. Atmosferik engelleme olayının kış aylarında daha fazla soğutucu etkiye sahip olduğu açıkça görülmektedir.

Yaz mevsiminde, engelleme olayı en doğudaki sektörde (60^o – 90^o Doğu boylamları arasında) konumlandığı zaman Tx ve Tn değerlerinin görülme sıklığı en yüksek değerde olmaktadır. Kış mevsiminde ise Tx en yüksek görülme sıklığı değerine engellemenin ortalama konumu en batıdaki sektörde (20^o Batı – 0^o boylamları arasında) iken, Tn ise en doğudaki sektörde (60^o – 90^o Doğu) iken sahip olmuştur. Engelleme şiddeti, yaz aylarında Tx görülme sıklığını etkilemez iken Tn görülme sıklığını artırmaktadır. Kış için ise, engelleme şiddetinin artması, en yüksek Tx ve Tn değerlerini azaltmaktadır. Yaz mevsiminde en büyük Tx ve Tn değerleri engellemenin boylamsal uzunluğu büyüdükçe artmaktadır. Kış mevsiminde ise, en büyük Tx değeri engellemenin boylamsal uzunluğu arttıkça azalırken, en büyük Tn değeri artmaktadır.

Engelleme süresi yaz aylarında en büyük Tx değerini artırırken Tn için bu şekilde doğrusal bir ilişki söz konusu değildir. Yaz aylarında en büyük Tn değeri kısa süreli olaylarda görülürken en küçük Tn değeri ortalama süreli olaylarda görülmektedir. Kış mevsiminde, engelleme süresi Tx görülme sıklıklarında azalmaya sebep olurken Tn görülme sıklıklarında artmaya sebep olmaktadır.

1. INTRODUCTION

1.1 Atmospheric Blocking

The partial or full interruption of westerly flow in the mid-latitudes can be described as atmospheric blocking. If it is observed during winter, it can be the cause of cold spells and great amounts of snow for certain locations. For example, in March 1987 the snow depth reached 1 meter in many parts of the city (Tayanç et al. 1998) and it is the second coldest blocking event associated with very cold temperature anomalies. However, it can lead to the heatwaves or drought if it is observed in the warm season. During summer 2010 blocking event, western Russia impacted by a severe drought and Moscow recorded 37.8 oC for the first time in over 130 years (Lupo et al., 2014). Two major types of atmospheric blocking are Rex – type, named after the researcher who made the first definition of atmospheric blocking and omega-type named because of its shape. The Rex type blocking event observed in the study area can be seen in Figure 1.1. Rex type blocking events are more frequent in the Euro – Atlantic Region.

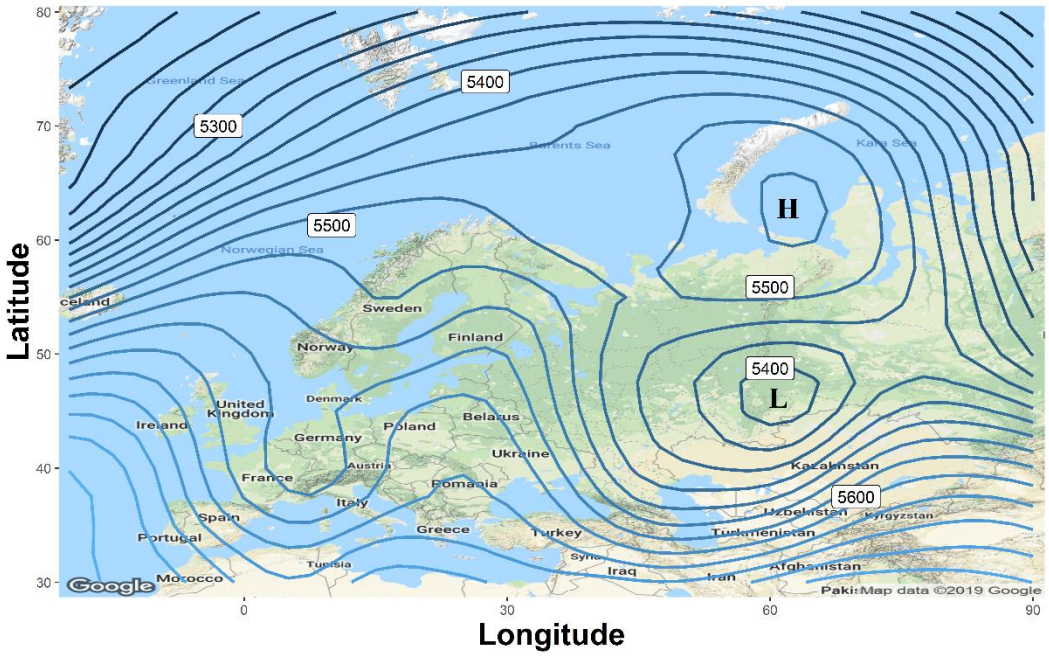

Figure 1.1 : Example of Rex – type blocking event.

The second blocking type is the omega – type blocking event that is more frequent in the Pacific Region. The example of an omega – type blocking event can be seen in Figure 1.2.

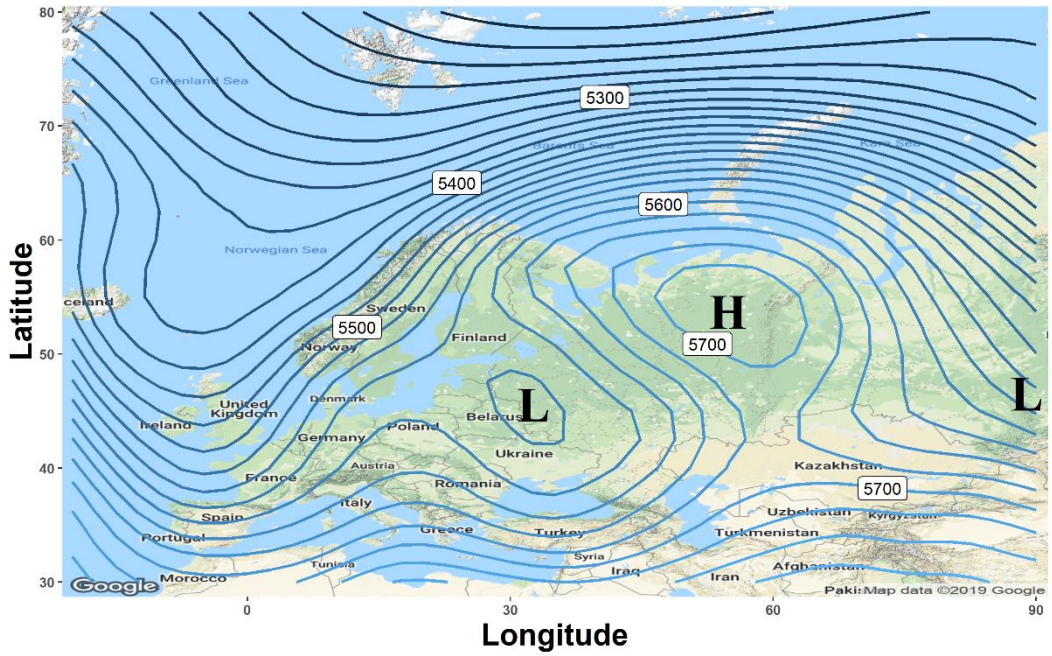

Figure 1.2 : Example of omega – type blocking event.

The annual average number of block onset by longitude is seen in Figure 1.3. As seen in Figure 1.3 there are two preferred blocking onset locations in the northern hemisphere. One of them is in the area covers North Atlantic and Europe, the other one is Pacific Ocean. Turkey is located in the area influenced by North Atlantic blocking events.

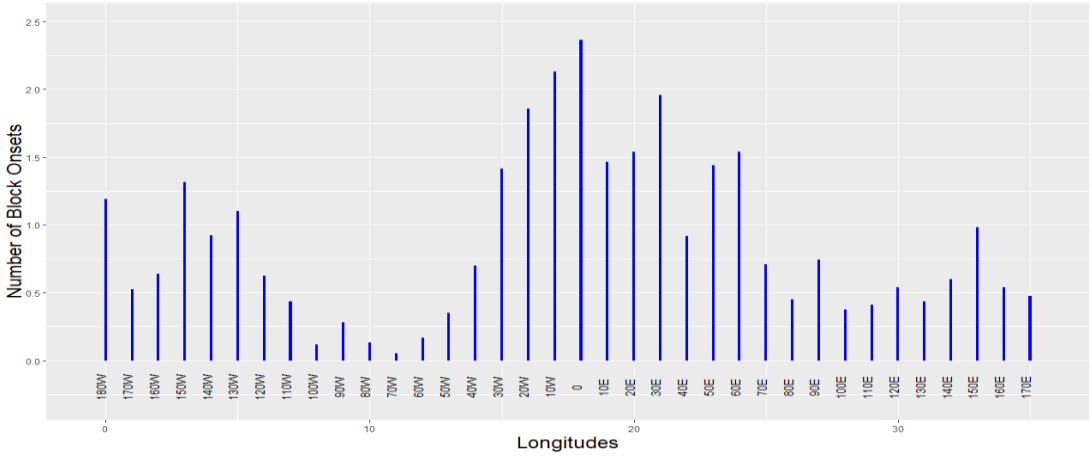

Figure 1.3 : The number of block onsets per year versus longitude (calculated by the University of Missouri blocking archive).

The first study related to the atmospheric blocking was introduced by Garriott (1904). During the 1940s some authors mentioned the effects of atmospheric blocking on local climates (e.g. Berggren et al., 1949; Elliott and Smith, 1949). After the second world war, the improvement of upper-level data coverage induced plotting upper-level maps and the number of studies related to the atmospheric blocking increased.

Rex (1950), made the first definition of atmospheric blocking as; the basic westerly flow must split into two branches that transport appreciable mass, a 45^{o} longitude extension of the double jet system, a change of zonal to meridional flow and the continuity of the pattern at least 10 days.

Treidl et al. (1981), stated that atmospheric blocking should exist north of 30^{o} N and persist at least 5 days. They also identified dipole structure of positive height anomaly around 60^{o} N and negative height anomaly around 40^{o} N. Lejenäs and Økland (1983, hereafter LO83), developed a blocking index based on the results of Treidl et al. (1981). The LO83 index considers the dipole structure and an event should satisfy this structure for at least 30^{o} longitudes.

Tibaldi and Molteni (1990, hereafter TM90) modified the LO index by introducing northward and southward gradients of 500 hPa geopotential height gradients. The southward gradient is considered to include the conversion of 500 hPa geopotential height by atmospheric blocking. The northward gradient also considered to satisfy the requirement that the average wind is westerly poleward of the block. Details on TM90 may be found in Section 2.2.1.

There are also some other 1-D and 2-D blocking indices that use 500 hPa geopotential height maxima or gradients.

Pelly and Hoskins (2003), introduced a new blocking index based on the potential vorticity field. As shown by Pelly and Hoskins (2003), atmospheric blocking can be identified by the breaking of upper – level Rossby waves on the dynamical tropopause.

So the blocking detecting algorithms can be divided into two main branches: use of the 500 hPa geopotential height data or potential vorticity data.

1.2 Literature Review

The influence of atmospheric blocking on observed regional surface temperature is widely investigated because the temperature is a variable of interest to the general public. Diao et al. (2015) demonstrated that Eastern Atlantic blocking accompanies frequent cold extremes in Europe. Diao et al. (2015) argue that not only does local cooling occur upstream and downstream of the blocking event, but also increased surface air temperatures are the result of atmospheric blocking where they reside. The composite maps examined in this study demonstrated that from 4 days to one day before block onset, positive anomalies of geopotential height are located over northern Europe when negative anomalies are located over southern Europe.

Antokhina et al. (2018) investigated the effect of atmospheric blocking on surface temperature anomalies for western Siberia during the period from 2004 to 2016. They detected 14 events located over western Siberia and divided these blocking events into two groups. For the first group (10 events), the surface temperature anomalies show a dipole pattern: north(south) of the domain observed positive (negative) anomalies or no temperature anomalies. The second group (four events) was non-dipole.

Sillmann et al. (2011) investigated the influence of North Atlantic Blocking on 2 m minimum temperatures, not only in the re-analysis data (ERA (ECMWF Re-Analysis) - 40) but also for 20th century and future simulations (ECHAM5/MPI-OM (developed at the Max Planck Institute for Meteorology in Hamburg, Germany). According to the distribution of ERA – 40 and 20th Century data, the Baltic Sea coastline is a primary area that is influenced by atmospheric blocking. During the winter season, long – lasting atmospheric blocking events are correlated with lower minimum temperatures for the vast majority of Europe.

The linkage between atmospheric blocking and precipitation is also investigated by many researchers due to the impacts of precipitation on daily activities. Rabinowitz et al. (2018) investigated the relationship between heavy rainfall events associated with atmospheric rivers in the midwest United States of America (USA) and Pacific Region blocking events during different El Nino Southern Oscillation (ENSO) phases. They found 16 heavy rainfall events were observed during the 2000-2015 period, and seven of these events were observed in La Nina (LN) years even though only three LN events occurred during this time. Also, four and five of the 16 events were observed during

El Nino (EN) and Neutral (NEU) years, respectively, although there were five and nine EN and NEU years, respectively. There was no statistical relationship between rainfall amounts and blocking characteristics due to the small sample size.

Rimbu et al. (2015) explored the linkage between summer precipitation extremes and atmospheric blocking events over Romania during the period 1962 – 2010. The R90p (90^{th} percentile is used as the threshold) index is used to determine extreme rainfall events. Rimbu et al. (2015) determined that blocking events in the sectors (0^o – 40^o E and 50^o – 70^o E) are associated with a significant portion of the extreme precipitation variability during summer over Romania.

Sousa et al. (2016), examined the relationship between blocking locations and European precipitation regimes on both the seasonal and annual time scale. In the regions directly under the influence of blocking, there was a decreased frequency of moderate rainfall events resulting in a reduction of total precipitation. On the other hand, there was an increase in the frequency of extreme rainfall events on the southern flank of blocking events, causing an overall precipitation increase in these regions.

Nunes et al. (2017) investigated the monthly precipitation extremes for two global regions (the central USA and southwest Russia). Nunes et al. (2017) used the meteorological data from Columbia, Missouri during the period of 1889 – 2014 within the central USA and from Belgorod surface weather station from 1944 to 2014 for southwest Russia. Monthly departures greater than three standard deviations from mean seasonal temperature and the three wettest and driest months for precipitation were used as the criterion to define an extreme event. In the central USA, extreme wet and dry years were associated with NEU years, whereas in southwest Russia EN and NEU years was responsible for most of the precipitation extremes.

Sousa et al. (2017) investigated the maximum temperature (Tmax) and minimum temperature (Tmin) variations in Europe during the period 1948 – 2012 for both blocking and transient ridge situations. The composite Tmax, Tmin anomalies during winter and summer for both blocking and ridge conditions with respect to European regions were obtained. In winter it was shown that during blocking episodes negative anomalies were observed for both Tmax and Tmin, but not for ridge events. In contrast, positive Tmax and Tmin anomalies observed during ridge situations. During the summer, there was not the opposite signature for blocking and ridge conditions.

Whan et al. (2016) studied the impacts of upstream atmospheric blocking on wintertime minimum extreme temperatures in North America using numerous data sets. They used the blocking frequency (BF) in the northern Pacific Ocean as a covariate when investigating the variation in minimum extreme temperatures by utilizing generalized extreme value theory (GEV). Whan et al. (2016) determined that blocking has different impacts on local temperature regimes depending on the location and scale of the event and the location parameters of GEV.

Rimbu et al. (2014) examined the relationship between not only a blocking index but also other large – scale general circulation patterns in association with large winter temperature extremes in Romania. High blocking activity is related to cold air advection and low blocking activity is related to warm air advection in Romania. Brunner et al. (2017) examined the linkage between atmospheric blocking events and European extreme temperatures during the spring season by using E – Obs temperature data set. They found that blocking occurring over central Europe is correlated with warmer conditions while blocking located over the Atlantic and Scandinavia is associated with the cold spells.

Luo et al. (2015) investigated the December 2013 snowstorm that affected the vast majority of the Middle East, including Turkey. Luo et al. (2015) related cold air advection into the Middle East that produced snowfall to an omega-shaped European blocking event, which is the ideal location for the transport cold air into the Middle East. Yao et al. (2016) examined the impacts of the North Atlantic Jet on Middle East snowstorms associated with downstream blocking and a positive North Atlantic Oscillation (NAO) index. Yao et al. (2016) concluded that the strength of the North Atlantic Jet changes the tilt of the block axis in association with a positive NAO during European dipole blocking events.

There are some studies about the influences of synoptic scale and large scale patterns on meteorological parameters over Turkey. Türkeş and Erlat (2009) investigated the relationship between winter mean temperatures and the NAO during the period 1950 - 2003 within Turkey. Cold temperatures were observed over almost all of the 70 surface stations during the positive phase of NAO, and northeasterly flow dominated the period during cold weather. Conversely, during the negative phase of the NAO, westerly flow persists over Turkey and warm temperature anomalies were observed over the vast majority of the country.

Baltacı et al. (2017) investigated the relationship between teleconnection patterns and Turkish extreme events for the period 1965 – 2014. Above normal precipitation in the western part of Turkey was linked to the positive phase of Arctic Oscillation (correlation coefficient (CC) around -0.5). In contrast, positive precipitation anomalies were observed over the Black Sea and Aegean Regions during the positive phase of the East Atlantic - Western Russia pattern.

Some researchers focused on the extreme events over Turkey. Yesilırmak and Atatanır (2016) examined the precipitation concentration in western Turkey by using several indices and concluded that mostly non-significant decreasing trends were observed for all indices. Kömüşçü and Çelik (2012) studied the Marmara flood took place in 2009. They emphasized that, besides the favorable meteorological conditions, urbanization played a major role in the worst flood occurred in the region in recent decades.

Unal et al. (2013) investigated the summer heat waves over western Turkey from 1965 to 2006. They concluded that the number of hot days, heat waves and heat wave duration increased within this period. Deniz and Gonencgil (2015) examined the trends in summer daily maximum temperatures for Turkey 1970 – 2006. They demonstrated that 59 percent of the stations have an increasing trend in the frequency of warm, hot and extremely hot days at the 0.05 confidence level or greater. On the other hand, 34 percent of the stations have a significant decreasing trend in the frequency of cool, cold and extremely cold days.

Toros (2012) analyzed the Tmax and Tmin during winter as well as summer. He summarized that there is significant warming in both annual maximum and minimum temperature observations with trends in summer, which are stronger than those during the winter.

On the other hand, the effects of blocking on Turkey has not been studied widely. Tayanç et al. (1998) is the first study that mentions blocking in association with a blizzard event, investigating one of the most famous blizzards that occurred in Istanbul, Turkey. This event lasted from 3 - 10 March 1987. The cause of the blizzard was a persistent cyclone associated with the block that was located over the Balkan region of Europe. Demirtaş (2017) examined the 2012 winter season which was associated with prolonged cold spells in Europe (including Turkey) due to an omega-shaped blocking event centered over Siberia. The European cold waves persisted for

time periods of 2 to 22 days, and in Turkey anywhere from 4 to 18 days, depending on the location within the country.

In addition, atmospheric blocking was observed to be associated with several extreme events in Turkey, including a flash flood event during 7 – 10 September 2009, during which 31 people died (Kömüşçü and Çelik, 2013). Also, blocking was associated with a devastating cyclone that caused strong winds (>80 kts) and fatal incidents, including forest fires during the period of 18 – 22 April 2012 (Sırdaş et al., 2017). One of the wettest winters in the history of Turkey occurred in 1985 (Türkeş and Erlat, 2005). However, blocking was not the focus of these studies which investigated the severe weather phenomena.

1.3 Purpose of the Thesis

Atmospheric blocking effects the regions not only it was located but also distant regions, since it disrupts the westerly flow in high levels and split the flow into two meridional branches. Turkey is located over the same latitudes as the cyclonic part of the Rex-type blocking event or the flanks of the omega-type blocking event. So, it is under the influence of blocking when blocking occurs at the longitudes close enough to Turkey. The scope of this thesis is to put forth the effects of the atmospheric blocking on surface temperature, precipitation and extreme temperature parameters in a climatological perspective for Turkey.

The thesis is organized as follows: The data and methodology used in this work are introduced in Chapter 2. This includes the data for blocking detection and meteorological parameters, the definition of blocking and its characteristics and institution of the variables to represent the meteorological parameters. Then, the results for atmospheric blocking were explained in Chapter 3. Results for temperature anomalies, mean precipitation frequency and extreme temperature are presented in Chapter 4, 5 and 6. Finally, the work is summarised in Chapter 7.

2. DATA AND METHODOLOGY

2.1 Data

2.1.1 Blocking data

The 500 hPa geopotential height data are provided by the National Centers for Environmental Prediction (NCEP) and National Center for Atmospheric Research (NCAR) Reanalysis-1 dataset (Kalnay et. al. 1996), and these were used to detect atmospheric blocking events. The data are available for 1948 to present with 6-h temporal resolution and 2.5º x 2.5º spatial (latitude-longitude) resolution. There are numerous data types available for both the surface and pressure levels. The NCEP – NCAR Reanalysis 500 hPa data set is used in several studies to detect blocking (e.g. de Vries et al., 2013; Mokhov et al., 2014; Sitnov et al., 2014). The daily geopotential data (0000 UTC) were used in this study for the period 1 January 1977 – 31 December 2016. The zonal and meridional boundaries of the study region are 20º W - 90º E and 30º N – 90º N, respectively. The domain is shown in Figure 2.1.

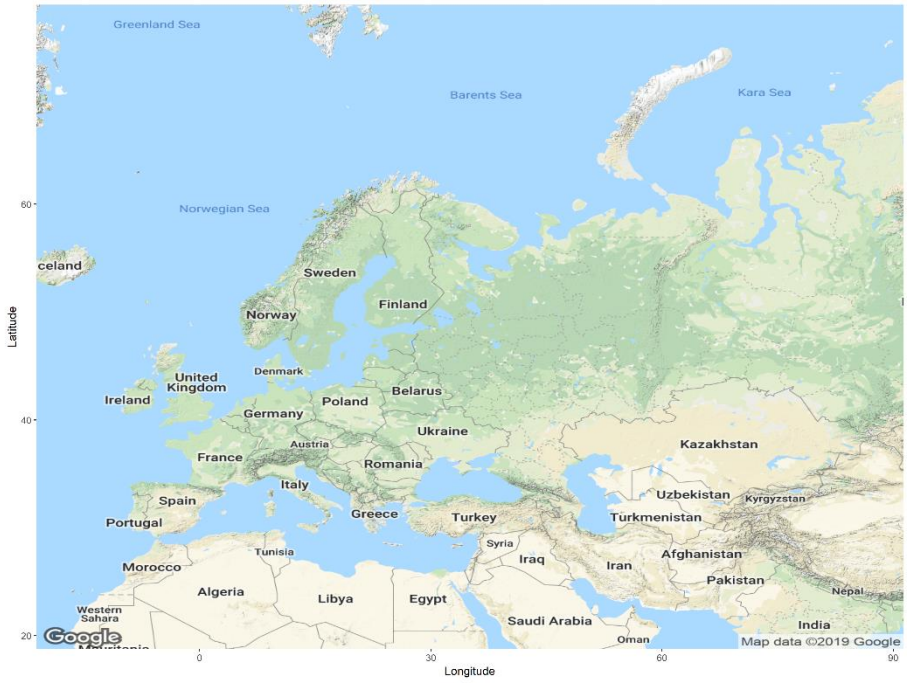

Figure 2.1 : Study domain for blocking detection.

2.1.2 Meteorological data

Turkey is located on both Europe and Asia continents and has complex topography. The largest portion of the country is in southwest Asia. The northern portion is in extreme southeast Europe. The daily mean, maximum and minimum temperature and precipitation data were provided by Turkish State Meteorological Services at 77 stations distributed across the country for the aforementioned period. The location of the stations is presented in Figure 2.2 and the information about the stations is presented in Table 2.1.

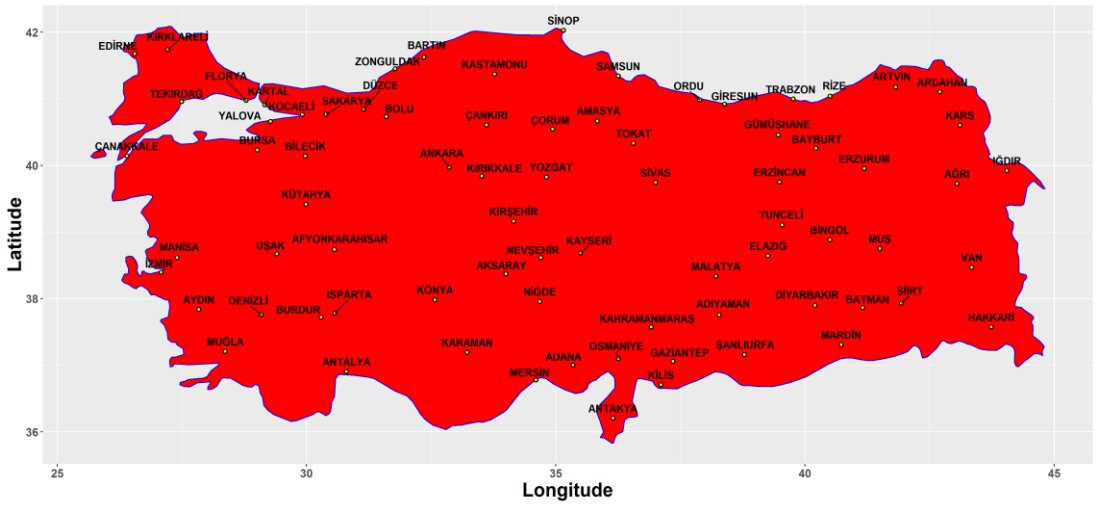

Figure 2.2 : The location of the stations used for the study.

Table 2.1 : The information about the stations.

No	Name	Latitude (oN)	Longitude (o E)	Altitude (m)
17020	BARTIN	41.6248	32.3569	33
17022	ZONGULDAK	41.4492	31.7779	135
17026	SİNOP	42.0299	35.1545	32
17030	SAMSUN BÖLGE	41.3441	36.2563	4
17033	ORDU	40.9838	37.8858	5
17034	GİRESUN	40.9227	38.3878	38
17040	RİZE	41.0400	40.5013	3
17045	ARTVİN	41.1752	41.8187	613
17046	ARDAHAN	41.1061	42.7055	1827
17050	EDİRNE	41.6767	26.5508	51
17052	KIRKLARELİ	41.7382	27.2178	232
17056	TEKİRDAĞ	40.9585	27.4965	4
17066	KOCAELİ	40.7663	29.9173	74
17069	SAKARYA	40.7676	30.3934	30
17070	BOLU	40.7329	31.6022	743

Table 2.1 (continued): The information about the stations.

No	Name	Latitude (oN)	Longitude (o E)	Altitude (m)
17072	DÜZCE	40.8437	31.1488	146
17074	KASTAMONU	41.3710	33.7756	800
17080	ÇANKIRI	40.6082	33.6102	755
17084	ÇORUM	40.5461	34.9362	776
17085	AMASYA	40.6668	35.8353	409
17086	TOKAT	40.3312	36.5577	611
17088	GÜMÜŞHANE	40.4598	39.4653	1216
17089	BAYBURT	40.2547	40.2207	1584
17090	SİVAS	39.7437	37.0020	1294
17094	ERZİNCAN	39.7523	39.4868	1216
17096	ERZURUM HAVALİMANI	39.9529	41.1897	1758
17097	KARS	40.6042	43.1073	1777
17099	AĞRI	39.7253	43.0522	1646
17100	IĞDIR	39.9227	44.0523	856
17112	ÇANAKKALE	40.1410	26.3993	6
17116	BURSA	40.2308	29.0133	100
17119	YALOVA	40.6589	29.2796	4
17120	BİLECİK	40.1414	29.9772	539
17135	KIRIKKALE	39.8433	33.5181	751
17140	YOZGAT	39.8243	34.8159	1301
17160	KIRŞEHİR	39.1639	34.1561	1007
17165	TUNCELİ	39.1058	39.5408	981
17186	MANİSA	38.6153	27.4049	71
17188	UŞAK	38.6712	29.4040	919
17190	AFYONKARAHİSAR BÖLGE	38.7380	30.5604	1034
17192	AKSARAY	38.3705	33.9987	970
17193	NEVŞEHİR	38.6163	34.7025	1260
17196	KAYSERİ BÖLGE	38.6870	35.5000	1094
17199	MALATYA	38.3367	38.2173	950
17201	ELAZIĞ BÖLGE	38.6443	39.2561	989
17203	BİNGÖL	38.8847	40.5007	1139
17204	MUŞ	38.7509	41.5023	1322
17210	SİİRT	37.9319	41.9354	895
17037	TRABZON BÖLGE	40.9985	39.7649	25
17220	İZMİR BÖLGE	38.3949	27.0819	29
17234	AYDIN	37.8402	27.8379	56
17237	DENİZLİ	37.7620	29.0921	425
17238	BURDUR	37.7220	30.2940	957
17240	ISPARTA	37.7848	30.5679	997
17244	KONYA HAVALİMANI	37.9837	32.5740	1031
17246	KARAMAN	37.1932	33.2202	1018
17250	NİĞDE	37.9587	34.6795	1211
17255	KAHRAMANMARAŞ	37.5760	36.9150	572

Table 2.1 (continued): The information about the stations.

No	Name	Latitude (oN)	Longitude (o E)	Altitude (m)
17261	GAZİANTEP	37.0585	37.3510	854
17262	KİLİS	36.7085	37.1123	640
17265	ADIYAMAN	37.7553	38.2775	672
17270	ŞANLIURFA	37.1608	38.7863	550
17275	MARDİN	37.3103	40.7284	1040
17280	DİYARBAKIR HAVALİMANI	37.8973	40.2027	674
17282	BATMAN	37.8636	41.1562	610
17285	HAKKARİ	37.5745	43.7388	1727
17292	MUĞLA	37.2095	28.3668	646
17300	ANTALYA HAVALİMANI	36.9063	30.7990	64
17340	MERSIN	36.7808	34.6031	7
17351	ADANA BÖLGE	37.0041	35.3443	23
17355	OSMANIYE	37.1021	36.2539	94
17372	ANTAKYA	36.2048	36.1513	104
17636	FLORYA	40.9758	28.7865	37
17130	ANKARA BÖLGE	39.9727	32.8637	891
17155	KÜTAHYA	39.4171	29.9891	969
17172	VAN BÖLGE	38.4693	43.3460	1675
17638	KARTAL (İSTANBUL)	40.9100	29.1600	27

2.2 Methodology

2.2.1 Detection of blocking and blocking index

The blocking detection method used in this study was described in TM90, which is based on the original objective criterion published by LO83. For the TM90 method, two 500 hPa geopotential gradients are computed for each longitude and every day as in expression (2.1);

$$\mathrm{GHGS} = \frac{Z_{\lambda,\varphi_0} - Z_{\lambda,\varphi_S}}{\varphi_0 - \varphi_S}$$

$$GHGN = \frac{Z_{\lambda,\varphi_N} - Z_{\lambda,\varphi_0}}{\varphi_N - \varphi_0} \qquad (2.1)$$

$\varphi_S = 40^o + \Delta$, $\varphi_0 = 60^o + \Delta$, $\varphi_N = 77.5^o + \Delta$ and $\Delta = -5^o, -2.5^o, 0, 2.5^o, 5^o$. (2.2)

where $Z_{\lambda,\varphi}$ is the geopotential height at the longitude λ and latitude φ. The GHGS (Geopotential Height Gradient in Southern part of φ_0) is proportional to the zonal component of the geostrophic wind and GHGN (Geopotential Height Gradient in Northern part of φ_0) is included to exclude non-blocked flows. This modified version

of TM90 is based on the availability of the NCEP - NCAR data with 2.5 x 2.5-degree resolution. An arbitrary longitude is accepted as blocked when both GHGS and GNGN verify the condition expressed by (2.3) for at least one of the five Δ values and simultaneously the geopotential height gradient at φ_0 is positive. By allowing five Δ values, this criterion provides for more blocking opportunities and better spatial resolution instead of three Δ proposed by TM90;

$$\text{GHGS} > 0$$

$$\text{GHGN} < -10 \text{ gpm} / {}^{o}\text{lat}$$

$$Z(\lambda, \phi_0) - \overline{Z(\lambda, \varphi_0)} > 0 \qquad (2.3)$$

A pattern can be assumed as blocked when a considerable number of adjacent longitudes are simultaneously blocked since blocking patterns are large-scale phenomena. In this dissertation, consistent with (Barriopedro et al., 2006) five or more adjacent grid points (12.5^{o}) is required to confirm that a blocking pattern exists, with the allowance of one non-blocked longitude between the blocked longitudes.

2.2.2 Blocking center detection

Before the description of the blocking center, a latitude-longitude box is defined in the blocking region. The longitude limits of this box are 5^{o} west of the first blocked longitude and 5^{o} east of the last blocked longitude. Latitude limits are the northward of the maximum value of ϕ_S and the southward of the minimum value of ϕ_N. Now, the blocking center can be described. The longitude of the blocking can be described as that longitude within the box with maximum latitudinally averaged geopotential height. Similarly, the latitude of the blocking can be described as that latitude within the box with maximum longitudinally averaged geopotential height.

2.2.3 Blocking intensity

The methodology introduced in Lupo and Smith (1995, hereafter LS95) and Wiedenmann et al. (2002, hereafter WI02) was also followed in order to compute a blocking intensity (BI) index. LS95 obtained this index by proportioning the local maxima of geopotential height to the reference contour line that can be described as the contour that covers upstream and downstream troughs. The slightly modified version done by WI02 can be described as in (2.4)

$$\boldsymbol{BI = 100 * \left[\frac{Z_{BC}}{RC} - 1.0\right]}$$

$$\boldsymbol{RC = \left[\frac{Z(\lambda_u,\phi)+Z(\lambda_d)}{2}\right]} \quad (2.4)$$

where $\boldsymbol{Z_{BC}}$ is the geopotential height value of the blocking center and RC is the reference contour that is calculated by the averaging the geopotential height value of the lowest trough axis upstream $\boldsymbol{Z(\lambda_u, \phi)}$ and downstream $\boldsymbol{Z(\lambda_d, \phi)}$located at the same latitude as the blocking center. The position of $\boldsymbol{\lambda_u}$ was fixed 10° westward of the half-extension of from the blocking center and $\boldsymbol{\lambda_d}$were fixed 10° eastward of the half-extension from the blocking center in longitude in order to ensure that they are located in the blocking region.

$\frac{\boldsymbol{Z_{BC}}}{\boldsymbol{RC}}$ gets the value between 1 and 1.1 so the BI is limited between 0 and 10. LS95 classified the blocking events as weak (BI < 2.55), moderate (2.55 < BI < 4.55) and strong (4.55 < BI).

2.2.4 Minimum duration for blocking

There is no temporal persistence criterion accepted by all blocking studies, even though duration is one of the most important characteristics of blocking event. Most authors use five days as the minimum duration criteria (Treidl et al., 1981; LS95; Shabbar et al., 2001; Scherrer et al., 2006), and this is used for our study as well.

2.2.5 Temporal tracking of blocking

The temporal algorithm was executed for tracking blocking events (except step two) as was described in (Barriopedro et al., 2006). According to this algorithm, the blocking event must last at least five days, a non-blocked day between two blocked days considered as blocked and it is considered as the same blocking event if the area blocked at day i intersects the area blocked at day i+1.

2.2.6 Blocking characteristics classification

The study domain is divided into four sectors; 20° W – 0° E (hereafter S1), 0 – 30° E (hereafter S2), 30 – 60° E (hereafter S3), 60 – 90° E (hereafter S4), respectively to be consistent with Efe et al. (2019). Also, sectors two, three, and four are consistent with those defined in Sousa et al. (2016). The block intensity (BI) is divided into three sub-

categories, weak, moderate and strong as described in LS95. The block duration and block size are divided into three sub-categories by using percentiles: short-term (small) for the values smaller than the 25^{th} percentile, moderate (moderate) for the values between 25^{th} and 75^{th} percentile and persistent (large) for the values greater than the 75^{th} percentile.

2.2.7 Temperature anomalies

The anomalies during blocked days were stratified by season (December, January, and February for winter; March, April, and May for spring; June, July, and August for summer and September, October and November for fall). The seasonal temperature anomalies for all stations are categorized into five classes: Very Strong Negative (anomaly < μ-2σ), Strong negative (μ-2σ < anomaly < μ-σ), Moderate (μ-σ < anomaly < μ+ σ), Strong Positive (μ+σ < anomaly < μ+2σ) and Very Strong Positive (μ+2σ < anomaly) where μ and σ represents the seasonal mean and standard deviation of the temperature anomaly, respectively.

2.2.8 Precipitation frequency

The precipitation frequency value is calculated as the ratio between the number of days with precipitation to the total number of days. Mean precipitation frequency represents the overall average of precipitation frequency.

2.2.9 Extreme temperature definition

The extreme cold temperature (Tn) for each season is defined as the minimum temperature that is lower than the first percentile of all minimum temperature values during winter and summer. The extreme warm temperature (Tx) for each season is defined as the maximum temperature that is greater than the 99^{th} percentile of all maximum temperature values. The frequency of extreme events during blocking is calculated as the proportion of the number of days with extreme events to the total number of blocking days.

2.2.10 Statistical relationships

The Pearson correlation coefficient (Pearson, 1896) is used to determine the relationship between blocking properties and temperature anomalies and MPF. The

significance of the relationship was tested by using the t-distribution with N – 2 degrees of freedom where N is the length of data.

All uncredited figures are illustrated via ggplot2 R-package (Wickham, 2019). All calculations are performed using R-programming (R Core Team 2019; Wickham et al. 2019)

3. BLOCKING CLIMATOLOGY

In this section, the statistical characteristics of atmospheric blocking events will be introduced. The statistical characteristics of atmospheric blocking events with respect to seasons in the study domain are calculated and shown in Table 3.1.

Table 3.1 : The characteristics of the blocking events in the domain.

	Winter	**Spring**	**Summer**	**Fall**	**Annual**
Mean Duration (Days)	9.2	9.2	8.4	8.1	8.8
Count	2.7	3.9	2.5	2.6	11.7
Intensity	2.65	2.31	1.91	2.36	2.41
Longitudinal Extent (Longitudes)	29	27	25	25	28

3.1 Blocking Numbers

The annual blocking numbers in the study area is shown in Figure 3.1. The mean number is 11.7 events per year (Table 3.1). The lowest annual blocking number is seen in several years with the value of 9. The highest annual blocking number is 18 in 1996.

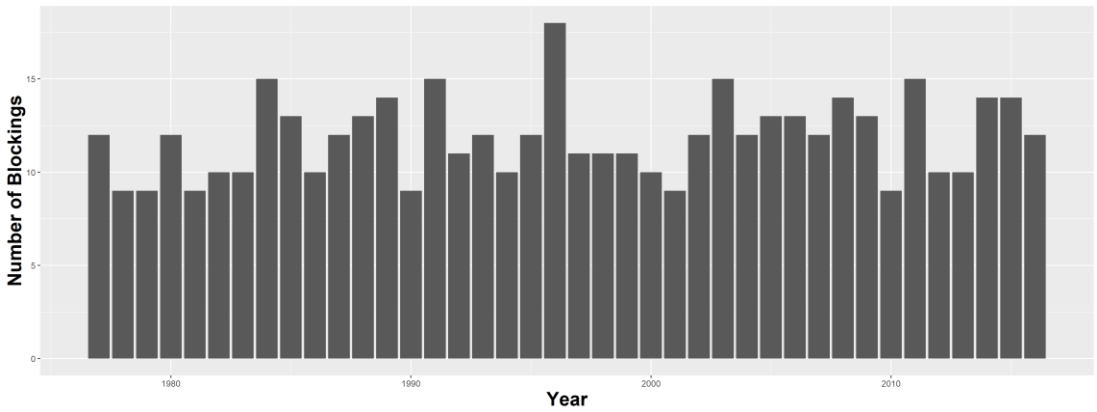

Figure 3.1 : Annual blocking numbers.

The blocking occurrence stratified by season is seen in Figure 3.2. In the winter, the lowest occurrence is once a year in some years when the maximum number is 6 in 1984 (Figure 3.2a) and the mean number is 2.7 (Table 3.1). In the spring, the lowest occurrence is once a year in 1997 when the maximum number is 7 in 1991 (Figure

3.2b) with a mean of 3.9 events (Table 3.1). In the summer, no blocking was observed in 1985 and 1993 while 5 events were observed in 1983, 1988 and 1997 (Figure 3.2c) and the seasonal average is 2.5 events (Table 3.1). In the fall, 1983 and 2012 years have no blocking events. On the other hand, 5 events were observed in 1993, 1996 and 2003 (Figure 3.2d). The mean occurrence for fall is 2.6 events (Table 3.1). Summarizing, the mean occurrence for atmospheric blocking events is nearly the same during winter, summer and fall at 2.7, 2.5 and 2.6 events, respectively. In contrast, spring has more blocking occurrences than any other season (3.9 events).

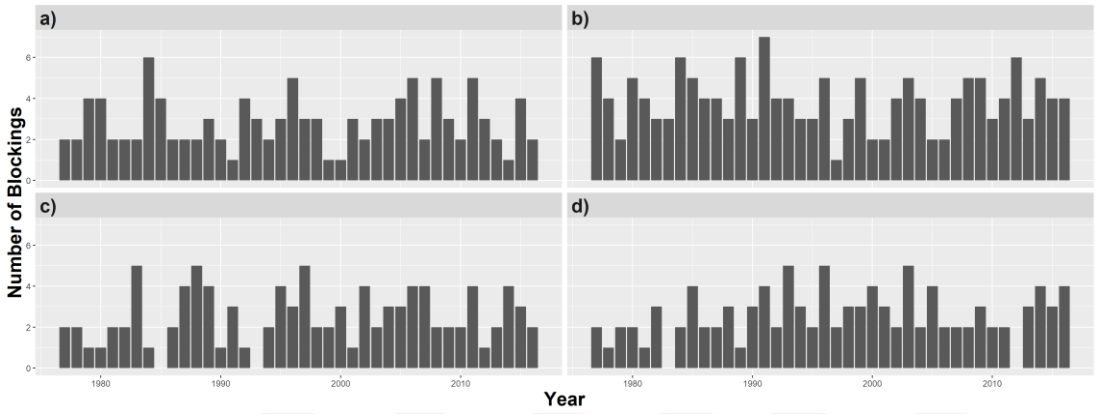

Figure 3.2 : Seasonal blocking numbers in (a) winter, (b) spring, (c) summer, and (d) fall.

3.2 Blocking Intensity

The annual mean blocking intensity of atmospheric blocking for the study area is shown in Figure 3.3. The annual mean intensity is 2.41 (Table 3.1) with the minimum and maximum values of 1.89 (2010) and 3.04 (in 1979), respectively.

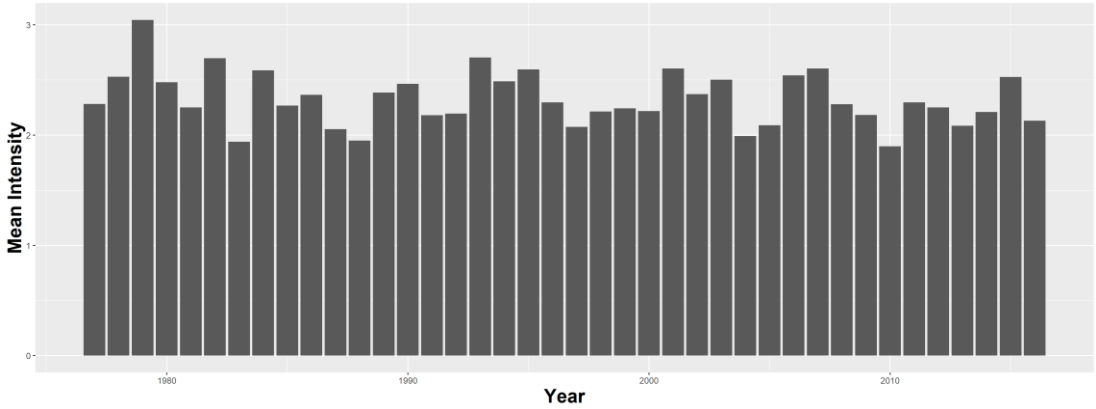

Figure 3.3 : The annual average of mean blocking intensity.

The mean intensity stratified by season is seen in Figure 3.4. The minimum, mean and maximum mean intensity values observed in winter is 1.51 (in 2011), 2.65 and 4.36 (in 1994), respectively (Figure 3.4a and Table 3.1). In the spring, the mean intensity is 2.31 while the minimum and maximum values are 1.56 (observed in 2008) and 3.27 (1997), respectively (Figure 3.4b and Table 3.1). In the summer, 2012 observed the minimum mean intensity with the value of 0.89 while the maximum mean intensity is observed in 2001 with the value of 2.75. The summer season average for mean intensity is 1.91 (Figure 3.4c and Table 3.1). Lastly, the fall season was associated with the minimum mean intensity of 1.37 (in 2014), an average of 2.36 and the maximum of 4.41 (in 1979) (Figure 3.4d and Table 3.1). The mean seasonal values for BI range between 1.91 and 2.65 in the study area. The most intense blocking events are observed in winter (2.65), while the weakest blocking events are observed in summer (1.91). This is consistent with the results of WI02 and others for the entire NH. Spring and fall have nearly the same values for BI, 2.31 and 2.36, respectively. The overall mean BI is 2.41 in the study domain.

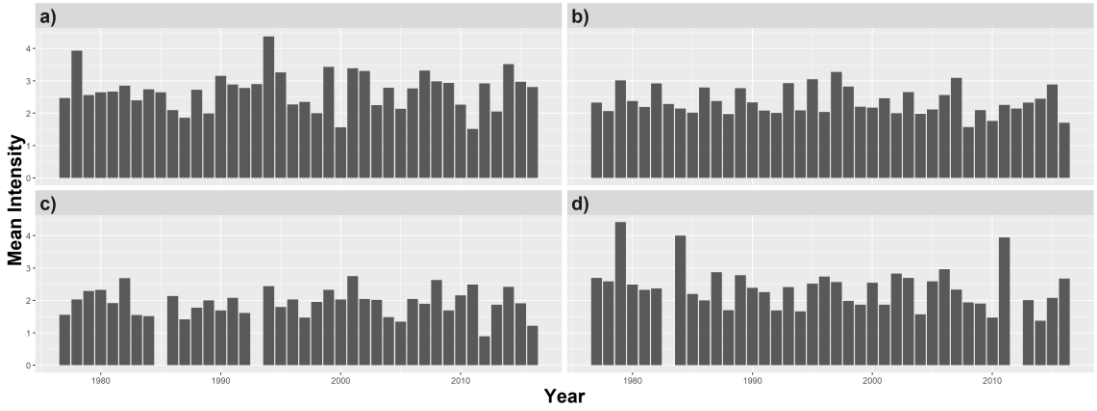

Figure 3.4 : Same as Figure 3.2 but for mean blocking intensity.

3.3 Mean Duration

The annual mean duration of atmospheric blocking for the study area is shown in Figure 3.5. The annual mean duration is 8.8 (Table 3.1) days with the minimum and maximum values of 6.7 (2009) days and 14.1 (in 2010) days, respectively.

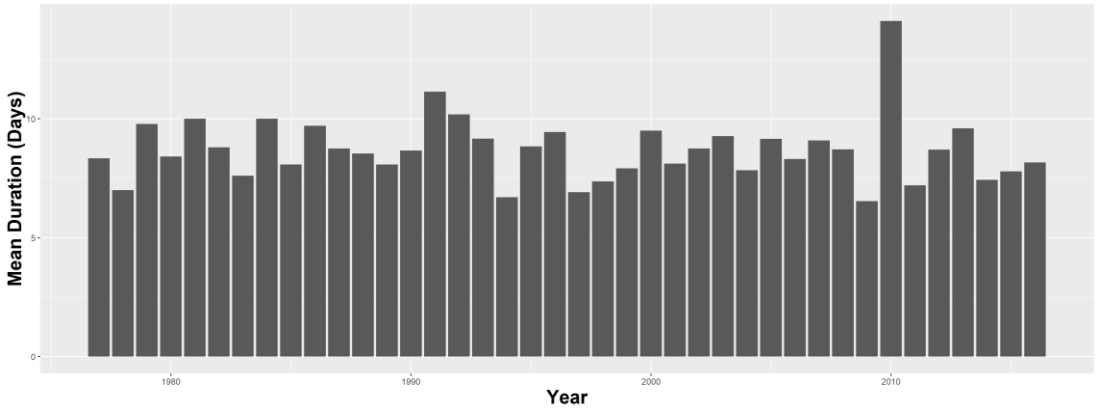

Figure 3.5 : The annual average of blocking duration.

The mean duration stratified by season is seen in Figure 3.6. The minimum, the mean and maximum mean duration values in winter are 3.0 (observed in 2014), 9.2 and 29.0 (observed in 1991) days, respectively (Figure 3.6a and Table 3.1). In the spring, the mean duration is 9.2 days while the minimum and maximum values are 5.8 (observed in 2012) and 19.5 (in 1979) days, respectively (Figure 3.6b and Table 3.1). In the summer, the years 1978 and 1992 have minimum mean duration with a value of 5 days while the maximum mean duration is seen in 2010 with a value of 21.5 days. The summer season average for the mean duration is 8.4 days (Figure 3.6c and Table 3.1). Lastly, the fall season has a minimum mean duration of 5 days (in 1979), an average of 8.1 days and a maximum of 15 days (in 1977 and 1987) (Figure 3.6d and Table 3.1. The maximum value for mean block duration occurs during the winter and spring seasons at 9.2 days. The fall season has the minimum block duration at 8.1 days, while the overall value for the mean duration is 8.8 days.

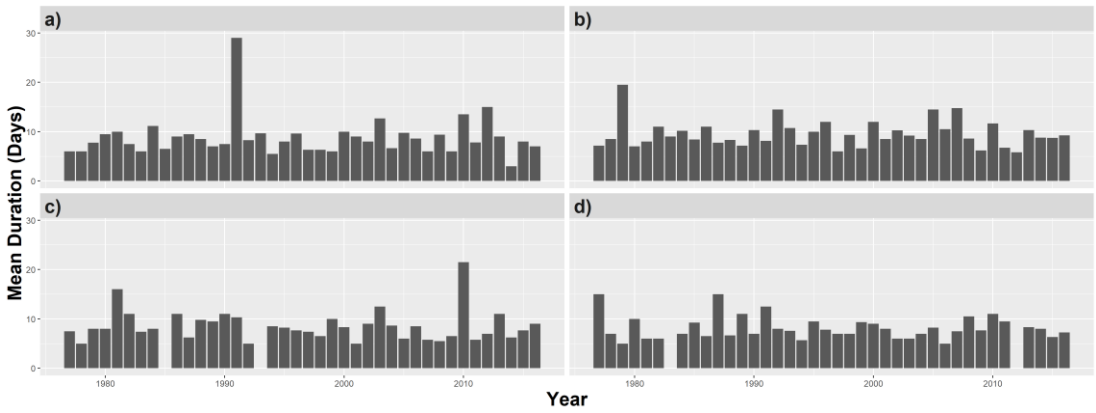

Figure 3.6 : Same as Figure 3.2 but for the mean duration.

3.4 Longitudinal Extent

The annual average longitudinal extent of atmospheric blocking for the study area is shown in Figure 3.3. The observed annual mean longitudinal extent is 28 longitudes (Table 3.7) with the minimum and maximum values of 22.59 (in 2004) and 31.32 (in 1993), respectively.

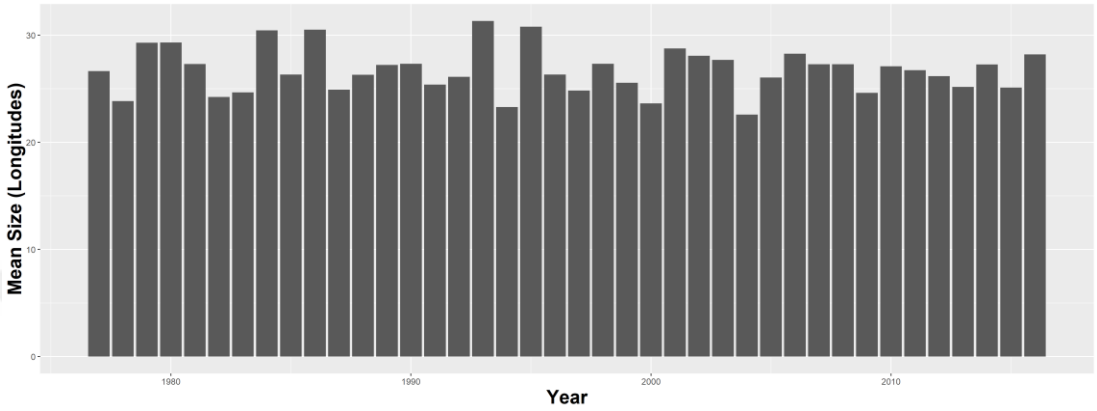

Figure 3.7 : The annual average of blocking extent.

The mean longitudinal extent stratified by season is seen in Figure 3.8. The minimum, mean and maximum mean longitudinal extent values in winter is 19.72 (observed in 2000), 29 and 47 (observed in 1986) longitudes, respectively (Figure 3.8a and Table 3.1). In the spring, the mean duration is 27 longitudes while the minimum and maximum values are 20.11 (observed in 1983) and 39.19 (in 1995) longitudes, respectively (Figure 3.8b and Table 3.1). In the summer, 1987 had the minimum mean longitudinal extent with the value of 17.90 longitudes while the maximum mean extent was seen in 2010 with the value of 37.18 longitudes. The summer season average for the mean longitudinal extent is 25 longitudes (Figure 3.8c and Table 3.1). According to Figure 3.8d and Table 3.1, the fall season has the minimum mean longitudinal extent of 15 longitudes (in 1981), an average of 25 longitudes and the maximum of 33.43 longitudes (in 1984). The seasonal longitudinal extent fluctuates between 25 and 29 degrees longitude. Summarizing, the longitudinal extent of atmospheric blocking is the largest in winter (29 degrees longitude), while spring (27 degrees longitude) had the second largest extent, and summer and fall had a nearly the same longitudinal extent (25 degrees longitude). The overall mean extent for atmospheric blocking is 28 degrees longitude.

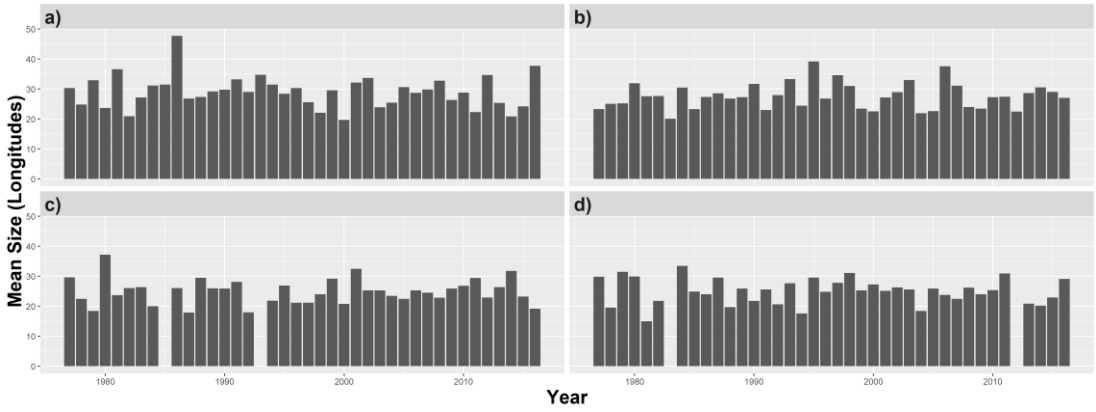

Figure 3.8 : Same as Figure 3.2 but for blocking longitudinal extent.

3.5 Relationship Between Blocking Parameters

The block longitudinal extent and duration (CC = 0.30, 0.30, 0.18 (Not Statistically Significant(NSS)), 0.40 for winter, spring, summer and fall, respectively) as well as block size and intensity (CC = 0.50, 0.56, 0.54, 0.65 for winter, spring, summer and fall, respectively) were positively correlated here with the statistical significance at the 95% confidence level except block size and duration in summer , and these results are consistent with LS95, especially for the winter season. LS95 showed these relationships were strongest in the Atlantic sector as well.

3.6 Sample Blocking Events in Different Sectors

Examples of blocking events that are located in different sectors are shown in the 500 hPa height field (Figure 3.9). These events are also the most intense (BI) events observed within those sectors. The representative blocking event located in S1 is a Rex-type event (Figure 3.9a). Turkey is under the influence of the flow associated with the cyclone located over southeast Europe. The height gradient around the blocking high is relatively weak. The flow is westerly over the entire country, transporting more humid air from the Aegean and Mediterranean Sea into Turkey. The blocking event located in S2 is an omega type event (Figure 3.9b). Turkey is located on the downstream flank of the blocking high. There is dry air transport from Europe into the northern part of the country and humid air transport from the Mediterranean into the southern part. The geopotential height gradient is the strongest compared to the other three events indicating stronger flow. The blocking event located in S3 is also an omega type event (Figure 3.9c). It has the weakest geopotential height gradient over

Turkey and the flow is nearly zonal. The sample for S4 is also an omega-type blocking event (Figure 3.9d). Turkey is located on the upstream flank of the blocking high. The geopotential height gradient is weak over the northern part of the country but stronger over the southern part.

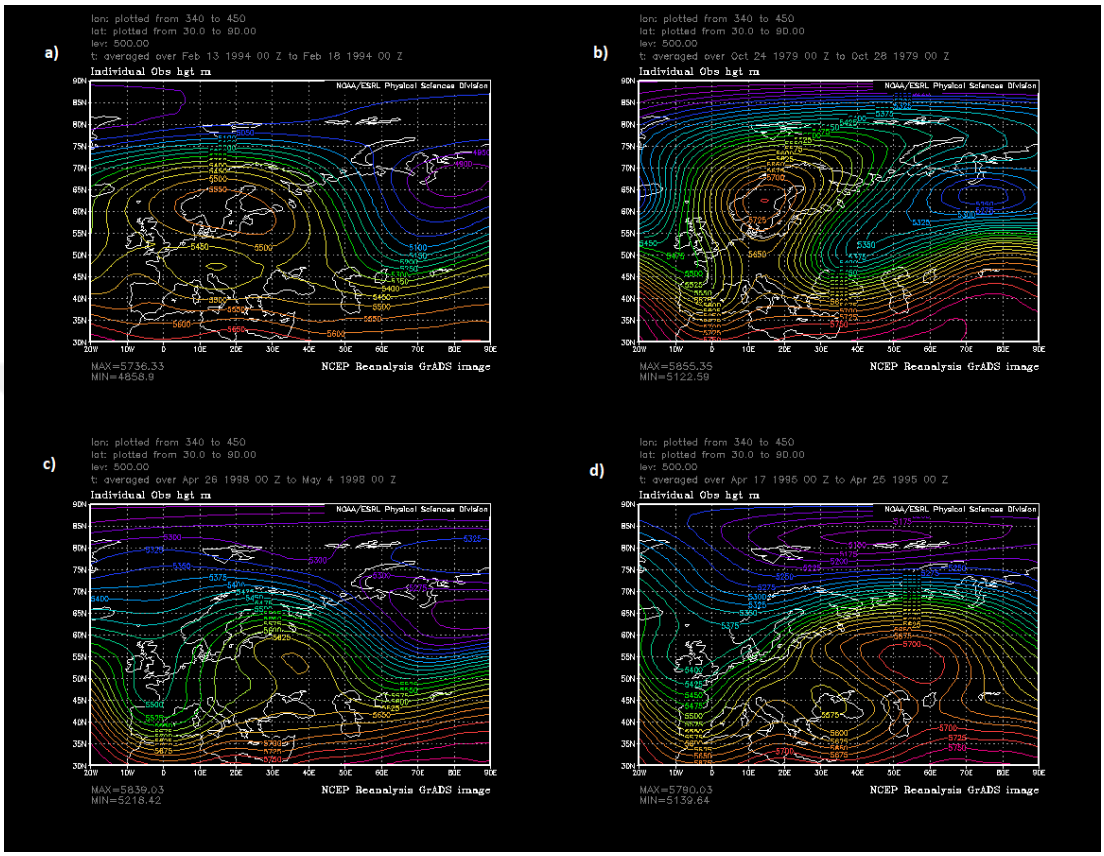

Figure 3.9 : The 500 hPa height (m) field showing sample blocking events with the blocking center located in (a) S1, (b) S2, (c) S3 and (d) S4. Height contour interval is 60 m.

4. TEMPERATURE

4.1 General Pattern of Temperature Anomalies

In this section, the mean seasonal temperature anomalies during blocked and non-blocked days are examined. Then, the difference between these seasonal anomalies is studied to emphasize the difference in regional weather between blocking and non-blocking conditions.

4.1.1 Temperature anomaly during blocked days

The seasonal mean temperature anomalies during blocked days vary between -2.1^{o} C and 0.8^{o} C (Figure 4.1). The Kırklareli station in the Marmara Region of Turkey had the highest negative temperature anomaly in winter with -2.1^{o} C, although the Ağrı station in the East Anatolia Region has the highest positive temperature anomaly during spring with 0.8^{o} C. The stations in Trakya sub-region of Marmara Region have the negative temperature anomalies around -2.0^{o} C in winter.

As seen in Figure 4.1 there are mainly four temporal patterns for the mean seasonal temperature anomalies. The first pattern (P1b) can be characterized with the minimum temperature anomaly in winter, increasing towards 0.0^{o} C or above during spring, slightly increasing or decreasing during the summer with respect to spring, and then a sharp decrease toward negative values in fall. For this pattern, the highest negative temperature anomaly was observed during the winter. This pattern is usually observed for the cities that are on the shore of the Black Sea, Marmara Sea, and the northern part of the Aegean Sea. The same pattern is observed for the Kutahya, Tokat, Nevşehir, Kayseri and Yozgat stations even though they are located in the continental inner part of Turkey.

The second pattern (P2b) is characterized by the cold seasons (winter and fall) observing negative temperature anomalies with nearly the same magnitude. During the warm seasons (spring and summer), the temperature anomalies were close to 0.0^{o} C. This pattern is observed within Central Anatolia and the inner part of the Aegean Region and the Black Sea Region. For a majority of the cities that have this pattern,

the temperature anomaly during the summer season was about 0.2° C lower than that for the spring season. For the other stations with this pattern, the warm season temperature anomalies are of similar magnitude.

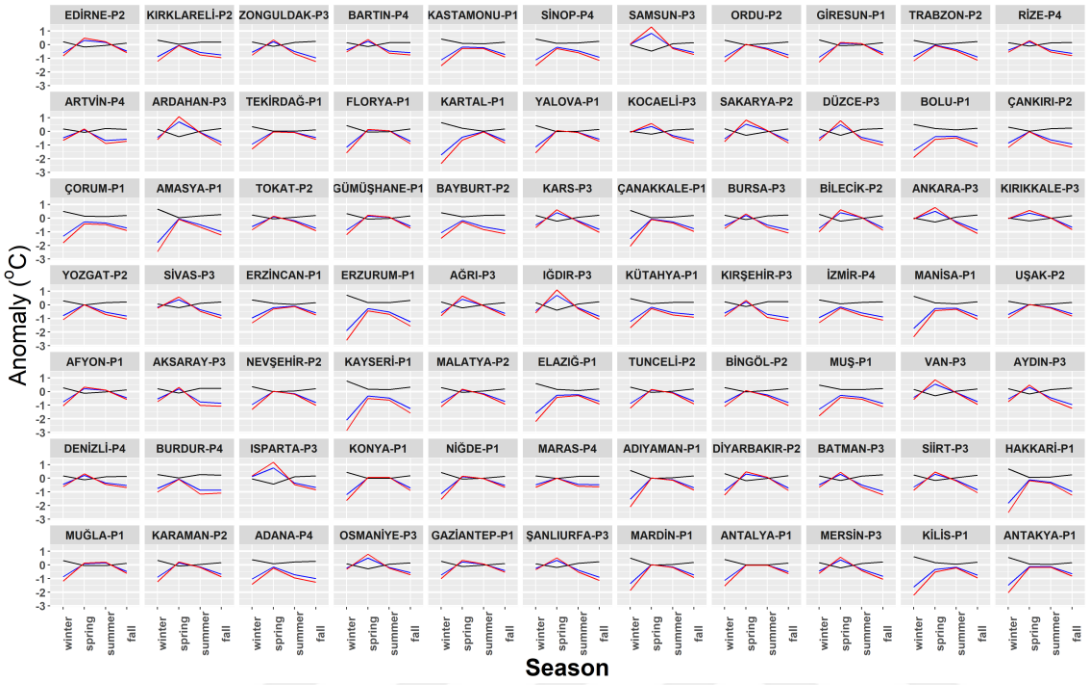

Figure 4.1 : Mean seasonal temperature anomaly during blocked days (blue line), non-blocked days (black line), temperature anomaly difference between blocked and non-blocked days (red line).

The third pattern (P3b) can be described as negative temperature anomalies in winter, then anomalies increasing up to +0.5° C in spring, and finally decreasing towards negative values in both summer and fall. This pattern is observed within the Eastern and Southeast Anatolia Regions. This pattern, however, can be split into two sub-categories. The first sub-category is associated primarily with northern cities and has lower temperature anomalies during the winter than in the summer. For the other sub-category, the pattern has nearly identical anomalies for both winter and summer or even lower summer season temperature anomalies, and this pattern is observed primarily within the southernmost part of Southeast Anatolia Region.

The fourth pattern (P4b) is observed within the cities of the Mediterranean Sea Region and south of the Aegean Region. For this pattern, the spring season was associated with the warmest temperature anomalies just around 0° C and the other seasons have nearly the same negative anomalies.

4.1.2 Temperature anomaly during non-blocked days

Temperature anomalies during non-blocked days varied between -0.5^{o} C (Ağrı in spring) and 0.8^{o} C (Edirne in fall). Similarly, the temperature anomaly during non-blocked days can be categorized as four similar groups with different behavior (Figure 4.1).

The first pattern (P1n) can be described as follows; the highest positive temperature anomalies were observed during the winter season, then decreasing values for temperature anomalies in the warm seasons and increasing values in the fall. This pattern is observed within the cities of the coastal region of the Black Sea, Marmara Sea, and northern Aegean Region. The mean seasonal anomalies are all positive in this pattern except at Rize and Ordu. This region has nearly the same type of pattern as that for P1b blocked days, but of opposite sign in character.

The second pattern (P2n) is characterized by positive temperature anomalies with the same magnitudes in cold seasons and anomalies around 0.0^{o} C in warm seasons, but of opposite sign as P2b. Analogous to the P2b, this pattern is observed within the Central Anatolia Region and inner parts of the Aegean Region and Black Sea Region. The northern cities have lower anomalies in the spring than in the summer (0.2^{o} C lower). However, the southern cities have nearly equal anomalies around 0.0^{o} C.

The third pattern (P3n) is observed within the Eastern and Southeastern Anatolia Regions. This pattern is associated with a positive temperature anomaly in the winter, a negative minimum during spring, and then a linear increase for the summer and fall seasons. The fall season has the greatest positive temperature anomaly for most of the stations. Only Erzincan and Sivas have the greatest temperature anomalies in winter.

Finally, the fourth pattern (P4n) is observed along the shore of the Mediterranean Sea and the southern part of the Aegean Sea. For this pattern, the temperature anomalies within all seasons are close to 0.0^{o} C. Spring is associated with a negative anomaly, and the other seasons have positive anomalies of almost the same magnitude.

4.1.3 Temperature anomaly difference between blocked and non-blocked days

In this sub-section, the temperature anomaly difference between blocked and non-blocked days are examined to emphasize the effect of blocking (Figure 4.1) and the patterns described previously are more evident. The first pattern(P1d) can be described

as having minimum differences for the winter season values, increasing for the spring and then with similar values for the summer, and finally decreasing in fall. All the differences for this pattern are negative for nearly all stations. For northern stations, the magnitudes of the differences in the winter are greater than the magnitudes of the differences in fall, obviously. However, for the southern stations, these differences are not evident.

For the second pattern (P2d), almost the same negative temperature anomaly differences are observed during the winter and fall seasons. For the spring and summer, the temperature anomaly differences are near 0.0^{o} C. Similar to the situation for blocked days, for the majority of the stations that have this pattern, the anomaly in the summer is lower than the anomaly in the spring. The rest of the stations have nearly the same anomalies during the spring and summer.

The third pattern (P3d) is characterized by negative temperature anomaly differences of approximately -1.0^{o} C during the winter season and then increased during the spring season. During the spring season, the anomalies vary between 0.5^{o} C – 1.0^{o} C. During the summer season, the anomaly difference is similar to the winter season, while for the fall the temperature anomaly difference reaches a minimum value.

In the last pattern (P4d), the differences are largest during the spring season, however, the other seasons have nearly the same differences. As seen in Figure 4.1, the seasonal anomaly difference curve has the same behavior with the seasonal anomaly curve during blocked days. These situations demonstrate the impact of blocking events on temperature anomalies although the blocking days are observed only approximately 30% of the study period.

4.2 500 hPa Conditions and 850 hPa Temperature Advection for the 10 Strongest Warm / Cold Anomalies

In this sub-section, the composite map of 500 hPa geopotential height for the ten events associated with the coldest and warmest conditions as well as representative temperature advection maps for these events are also investigated to explain the dynamics contributing to these temperature anomalies. The mean 500 hPa geopotential height during the blocking events associated with the ten coldest and the ten warmest surface temperature anomalies were stratified by seasons (Figure 4.2). Turkey is on

the downstream flank of the blocking ridge and exposed to cold air advection during these events (Figure 4.3). This is a similar configuration for eastern Pacific blocking events during cold conditions in the central USA (e.g., Nunes et al. 2017). On the other hand, Turkey is exposed to warm air advection during blocking events that are located east of the study region (Figure 4.3). As seen in Figure 4.3, the magnitude of the advection in upstream blocking events is greater than the magnitude of the advection in downstream blocking events in all seasons.

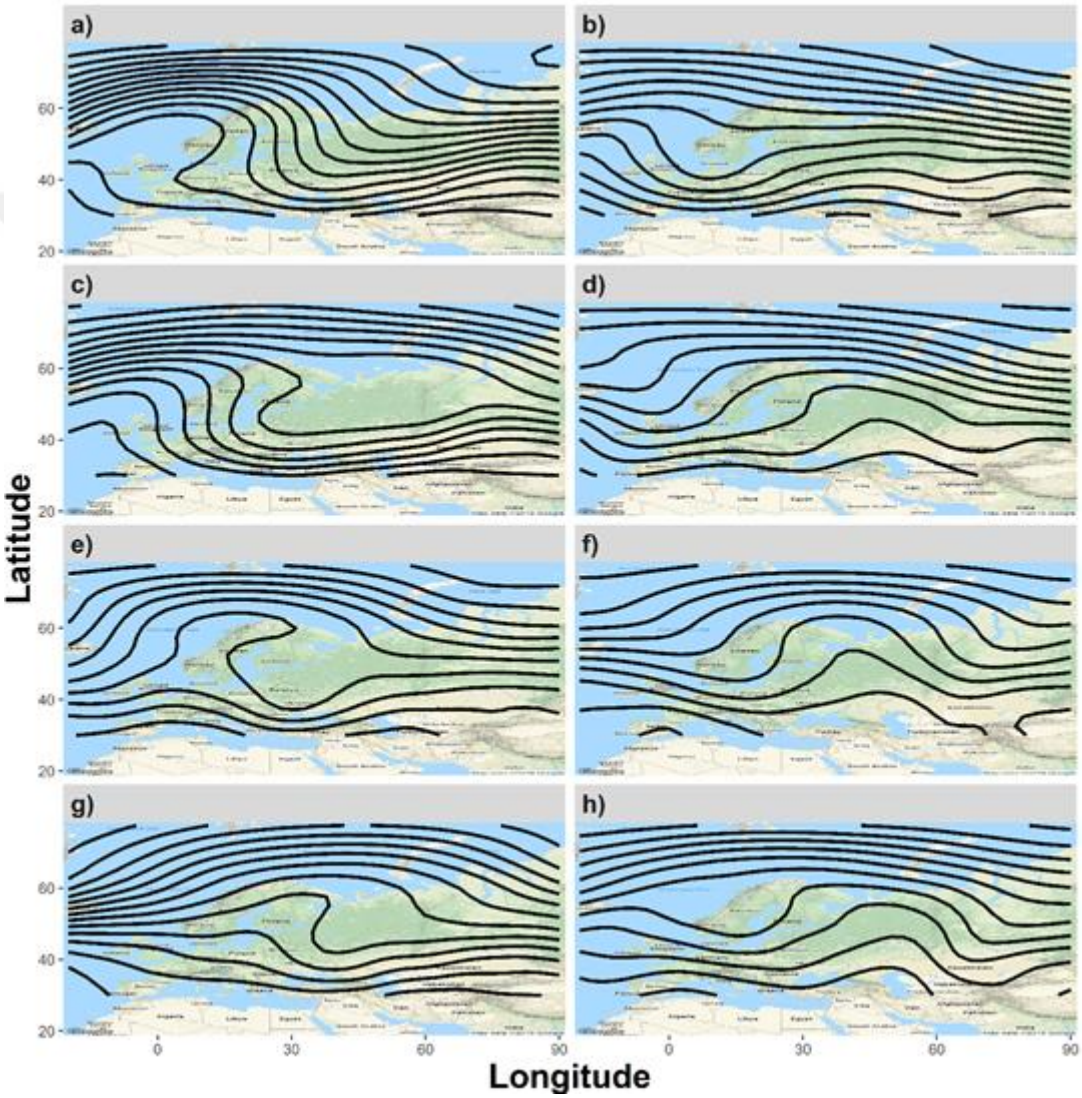

Figure 4.2 : The average 500 hPa value during (a) 10 coldest winter, (b) 10 warmest winter, (c) 10 coldest spring, (d) 10 warmest spring, (e) 10 coldest summer, (f) 10 warmest summer, (g) 10 coldest fall ,and (h) 10 warmest fall events.

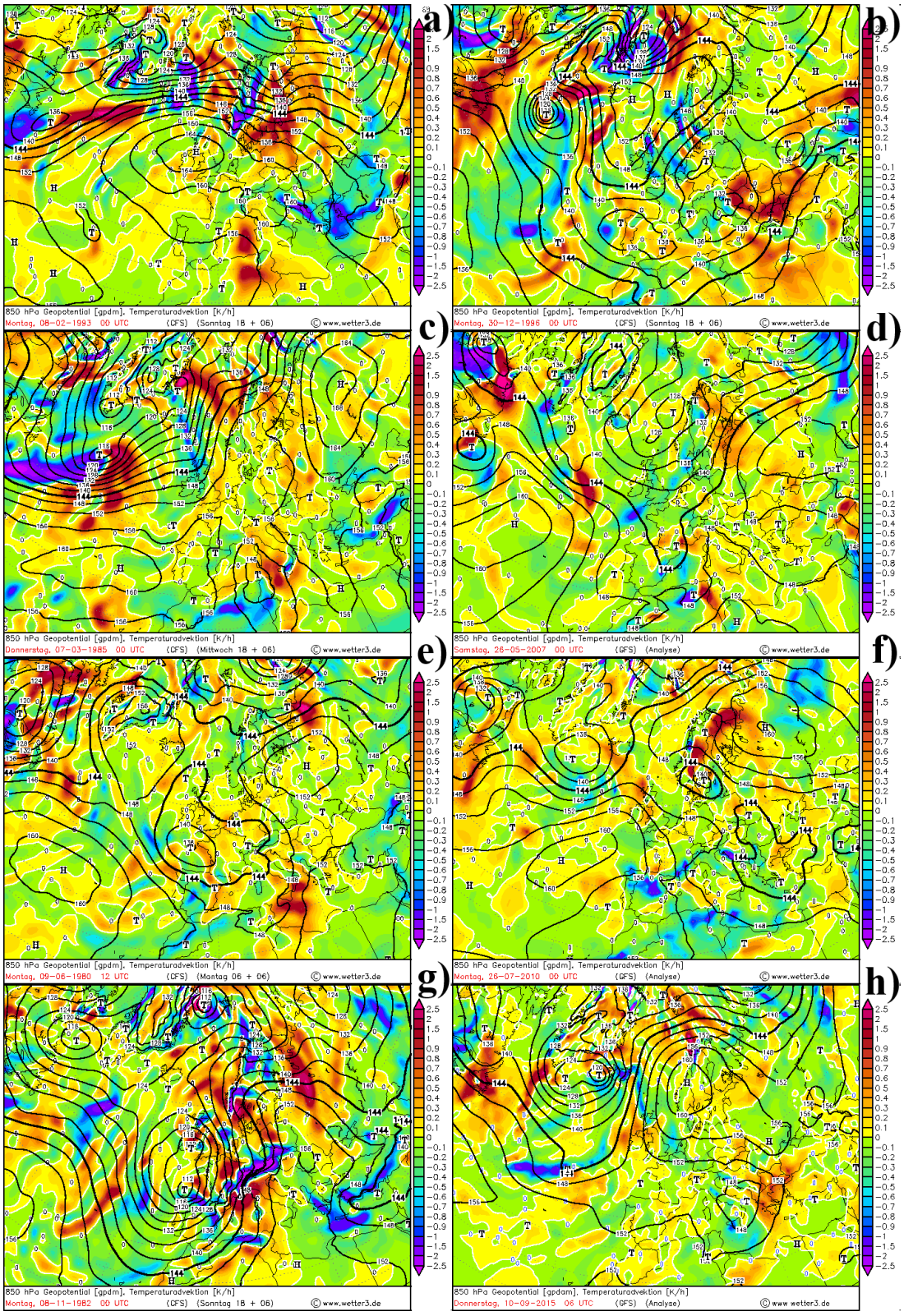

Figure 4.3 : The representative 850 hPa temperature advection for (a) 10 coldest winter, (b) 10 warmest winter, (c) 10 coldest spring, (d) 10 warmest spring, (e) 10 coldest summer, (f) 10 warmest summer, (g) 10 coldest fall, and (h) 10 warmest fall events.

Winter is the season during which negative temperature anomalies are observed across much of the country, while the northwest part of the country is most affected by cold air advection during cold events for all seasons (Figure 4.2 and 4.3). During the spring season, much of the country observes positive temperature anomalies, especially the central and eastern regions. The eastern part of the country experiences the strongest positive anomalies due to warm air advection (Figure 4.2 and Figure 4.3).

4.3 Temperature Anomaly Distribution During Blocked Days Stratified to Seasons

In this section, the average temperature anomaly for stations in certain regions of Turkey during the blocked days is stratified by seasons.

4.3.1 Winter

The mean temperature anomalies during the winter season are shown in Figure 4.4a. The spatial mean anomaly is -0.86^{o} C during the winter season with a standard deviation of 0.48^{o} C. As seen in Figure 4.4a, the whole country has negative anomalies except four cities in the eastern part of the country. Very strong negative temperature anomalies are observed in the north-western part of Turkey and strong negative anomalies are observed in the Marmara region and in some cities of Black Sea Region due to the strength of cold temperature advection during upstream blocking events and the weakness of warm temperature advection during downstream blocking events in this region (Figure 4.3a and b).

In the southeast part of the country, strong positive anomalies are observed in most places and a very strong positive anomaly was observed in only Muş. This situation is due to weak cold air advection in upstream blocking events and strong warm air advection in downstream blocking events (Fig. 4.3a and b). Moderate temperature anomalies were observed in the Central Anatolia Region, Mediterranean Region, Aegean Region and several cities from Black Sea Region due to moderate values of temperature advection during upstream and downstream blocking events.

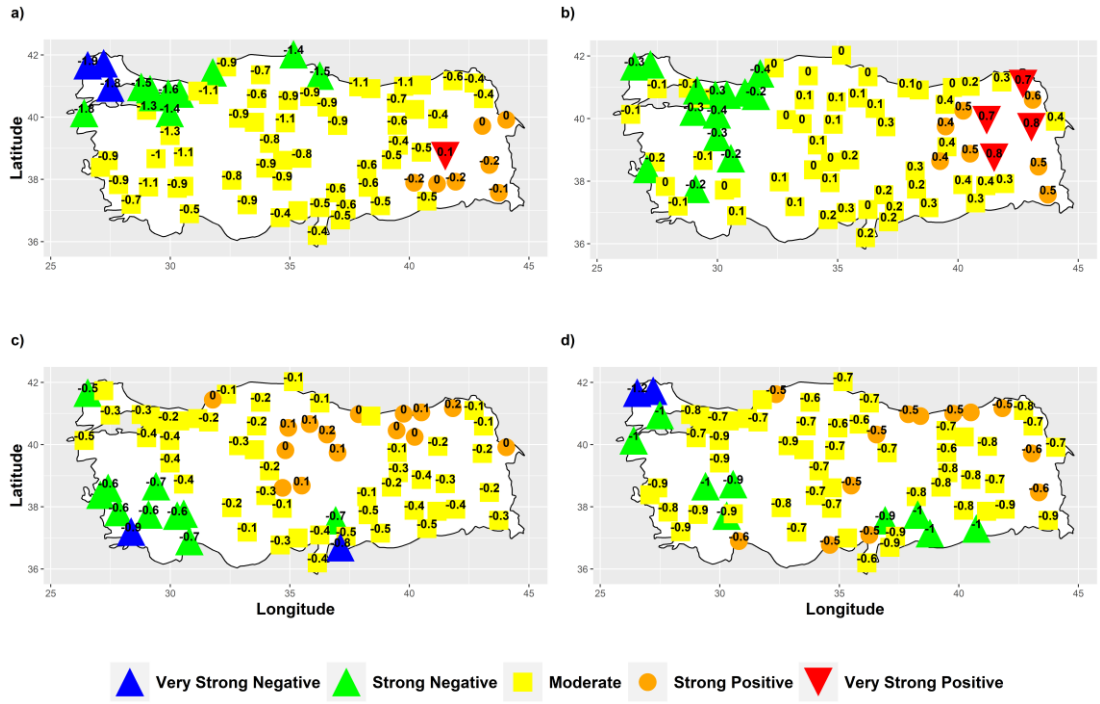

Figure 4.4 : Mean temperature anomalies in stations in (a) winter, (b) spring, (c) summer, and (d) fall during blocked days

4.3.2 Spring

The mean temperature anomalies during the spring season are shown in Figure 4.4b. The spatial average of the seasonal temperature anomaly is 0.11^{o} C with the standard deviation of 0.28^{o} C. During this season, it is shown that the western portion of the country has strong negative and moderate anomalies, the central region has moderate anomalies, and the eastern part has the moderate, strong positive and very strong positive anomalies. Similarly, the western area is strongly affected by cold air advection, the eastern region is strongly affected by warm air advection, and the central area is moderately affected by both advection types (Figure 4.3c and d). No very strong negative anomalies are observed during this season (Figure 4.4b) likely because the cold air advection in this season is not strong as the cold air advection the winter (Figure 4.3c). In detail, the continental region of northwest Anatolia, the eastern region of the Marmara Region, the western part of the Black Sea Region, and several of the stations in the Aegean Region have strong negative temperature anomalies. The remaining stations in the Marmara and Aegean Region have moderate anomalies. Almost the entire Central Anatolia Region, Black Sea coastline except for the western part, the Mediterranean coastline, and the Southern Anatolian Region have moderate temperature anomalies. Bayburt, Erzincan, Elazığ, Bingöl, Kars, Van and Hakkari

stations from East Anatolian Region has strong positive temperature anomalies. Lastly, Ardahan, Ağrı, Erzurum, and Muş have very strong positive anomalies.

4.3.3 Summer

The spatial average of temperature anomalies within Turkey during the summer season is -0.27^{o} C and the standard deviation is 0.24^{o} C (Figure 4.4c). The summer season temperature anomalies in Turkey did not show any district pattern. Only Muğla station from the Aegean Region and Kilis from the Southeast Anatolia Region have very strong negative anomalies due to the location of both of cities on the downstream flank of the ridge during cold air advection (Figure 4.2e and 4.3e). The southwest part of the country, Edirne from the Marmara Region, and Kahramanmaraş from the Mediterranean Region have strong negative temperature anomalies during the summer (Figure 4.4c). Similarly, these stations are located on the downstream flank of the ridge during cold air advection (Figure 4.2e and 4.3e).

The eastern cities of the Central Anatolia Region, several cities east of the Black Sea Region, Zonguldak from west Black Sea Region, and Iğdır from East Anatolia Region have strong positive temperature anomalies (Figure 4.4c). These regions are not typically exposed to cold temperature advection during upstream blocking events but are impacted by warm advection during downstream blocking events (Figure 4.2e, f, and 4.3 e,f). The rest of the country has moderate temperature anomalies, and very strong positive anomalies are not observed in any station.

4.3.4 Fall

The fall season temperature anomalies are negative throughout nearly the entire country. The spatial average of the anomaly is -0.75^{o} C, with 0.16^{o} C standard deviation. The distribution of temperature anomalies during the fall is complex (Figure 4.4d), and there is no prominent or coherent pattern. Edirne and Kırklareli have very strong negative temperature anomalies. The southwest part of the Marmara Region, the southeast Aegean Region, and the east of the South East Region have strong negative temperature anomalies. These regions are located on the downstream flank of the ridge during the cold blocking events and weakly affected from the warm temperature advection during downstream blocking events (Figure 4.3g and h).

Antalya, Mersin, Osmaniye from the Mediterranean Region, Kayseri from the Central Anatolia Region, Bartın from west of the Black Sea Region, east of the Black Sea Region and Ağrı, Van from the East Anatolia Region have strong positive temperature anomalies. These regions are located within the area where the height contours are zonally aligned during the cold events and more often affected by warm air advection during upstream blocking events (Figure 4.2 h and g). The rest of the country has moderate anomalies, while none of the stations observed very strong positive anomalies.

4.4 Relationship Between Blocking Parameters and Temperature Anomaly

Here the Pearson correlation coefficients are calculated and tested using the t-test in order to establish a statistical relationship. Additionally, we chose 28 representative situations and investigated the relationship between blocking parameters and temperature anomalies in order to test for pseudo-replication. However, this test did not significantly alter the conclusions below.

4.4.1 Blocking intensity vs. temperature anomaly

The relationship between BI and temperature anomaly is shown in Figure 4.5. The CC ranges between -0.31 and -0.18. The fall has a value of -0.31, the winter and summer have a value of -0.27 and the spring has a value of -0.18. As inferred from the CC values, there is a negative relationship between mean BI and mean temperature anomalies during blocking events during every season, in other words, stronger blocking events are associated with cooler surface temperatures. All these results are statistically significant at the 95% confidence level except during spring.

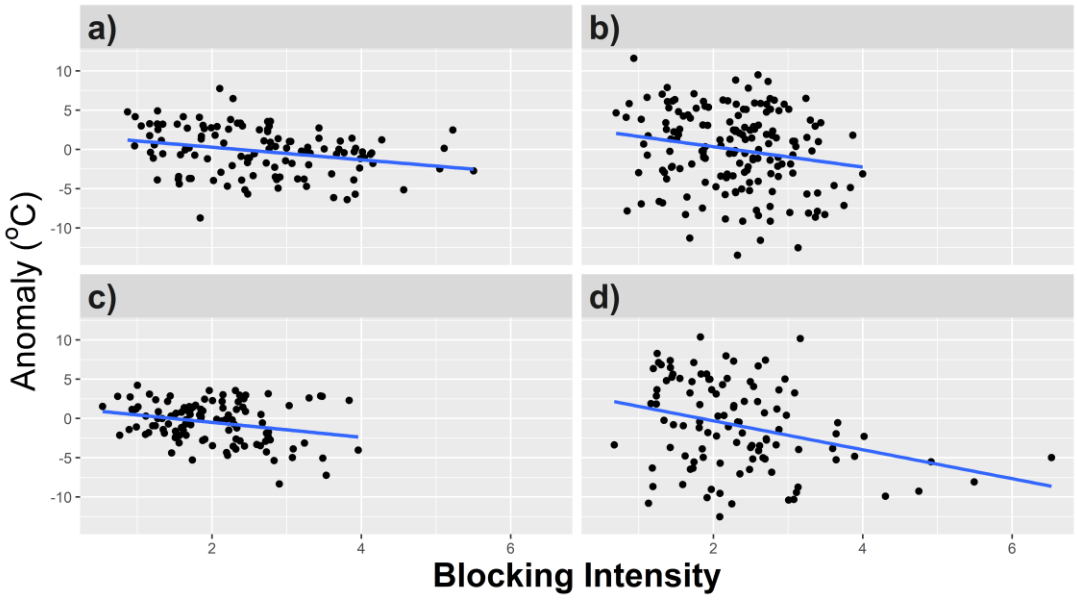

Figure 4.5 : The relation between blocking intensity and mean temperature anomaly during (a) winter, (b) spring, (c) summer, and (d) fall

4.4.2 Blocking duration vs. temperature anomaly

As seen in Figure 4.6, the CC varies between the -0.31 and 0.12. Only the winter season has a negative CC with the value of -0.31. This result indicates a negative relationship between mean blocking duration and mean temperature anomaly during blocking events in the winter. In the other seasons, there is no statistically significant relationship between blocking duration and the temperature anomalies. In the winter season, more persistent blocking events indicate colder temperatures (Figure 4.2). WI02 found a significant correlation between block duration and BI, especially in the winter. Thus, these results are consistent with WI02 and the BI results here. The colder anomalies are associated with stronger more persistent blocks located upstream of Turkey.

4.4.3 The longitudinal extent of blocking vs. temperature anomaly

The CC between the mean longitudinal extent of blocking and the mean temperature anomaly stratified to seasons varies between -0.24 and -0.10 (Figure 4.7). The winter and spring seasons were associated with values of -0.24 and -0.23, respectively, that means there is a relationship between the longitudinal extent of blocking and temperature anomaly. Larger blocks are associated with colder anomalies and stronger blocks are associated also with colder anomalies. LS95 found a relationship between larger blocks and stronger blocks, especially in the Atlantic region. The summer and

fall seasons were associated with correlation values of -0.10 and -0.14 that means there is no relationship between the longitudinal extent and temperature anomaly. The CCs are statistically significant at the 95% confidence level in all seasons

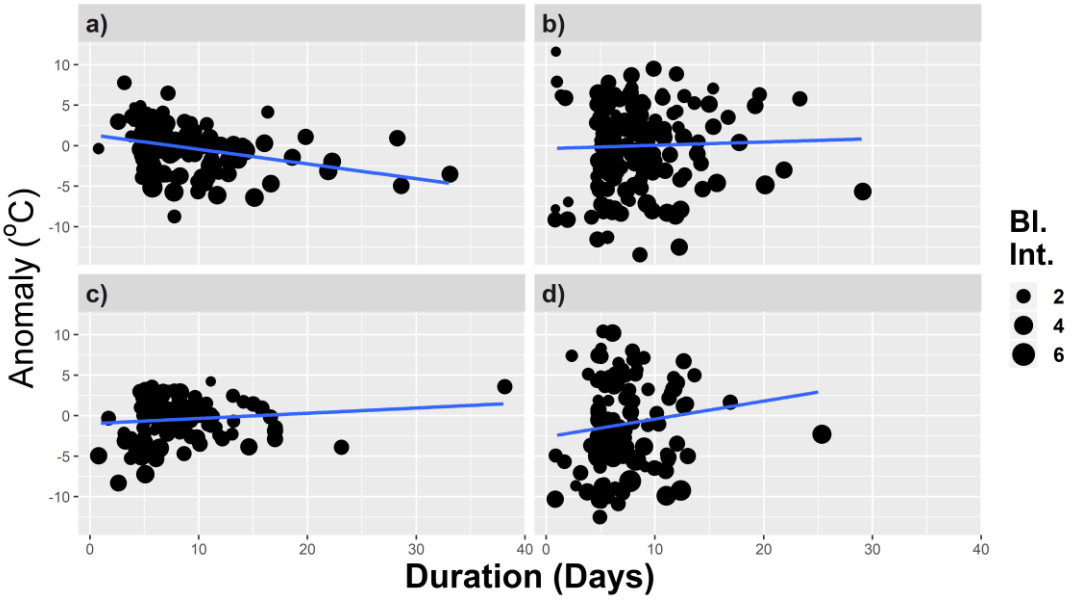

Figure 4.6 : The relation between blocking duration and mean temperature anomaly during (a) winter, (b) spring, (c) summer, and (d) fall. The size of the points indicates the different blocking intensity values.

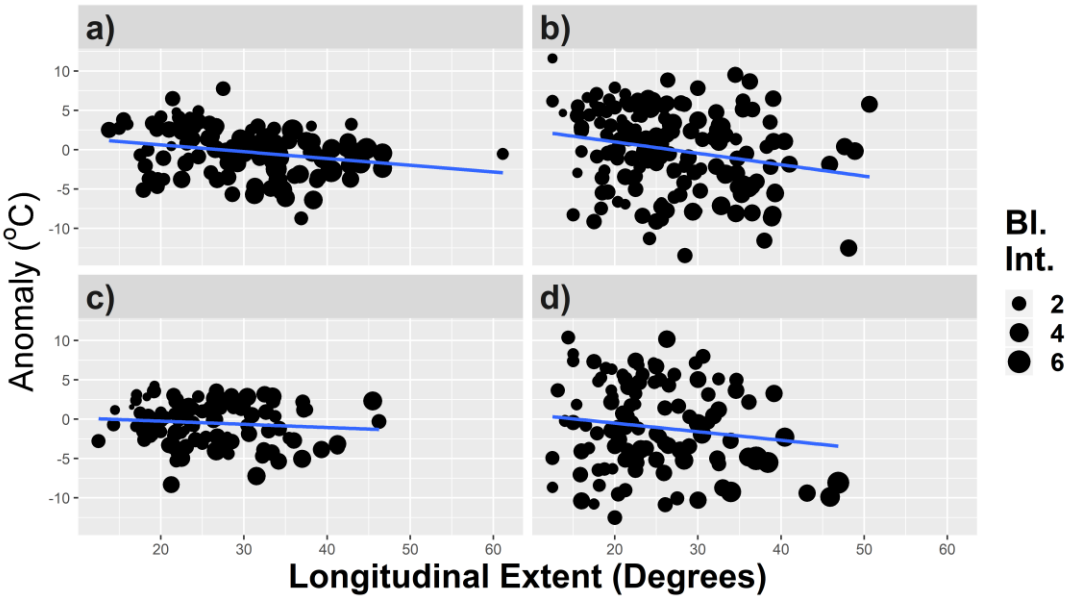

Figure 4.7 : The relation between blocking longitudinal extent in a number of longitudes and mean temperature anomaly during (a) winter, (b) spring, (c) summer, and (d) fall. The size of the points indicates the different blocking intensity values.

4.5 500 hPa Conditions During Strongest Temperature Anomalies

In this section, the average 500 hPa geopotential height conditions for two case studies representing the maximum and minimum temperature anomalies were examined.

4.5.1 Maximum positive anomaly

The average temperature anomaly for the region of Turkey during 8 – 13 September 2015 is 10.4^{o} C. The average geopotential height at 500 hPa level during this period are shown in Figure 4.8a. As seen in Figure 4.8a, there was a dipole blocking (Rex-type blocking) event centered at approximately 65^{o} N and 10^{o} E. The accompanying low center is located around 53^{o} N and 15^{o} E. Turkey is located in the southeastern part of the low-pressure center. Thus, there is warm air temperature advection carrying in the air from the Mediterranean and Sahara region west of Turkey. This blocking event dominated the weather of early September 2015 over Europe as well, and the BI for this event was 3.56; a value typical for the fall season over the Atlantic Region (see University of Missouri Blocking Archive: http://weather.missouri.edu/gcc). The result was generally cooler than normal conditions for northwest Europe and warmer than normal conditions over central and Eastern Europe, including Turkey (Weather Log, 2015).

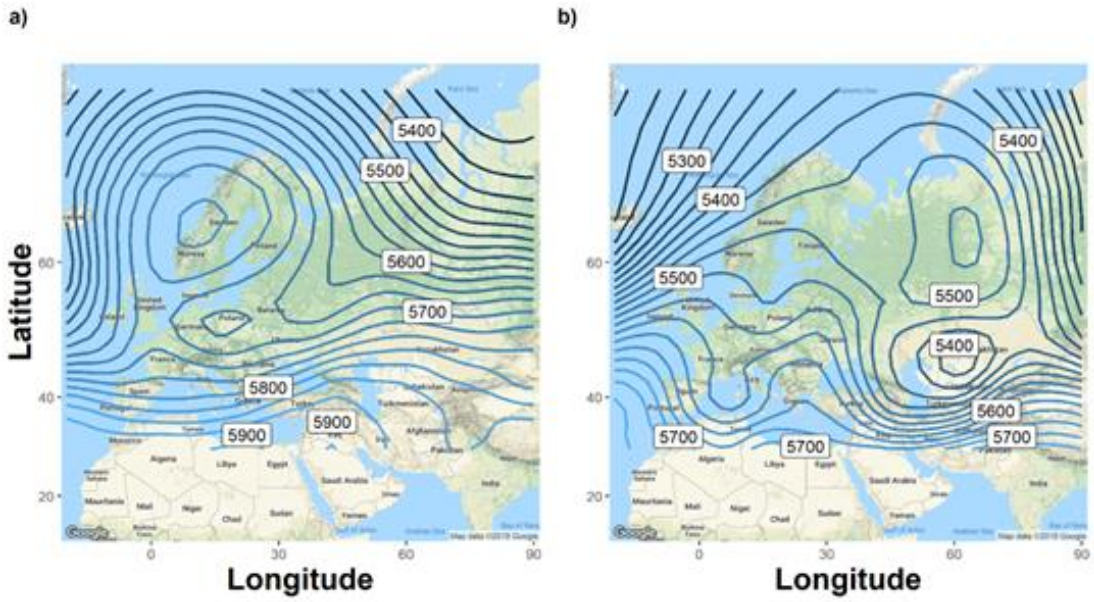

Figure 4.8 : The average 500 hPa geopotential height for the period of (a) 8 – 13 September 2015 (the blocking event with greatest temperature anomaly), and (b) 3 – 11 March 1985 (the blocking event with lowest temperature anomaly).

4.5.2 Maximum negative anomaly

The average 500-hPa geopotential heights during the period 3 – 11 March 1985 are shown in Figure 4.8b. During this period, the average temperature anomaly for Turkey was -13.7^{o} C. As seen in Figure 4.8b, the blocking event was located northeast of Turkey. The block center was located at approximately 60^{o} N and 60^{o} E. Similarly, this event is a Rex-type blocking event. The low center is located around 45^{o} N and 60^{o} E. During this period, cold air originating from the North Atlantic and possibly also from Russia was transported into Turkey. This blocking event was tilted positively (from southwest to northeast) and, thus, colder air was drawn from the polar regions directly towards the study region implying less modification of the surface airmass. This is consistent with Luo et al. (2015) and Yao et al. (2016), who demonstrated that the tilt of the blocking axis was important for impacting regional weather. The BI for this blocking event was also typical of the region and season and persisted for much of the first part of March 1985 (University of Missouri Blocking Archive). This event contributed likely to cooler than normal temperatures for this month and was noted by Radcliffe (1985).

5. PRECIPITATION

5.1 Annual Mean Precipitation Frequency Distribution

5.1.1 Annual MPF distribution during blocked days

Mean precipitation frequency (MPF) across Turkey during blocked days is shown in Figure 5.1. The MPF across Turkey for the study period during blocked days varies between 0.15 and 0.43. The highest precipitation frequencies were observed along the Black Sea coastline and the northeastern part of the Marmara Region during blocked events. The lowest MPF were observed in southern Turkey, especially along Mediterranean coastline and several cities in South Anatolia Region during blocked. Rize, Giresun, and Ordu are the cities that have the highest precipitation frequencies with values of 0.43, 0.39 and 0.36 during blocked days, respectively. Mersin, Karaman, and Osmaniye are the cities that have the lowest precipitation frequencies with the value of 0.15, 0.16 and 0.16 during blocked days, respectively.

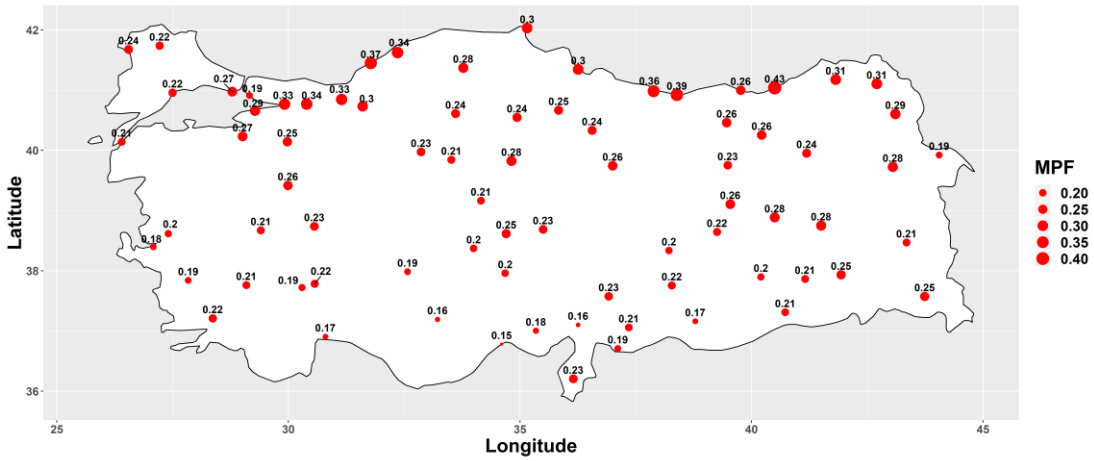

Figure 5.1 : MPF distribution during blocked days.

5.1.2 Annual MPF distribution for non-blocked days

The MPF across Turkey during non – blocked days is shown in Figure 5.2. The MPF across Turkey for the study period during non - blocked days varies between 0.12 and 0.38. The highest MPF values were observed along the Black Sea coastline and the

northeastern part of the Marmara Region during non-blocked events. The lowest MPF values were observed in southern Turkey, especially along Mediterranean coastline and several cities in South Anatolia Region during non-blocked days. Rize, Giresun, and Ordu are the cities that have the highest MPF with values of 0.38, 0.32 and 0.29 during non – blocked days, respectively. Osmaniye, Mersin, and Karaman are the cities that have the lowest MPF with the value of 0.12, 0.13 and 0.13 during non-blocked days, respectively.

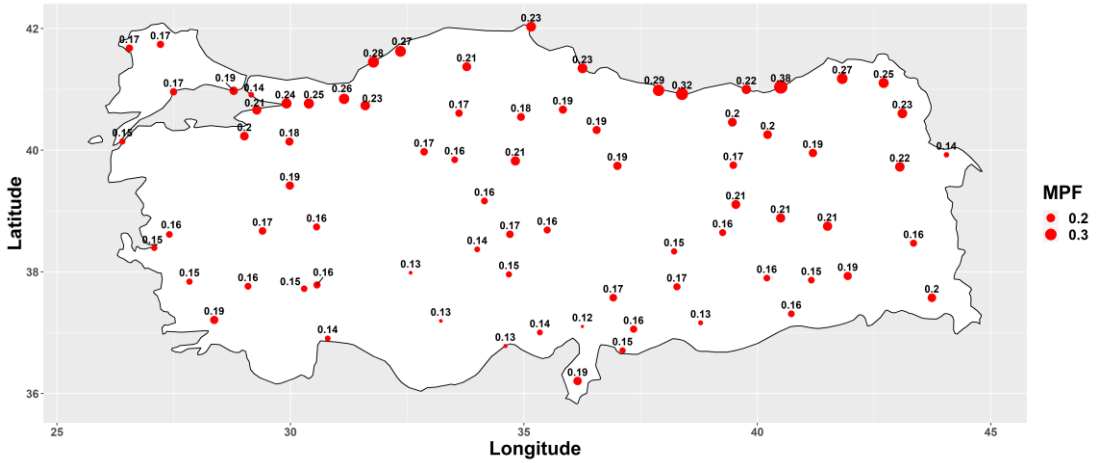

Figure 5.2 : MPF distribution during non – blocked days.

5.1.3 MPF change during blocked days with respect to non-blocked days

The ratio of MPF during blocked days with respect to non – blocked days is shown in Figure 5.3. Blocking events increase the MPF across the entire country. This increase in precipitation frequency ranges from 12% to 42% across Turkey. The inner part of Anatolia observed the higher ratio of MPF values whereas the western Black Sea region was associated with the lowest values. Konya, Kırklareli, and Çanakkale are the stations that have the highest MPF change with values of 48%, 42%, and 41%, respectively. Rize, Artvin, and Giresun have lowest MPF change with the values of 13%, 14%, and 18%, respectively. Thus, overall, blocking has an enhancing effect on the MPF across Turkey.

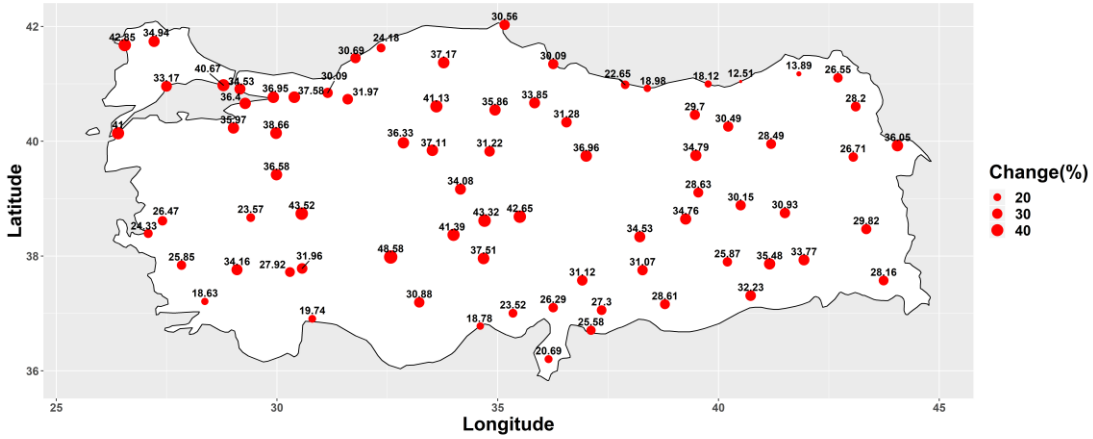

Figure 5.3 : Change in MPF (%) during blocked days with respect to non-blocked days.

5.2 Seasonal MPF Distribution

5.2.1 MPF distribution during blocked days

5.2.1.1 Winter

MPF during blocked days in all seasons is shown in Figure 5.4. During blocked days, the winter season has the highest MPF across the country with an average value of 0.31 (Figure 5.4a). During blocked days, the stations have MPF values in the range of 0.15 and 0.54. For blocked days, the inner part of Marmara Region, coastal parts of Black Sea Region and southwest part of East Anatolia Region have higher MPF values. During blocked days, Zonguldak, Rize, and Kocaeli have the highest MPF with the values of 0.54, 0.48 and 0.48, respectively. During blocked days, the vast majority of the inner part of Aegean Region, Central Anatolia Region, and Mediterranean Region have lower values. For blocked days, Iğdır, Osmaniye, and Erzincan have the lowest MPF with the values of 0.15, 0.19 and 0.21, respectively.

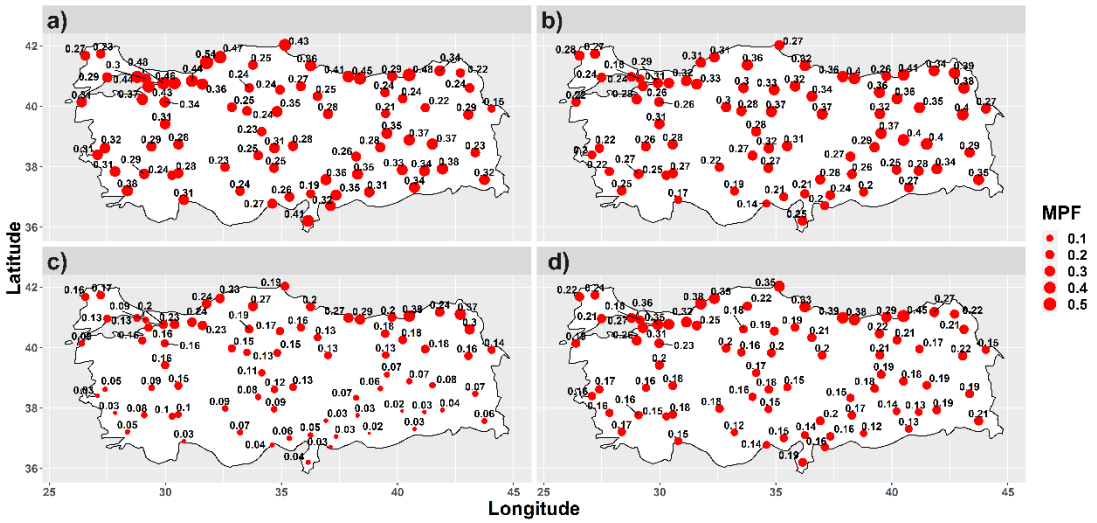

Figure 5.4 : MPF distribution during blocked days in (a) winter, (b) spring, (c) summer, and (d) fall.

5.2.1.2 Spring

During blocked days, the spring season observed an MPF of 0.29 across Turkey, with a minimum value of 0.13 and the maximum at 0.41 (Figure 5.4b). For blocked days, a large portion of East Anatolian Region and Black Sea Region have greater values. During blocked days, Rize, Giresun, and Muş have the highest MPF with the values of 0.41, 0.40 and 0.40, respectively. For blocked days, the coastal region of Aegean and Mediterranean Regions and west of the South East Anatolia Regions have the lower values of MPF. For blocked days, Mersin, Antalya, and Kartal are the stations with the lowest values of 0.14, 0.17 and 0.18, respectively.

5.2.1.3 Summer

Summer is the driest season across Turkey and MPF decreases sharply even on blocked days. During blocked days, MPF ranges between a value of 0.02 and a maximum value of 0.38 with a mean of 0.13 (Figure 5.4c). For blocked days, the cities in the northern part of the country, particularly along the Black Sea coastline, have higher MPF. For blocked days, Rize, Ardahan, and Kars have the highest MPF with the values of 0.38, 0.37 and 0.30, respectively. During blocked days, the Southeast Anatolia Region, south of East Anatolia Region, coastal line of the Mediterranean and Aegean Sea have lower MPF. For blocked days, Şanlıurfa, Diyarbakır, and Antalya have the lowest MPF values of 0.02, 0.02 and 0.03, respectively.

5.2.1.4 Fall

Lastly, during fall season blocked days**,** MPF fluctuates between 0.12 and 0.45 with the national average at 0.21 (Figure 5.4d). During blocked days, the coastal region of Black Sea Region and the eastern part of Marmara Region have higher values. For blocked days, Rize, Ordu, and Zonguldak have the highest MPF with values of 0.45, 0.39 and 0.38, respectively. During blocked days, the Southeast Anatolia Region and Mediterranean Region have lower values of MPF. For blocked days, Şanlıurfa, Karaman, and Mardin have the lowest MPF values of 0.12, 0.12 and 0.13, respectively.

5.2.2 MPF distribution during non – blocked days

5.2.2.1 Winter

MPF during non – blocked days in all seasons is shown in Figure 5.5. During non-blocked days, the winter season has the highest MPF across the country with an average value of 0.26 (Figure 5.5a). During non-blocked days, the stations have MPF values in the range of 0.10 and 0.40. For non-blocked days, the west part of the Marmara Region, the Black Sea coastline and southwest part of East Anatolia Region have higher MPF values. During non-blocked days, Zonguldak, Bartın, and Rize have the highest MPF with the values of 0.40, 0.39 and 0.39, respectively. During non-blocked days, Central Anatolia Region, northeast part of East Anatolia Region and the inner part of Aegean Region have lower values. For non-blocked days, Iğdır, Ardahan, and Erzurum have the lowest MPF with the values of 0.10, 0.16 and 0.16, respectively.

5.2.2.2 Spring

During non-blocked days, the spring season observed an MPF of 0.24 across Turkey, with a minimum value of 0.14 and the maximum at 0.36 (Figure 5.5b). For non-blocked days, the East Anatolia Region and east part of Black Sea Region have greater values. During non-blocked days, Rize, Giresun, and Ağrı have the highest MPF with the values of 0.36, 0.35 and 0.35, respectively. For non-blocked days, the European part of Marmara Region, the coastline of the Aegean and the Mediterranean Sea have the lower values of MPF. For non-blocked days, Mersin, Kartal, and Antalya are the stations with the lowest values of 0.13, 0.14 and 0.14, respectively.

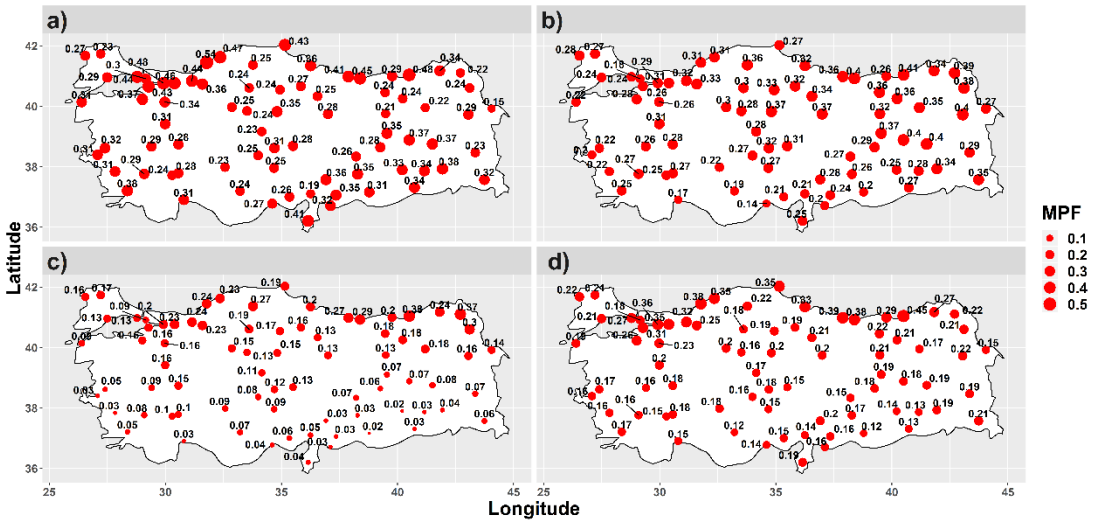

Figure 5.5 : MPF distribution during non-blocked days in (a) winter, (b) spring, (c) summer, and (d) fall.

5.2.2.3 Summer

Summer is the driest season across Turkey and MPF decreases sharply similar to the blocked days. During non-blocked days, MPF ranges between a value of 0.01 and a maximum value of 0.36 with a mean of 0.09 (Figure 5.5c). For non-blocked days, the Black Sea coastline, the northern part of East Anatolia Region and east of Marmara Region have higher MPF. For non-blocked days, Rize, Kars, and Ardahan have the highest MPF with the values of 0.36, 0.31 and 0.27, respectively. During non-blocked days, the Southeast Anatolia Region, the southern part of East Anatolia Region and coastline of both Aegean and the Mediterranean Sea have lower MPF. For non-blocked days, Kilis, Şanlıurfa and Mardin have the lowest MPF values of 0.01.

5.2.2.4 Fall

Lastly, during fall season non-blocked days, MPF fluctuates between 0.10 and 0.40 with the national average at 0.16 (Figure 5.5d). During non-blocked days, the northern regions have higher values. For non-blocked days, Rize, Giresun, and Ordu have the highest MPF with values of 0.40, 0.35 and 0.32, respectively. During non-blocked days, the southern regions have lower values of MPF. For non-blocked days, Şanlıurfa, Karaman, and Mardin have the lowest MPF values of 0.10.

5.2.3 MPF change during blocked days with respect to non-blocked days

In this part, the change of MPF during blocked days with respect to non-blocked days are investigated (Figure 5.6). The change of MPF in blocked days during all seasons are positive. Thus, we can conclude that blocking causes an increase in the frequency of rainy days.

5.2.3.1 Winter

In winter, the average change in MPF is 19%, with a minimum value of 1% and a maximum of 50% (Figure 5.6a). The higher changes occurred in the northeast part of the country (37% and higher), the southern part of Central Anatolia Region (28% and higher) and eastern part of the Marmara Region (31% and higher). Iğdır, Florya, and Ardahan observed the greatest changes with values of 50%, 39%, and 38%, respectively. The Aegean coastline (7% and lower), Mediterranean coastline (8% and lower), some cities in the northern part of the Central Anatolia Region (8% and lower) and the vast majority of Southeast Anatolia Region (18% and lower) observed lower changes. Kırklareli (1%), Adana (2%) and Osmaniye (2%) are the cities that observed the lowest changes.

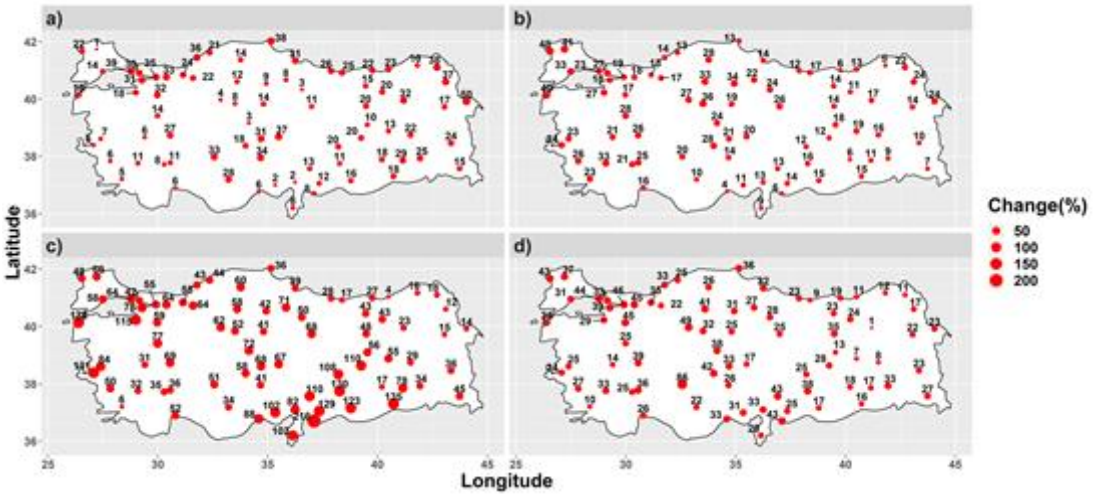

Figure 5.6 : Change in MPF (%) during blocked days with respect to non-blocked days during (a) winter, (b) spring, (c) summer, and (d) fall.

5.2.3.2 Spring

During the spring season, the minimum, mean and maximum of changes in MPF are 4%, 19% and 48%, respectively (Figure 5.6b). The Thracian part of the Marmara Region and several cities in the northern part of the Central Anatolia Region observed

greater changes (higher than 33% and 27%, respectively). Edirne, Kırklareli, and Çanakkale are all located in the Thracian part of the Marmara Region and observed the highest changes (48%, 41%, and 40%, respectively). The southern part of the East Anatolia Region, the South East Anatolia Region and the eastern part of the Mediterranean Region observed the lower changes (lower than 10%, 16%, and 13%, respectively). Artvin, Kilis, and Trabzon observed the lowest change values at 5%, 6%, and 6%, respectively.

5.2.3.3 Summer

During the summer season, the change in the MPF on the stations fluctuated between 4% and 216% with a mean of 60% (Figure 5.6c). This greater value of change in the summer is due to lower MPF during non-blocked days and blocked days. For example, the Kilis station has an MPF of approximately 0.01 during non-blocked days and 0.03 during blocked days, thus, the change is 216%. The southern part of the East Anatolia Region and the eastern part of the Mediterranean Region have higher changes (78% and 82% or higher, respectively). Kilis, Çanakkale, and Mardin observed the greatest changes with 216%, 135%, and 135%, respectively. The northeast part of the country observed lower changes (23% and lower). Rize, Muğla, and Kars observed the lowest changes (4%, 6%, and 12%, respectively).

5.2.3.4 Fall

During the fall season, the mean MPF changes were 28% nationwide with a minimum of 1% and a maximum of 86% (Figure 5.6d). The northeast part of the Central Anatolia Region, the Marmara Region and the cities in the neighborhood of the Mediterranean and the South East Anatolia Region have higher changes (32%, 37%, and 31% or higher, respectively). Konya, Ankara, and Kocaeli have the greatest changes with 86%, 49%, and 46%, respectively. The eastern part of East Anatolia Region, the eastern of the Black Sea coastline have smaller changes (23% or lower for both regions). Erzurum, Bingöl, and Muş have the lowest changes (1%, 7%, and 8%, respectively).

5.3 The Relationship Between Blocking Parameters and MPF

5.3.1 Blocking center vs. MPF

In this sub-section, the relationship between blocking center and MPF is investigated (Figure 5.7). The MPF ranges between 0.15 and 0.38 with an average of 0.25 when the block center is located in S1 (Figure 5.7a). The Black Sea coastline observes greater values while the southern part of the Central Anatolia Region and Mediterranean Region observes lower values. Rize (0.38), Zonguldak (0.35) and Giresun (0.31) have the highest values when the blocking center is located in S1. On the other hand, Mersin (0.15), Konya (0.17) and Iğdır (0.17) have the lowest values.

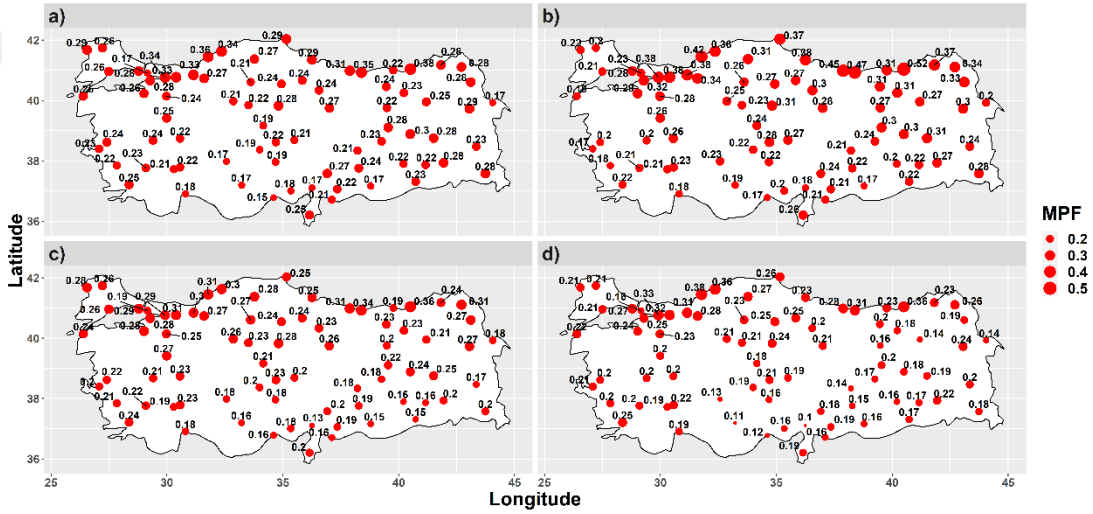

Figure 5.7 : MPF distribution for (a) S1, (b) S2, (c) S3 E and (d) S4

When the block center is located in S2, the minimum, mean and maximum MPF values are 0.17, 0.27 and 0.51, respectively (Figure 5.7b). The Black Sea coastline, the northeastern of the country have greater MPF values, while the Mediterranean Region, South East Anatolia Region, and Aegean Sea coastline have lower values. Rize, Giresun, and Ordu are the cities with the greatest MPF values (0.52, 0.47 and 0.45, respectively). Mersin, Şanlıurfa, and İzmir have the lowest MPF with a value of 0.17.

For S3, the MPF values vary between 0.13 and 0.36 with a mean value of 0.22 (Figure 5.7c). Generally, the MPF values are related to the latitudinal position of the stations when blocking center is located in the third sector. Northern stations, for example, Rize, Giresun, and Zonguldak have the greatest values, 0.36, 0.34 and 0.31, respectively. Southern stations, for example, Osmaniye (0.13), Şanlıurfa (0.15) and Mardin (0.15) are the stations with lowest values.

Lastly, for S4, the nationwide, the minimum, mean and maximum MPF values are 0.10, 0.21 and 0.38 respectively (Figure 5.7d). The eastern part of the Marmara Region and the western part of the Black Sea Region observe the highest MPF values whilst the Mediterranean Region and the South Anatolia Region observe the lowest values. Zonguldak (0.38), Rize (0.36) and Bartın (0.36) have the greatest MPF values, while Osmaniye (0.10), Karaman (0.11) and Mersin (0.12) have the lowest values.

5.3.2 Blocking intensity vs. MPF

The relationship between blocking intensity and MPF stratified to the seasons is shown in Figure 5.9. During the winter, the CC between blocking intensity and MPF is 0.18 and is NSS (Figure 5.9a). In spring, the CC is 0.10 and is NSS, also (Figure 5.9b). During summer, the data set has a weak positive relationship (CC = 0.35, statistically significant at a 95% confidence level) (Figure 5.9c). Lastly, during the fall season, data has statistically significant (at 95% confidence level) positive relationship (CC = 0.43) (Figure 5.9d).

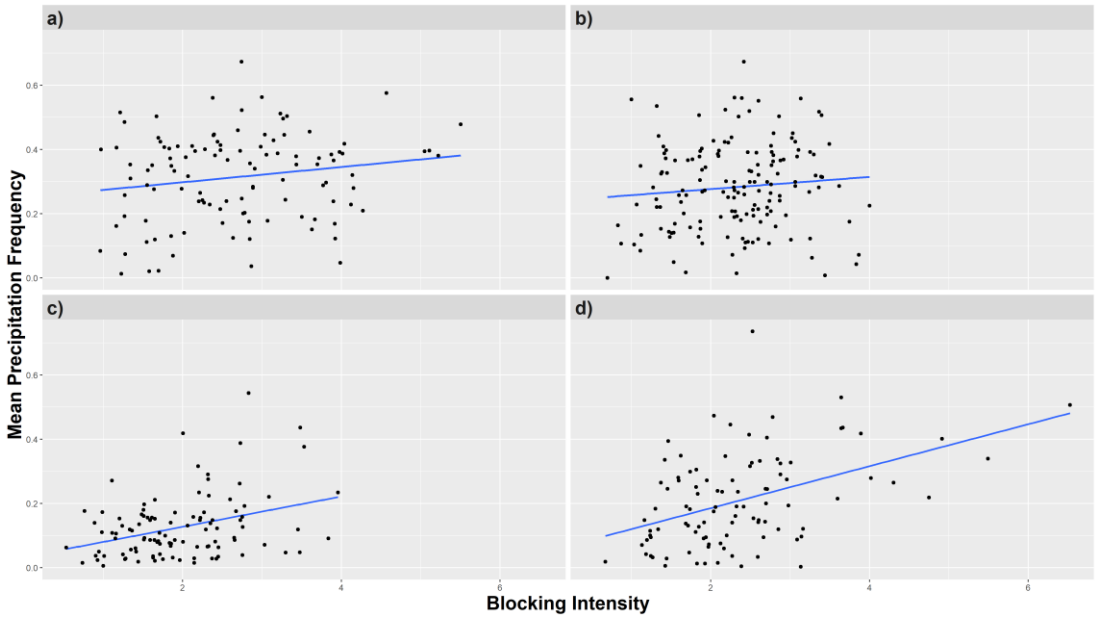

Figure 5.8 : The relationship between BI and MPF for (a) winter, (b) spring, (c) summer, and (d) fall.

5.3.3 Blocking duration vs. MPF

The relationship between blocking duration and MPF stratified to the seasons is shown in Figure 5.10. There is almost no relationship between blocking duration and MPF in all seasons. During the winter season, the CC is -0.01 (Figure 5.10a). During the

spring, there is a very weak relationship (CC = 0.10, NSS) between block duration and MPF for the data set (Figure 5.10b). During the summer, the data set has a CC of 0.03 (Figure 5.10c). Lastly, during the fall season, the CC is 0.02 for the entire data set (Figure 5.10d).

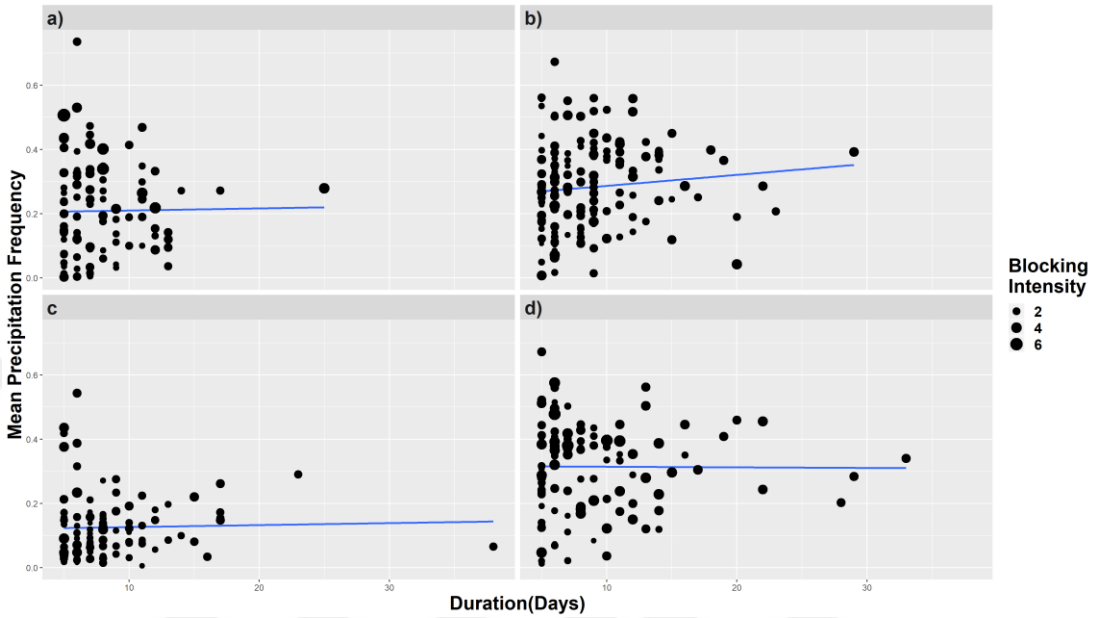

Figure 5.9 : The relationship between blocking duration and MPF for (a) winter, (b) spring, (c) summer and (d) fall.

5.3.4 Blocking longitudinal extent vs. MPF

The relationship between the longitudinal extent of blocking and MPF stratified to the season is shown in Figure 5.11. There is a positive relationship (CC = 0.15, NSS) during the winter (Figure 5.11a). In the spring, there is a weak relationship (CC = 0.26, statistically significant at the 95% level) for the data (Figure 5.11b). During summer, the CC is 0.29 (statistically significant at 95% level) (Figure 5.11c). Lastly, fall has a CC of 0.25 (statistically significant at the 95% level) (Figure 5.11d).

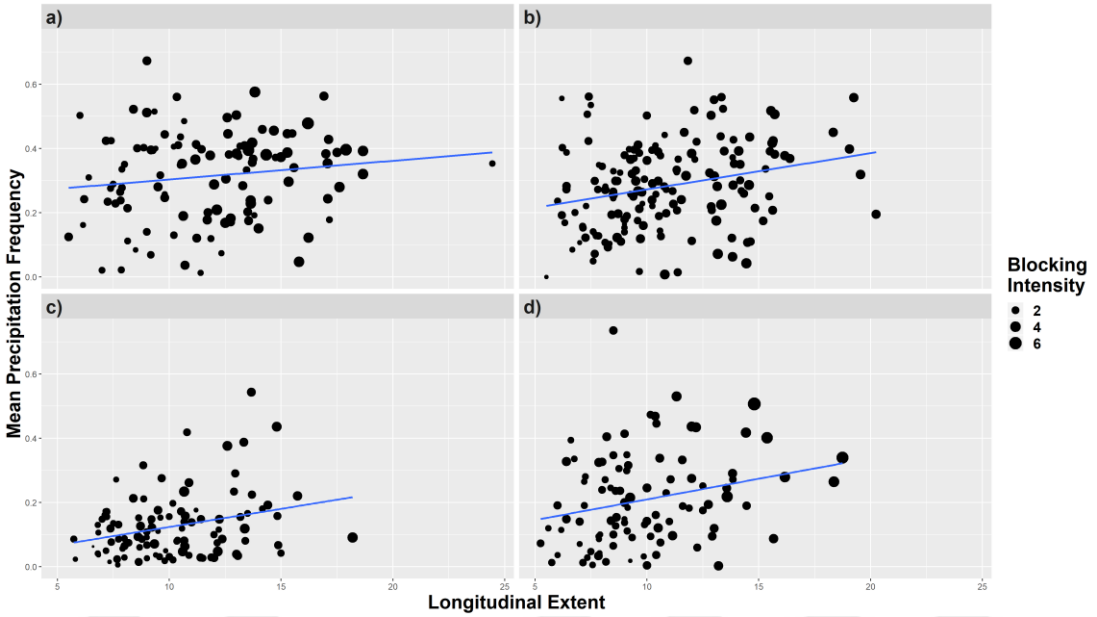

Figure 5.10 : The relationship between blocking longitudinal extent and MPF for (a) winter, (b) spring, (c) summer, and (d) fall.

5.4 500 hPa Conditions for the 10 Lowest / Highest MPF

The average 500 hPa geopotential height conditions during the 10 blocking events that have the lowest and the highest MPF values stratified by the season is shown in Figure 5.12. The dates for these events are shown in Table 5.1. The block center is located near 15^{o} E and 60^{o} N during the winter season for those events with higher MPF (Figure 5.12a). The mean BI during these events is 2.81. According to the 850 hPa charts, there was considerable water vapor advection from the Mediterranean Sea during the events that have the greatest MPF. The representative 850 hPa map is shown in (Figure 5.13a). The mean BI for the events with the lowest MPF values during the winter is 1.87 and the mean center position is located close to 20^{o} E and 60^{o} N (Figure 5.12b). Here, water vapor transport is in a different direction. In the representative 850 hPa map, the specific humidity is transported from the Balkans to Turkey (Figure 5.13b).

During the spring season, the highest MPF blocking events have a mean block center position near 20^{o} E and 60^{o} N (Figure 5.12c). The mean BI is 2.23 during these events. According to the 850 hPa charts, there was considerable water vapor advection from the Mediterranean Sea during the events that have the greatest MPF (Figure 5.13c). The BI during the lowest blocking events is 2.25 with the center location near 23^{o} E and 55^{o} N (Figure 5.12d). In the representative 850 hPa chart, the air masses are

transported from locales that have similar specific humidity to Turkey for the driest blocking events (Figure 5.13d)

Table 5.1 : The dates for the 10 wettest and driest blocking events.

		Dry		Wet	
Season	**No**	**Start**	**End**	**Season**	**No**
Winter	1	1984-02-23	1984-02-27	1991-12-01	1991-12-13
Winter	2	1984-12-01	1984-12-05	1994-12-01	1994-12-05
Winter	3	1987-01-11	1987-01-24	1998-12-08	1998-12-12
Winter	4	1989-01-24	1989-02-01	2001-11-30	2001-12-04
Winter	5	1992-01-11	1992-01-17	2001-12-07	2001-12-19
Winter	6	1998-01-16	1998-01-20	2002-01-04	2002-01-09
Winter	7	2005-12-10	2005-12-15	2009-02-19	2009-02-24
Winter	8	2006-02-21	2006-02-26	2009-12-12	2009-12-18
Winter	9	2008-01-18	2008-01-24	2011-01-27	2011-02-01
Winter	10	2011-01-15	2011-01-23	2014-12-29	2015-01-02
Spring	1	1980-05-31	1980-06-04	1977-03-16	1977-03-20
Spring	2	1985-03-03	1985-03-13	1987-03-06	1987-03-16
Spring	3	1986-03-09	1986-03-17	1987-04-12	1987-04-16
Spring	4	1986-03-19	1986-03-28	1988-04-17	1988-04-21
Spring	5	1986-04-23	1986-04-28	1996-02-29	1996-03-05
Spring	6	1989-04-02	1989-04-06	1998-05-13	1998-05-19
Spring	7	1993-02-25	1993-03-01	1999-03-29	1999-04-03
Spring	8	1994-04-14	1994-04-18	2001-05-04	2001-05-12
Spring	9	1997-03-08	1997-03-13	2002-03-23	2002-03-31
Spring	10	2004-04-09	2004-04-13	2002-04-03	2002-04-10
Summer	1	1977-07-06	1977-07-11	1979-06-01	1979-06-05
Summer	2	1987-07-13	1987-07-17	1982-06-01	1982-06-05
Summer	3	1987-07-19	1987-07-23	1984-05-31	1984-06-04
Summer	4	1991-07-28	1991-08-03	1988-06-16	1988-06-21
Summer	5	1995-07-29	1995-08-03	1992-06-01	1992-06-21
Summer	6	2000-07-12	2000-07-19	1995-05-31	1995-06-04
Summer	7	2004-07-20	2004-07-24	1997-06-07	1997-06-12
Summer	8	2005-07-09	2005-07-13	2010-06-23	2010-06-27
Summer	9	2006-08-04	2006-08-14	2011-05-31	2011-06-04
Summer	10	2008-07-19	2008-07-24	2014-06-02	2014-06-07
Fall	1	1981-08-28	1981-09-02	1979-10-24	1979-10-25
Fall	2	1986-11-17	1986-11-23	1985-10-14	1985-10-19
Fall	3	1988-09-14	1988-09-20	1989-11-09	1989-11-19
Fall	4	1994-09-18	1994-09-22	1993-11-10	1993-11-16
Fall	5	2000-11-06	2000-11-11	1996-10-23	1996-10-28
Fall	6	2001-09-14	2001-09-22	1997-11-17	1997-11-23
Fall	7	2008-11-01	2008-11-07	1998-11-29	1998-12-05
Fall	8	2010-11-18	2010-11-22	2005-10-15	2005-10-19
Fall	9	2013-09-06	2013-09-11	2006-10-13	2006-10-17
Fall	10	2016-11-20	2016-11-24	2009-10-31	2009-11-05

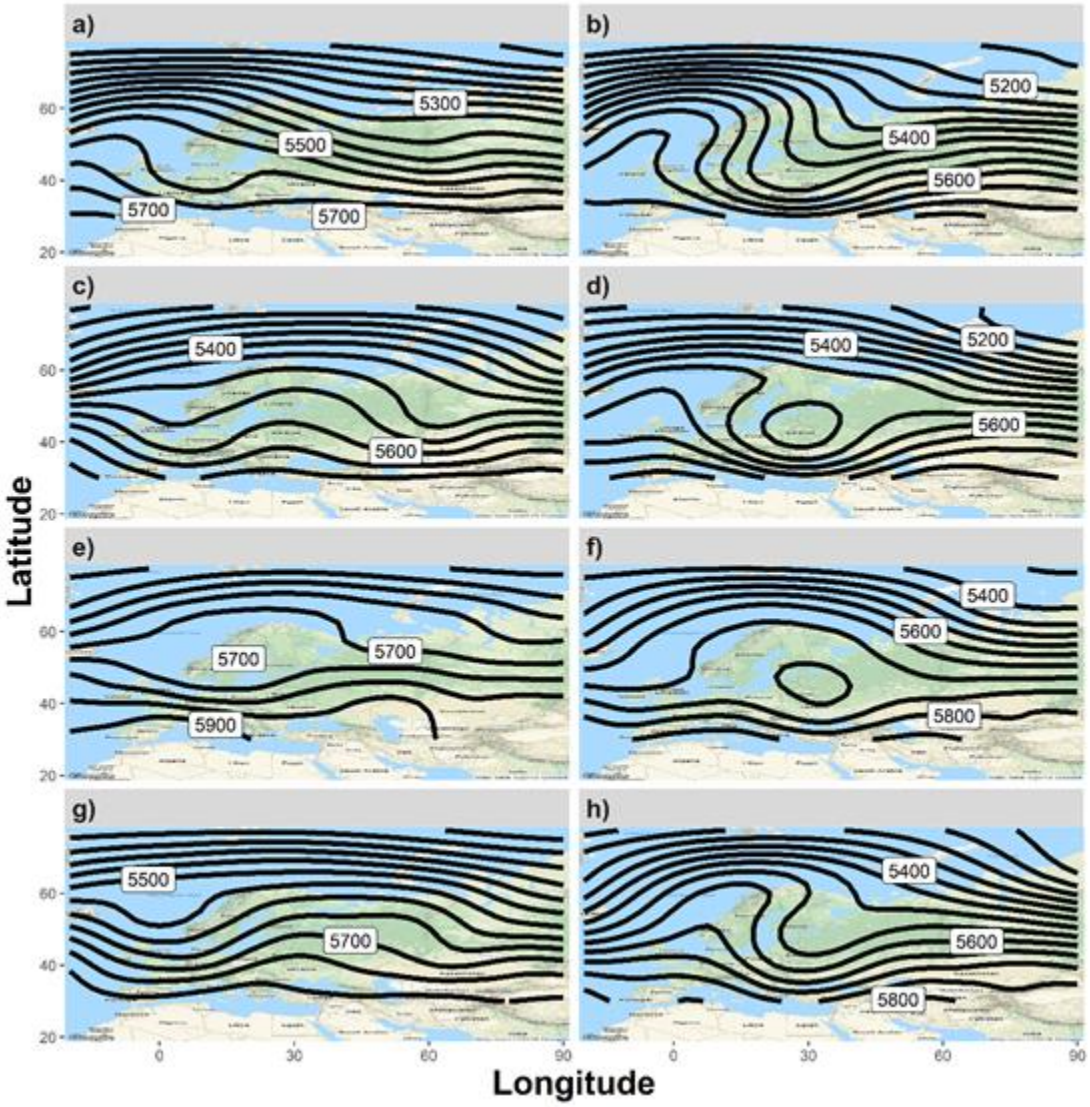

Figure 5.11 : The composite map of 500 hPa geopotential height data (m) of the 10 driest (lowest MPF) and wettest (highest MPF) events for the: (a) and (b) winter, (c) and (d) spring, (e) and (f) summer, and (g) and (h) fall season.

During the summer season, the highest events have a mean BI value of 2.34 and the blocking center is located near 35^{o} E and 65^{o} N (Figure 5.12e). According to the 850 hPa charts, there was considerable water vapor advection from the Mediterranean Sea during the events that have the greatest MPF (Figure 5.13e). A jet stream was observed where there were strong pressure gradients over the Mediterranean area (not shown). The mean BI during blocking events with the lowest MPF is 1.65 and the blocking center is located approximately at 35^{o} E and 65^{o} N similar to that of the highest MPF blocking events for this summer (Figure 5.12f). There is weak water vapor advection during dry events or water vapor transport from Turkey. In the representative 850 hPa chart, weak specific humidity advection occurred over the western and northern parts

of the nation while specific humidity transport into Turkey occurred over southeast of the country (Figure 5.13f).

For the fall season, an omega-shaped blocking event is observed in the average 500 hPa geopotential height map. The mean BI is 2.81 and the blocking center is located close to 20^{o} E and 65^{o} N (Figure 5.12g). According to the 850 hPa charts, there was considerable water vapor advection from the Mediterranean Sea region during the events that have the greatest MPF (Figure 5.13g). For the lowest MPF blocking events, the BI and blocking center are 1.87 and 35^{o} E and 60^{o} N, respectively (Figure 5.12h). There is weak water vapor advection during dry events, or there was water vapor transport out of the region of Turkey. In the representative 850 hPa chart, weak specific humidity advection occurred over the western part of the region while specific humidity divergence occurred over the east part of the country (Figure 5.13h).

5.5 Analysis of the Blocking Case with Greatest MPF

The average 500 hPa height for the blocking event that has the greatest MPF is shown in Figure 5.14. The blocking event within the study area occurred between 31 October 2009 and 05 November 2009. The omega-shaped blocking event was centered at approximately 30^{o} E and 65^{o} N. The upper-level downstream trough impacted Turkey during this blocking event and there was moist air advection from southern Europe, across the lifetime of this blocking event. The event was associated with BI, duration and longitudinal extent values of 2.52, 6 days and 20 degrees, respectively. The nationwide MPF was 0.73 and the mean total precipitation was 63.4 mm during this blocking event even though the duration was only six days. During this blocking event, heavy rainfall and flash flood events were observed in the Marmara Region (Gazete Vatan 2009), Şanlıurfa (a city in South Anatolia Region, Takvim 2009), and Trabzon (NTV 2009).

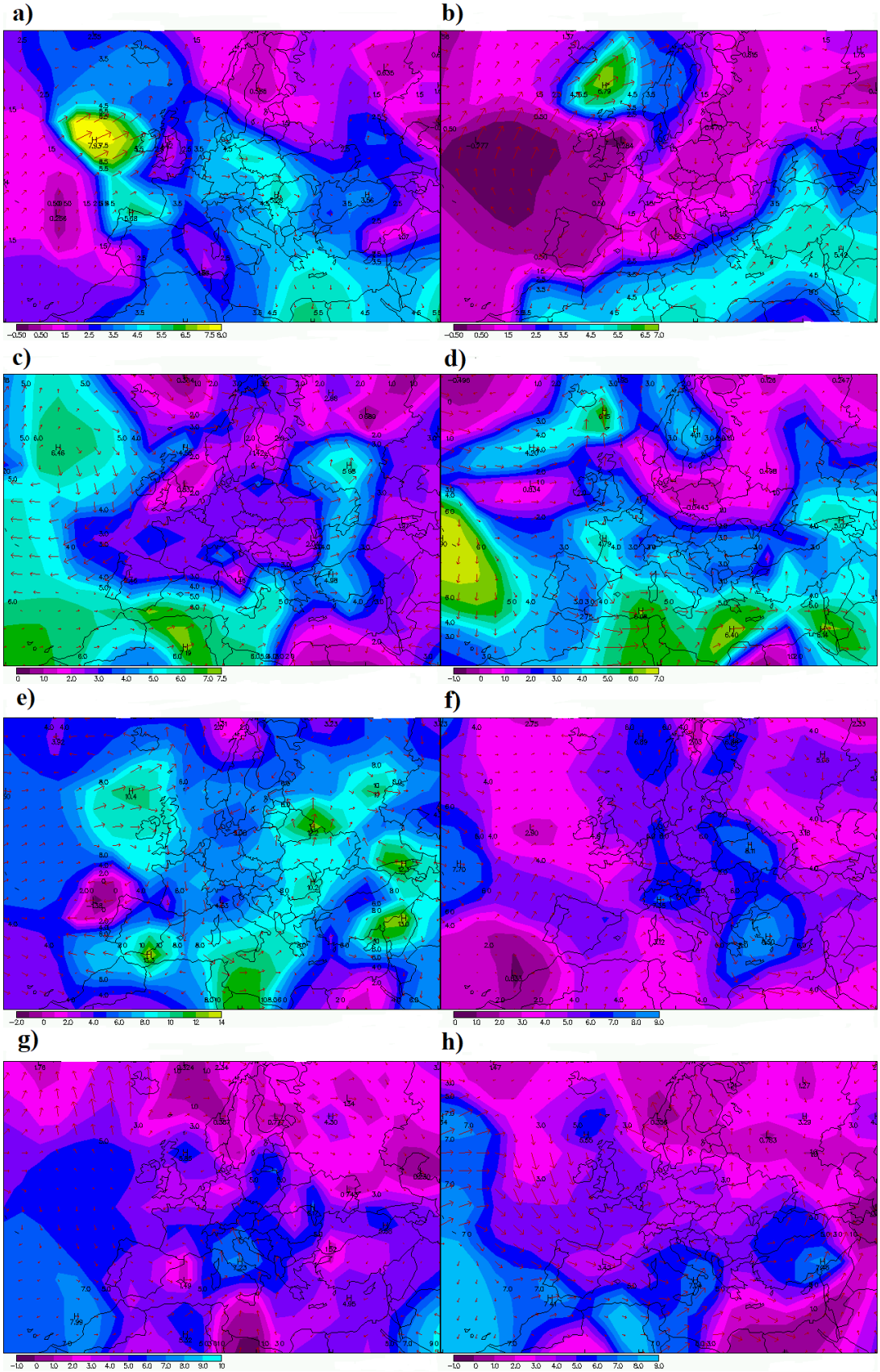

Figure 5.12 : The representative 850 hPa charts for (a) dry winter, (b) wet winter, (c) dry spring, (d) wet spring, (e) dry summer, (f) wet summer, (g) dry fall and (h) wet fall.

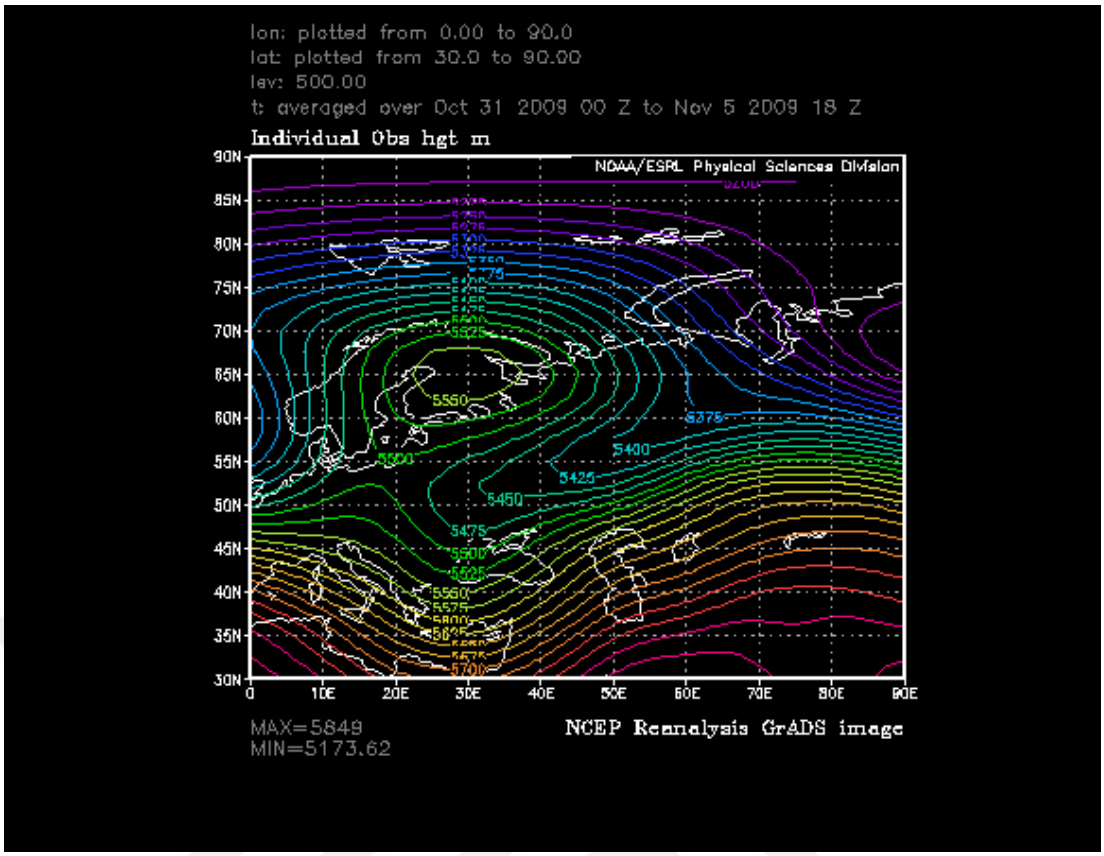

Figure 5.13 : The composite map of 500 hPa geopotential height (m) for 31 October to 5 November 2009 for the blocking event with the greatest MPF.

6. EXTREME TEMPERATURE

6.1 Summer Season

6.1.1 Extreme maximum temperature distribution

6.1.1.1 Tx distribution for all data

The mean Tx distribution during summer is seen in Figure 6.1. The Tx values fluctuate between 0.5 and 1.8 across the country. The most southern part of the country has Tx values lower than 0.6%. The western part of the country and Black Sea coastline have Tx values around 1.0%. The northern part of central Anatolia, the inner part of east Anatolia and some regions in the southern part of the country have Tx values greater than 1.5%. Blocking has an increasing impact on Tx frequency in the summer. The central regions have greater Tx distributions.

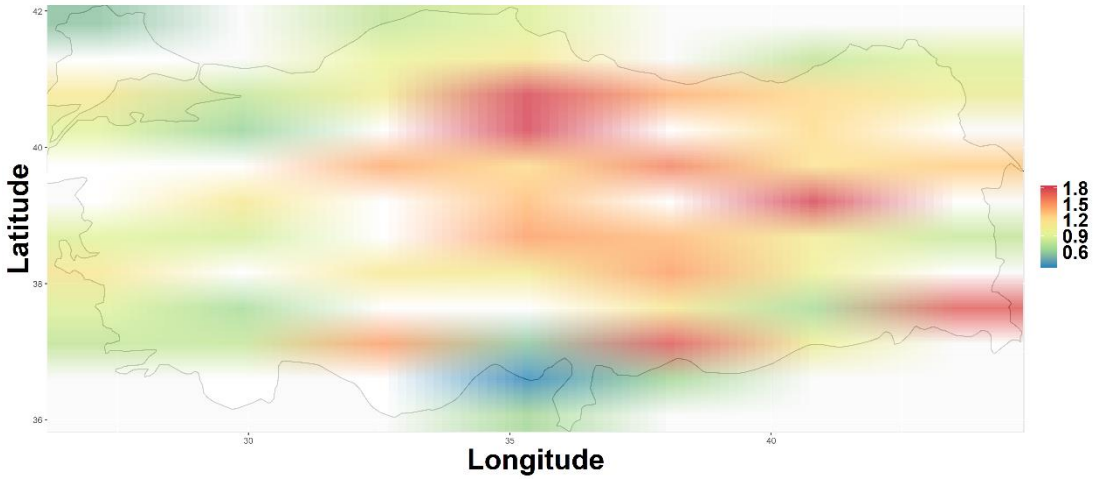

Figure 6.1 : The Tx frequency distribution during blocked days in summer.

6.1.1.2 Tx distribution for blocking center

In this section, the Tx frequency distribution for the block center location during summer is examined. The Tx distribution is seen in Figure 6.2. During the summer season, only one blocking event is located in S1. So, S1 was removed for the summer season results. When the block center is located in S2, the Tx frequency values have a minimum and maximum of 0.0 and 1.8. The eastern part of the country, an area from

the center and the most western part of the country have the greatest Tx frequency values while the rest of the country have values around 0.0% (Figure 6.2a). The Tx frequency values have a range of 0.0 and 2.7% when the block center is located in S3. The area around İzmir has the greatest Tx frequency. Minimum Tx frequency values are observed over a large area in the center, an area in the southeastern part of the country and an area over the most northern part of the country (Figure 6.2b). For S4, the Southeastern Anatolia Region has the greatest mean Tx frequency; approximately 2.0% with the maximum value of 6.4% at Van. Areas in the center of the country and in the northeastern part of the country have a Tx frequency value around 1.2% while the rest of the country has a Tx frequency below 0.5% (Figure 6.2c).

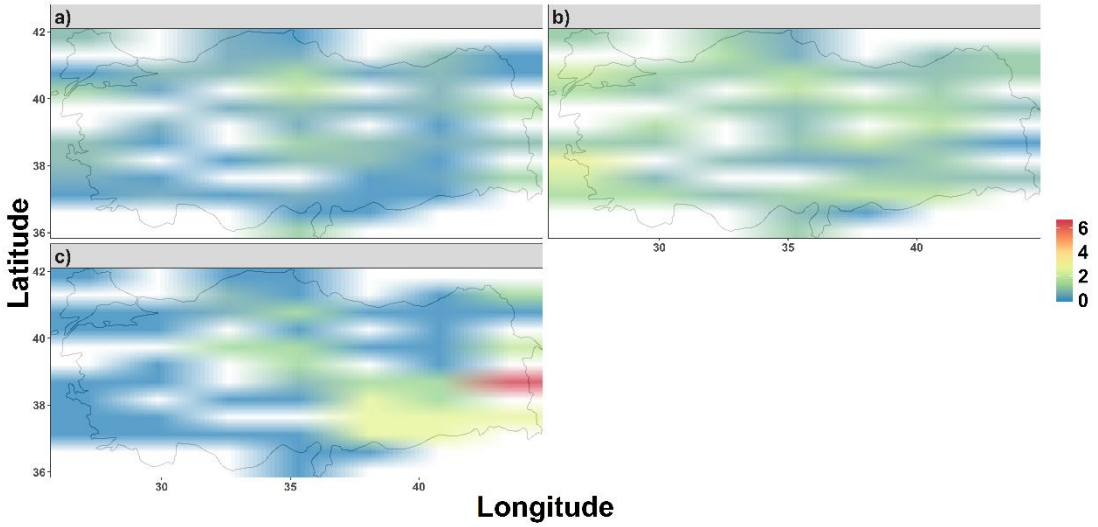

Figure 6.2 : The Tx frequency distribution for (a) S2, (b) S3 and (c) S4 during summer season blocked days.

6.1.1.3 Tx distribution for blocking intensity

The mean Tx frequency distribution stratified by BI during summer is seen in Figure 6.3. The BI is divided into three categories as stated in Chapter 2. However, there was no summer season blocking event classified as strong. The Tx frequency fluctuates between 0.0 and 2.5% for blocking event classified as weak. The area in the Marmara Region, the area around İzmir and the area around Hatay have the greatest Tx frequency values. The inner parts of the Marmara, Ege and Mediterranean Region have Tx values below 0.5% (Figure 6.3a). The minimum mean Tx distribution is 0.0% and the maximum is 2.8% when the block intensity is moderate. The area around Çorum

has the greatest Tx frequency while the areas in the most southern and northern parts of the country have the lowest frequencies (Figure 6.3b).

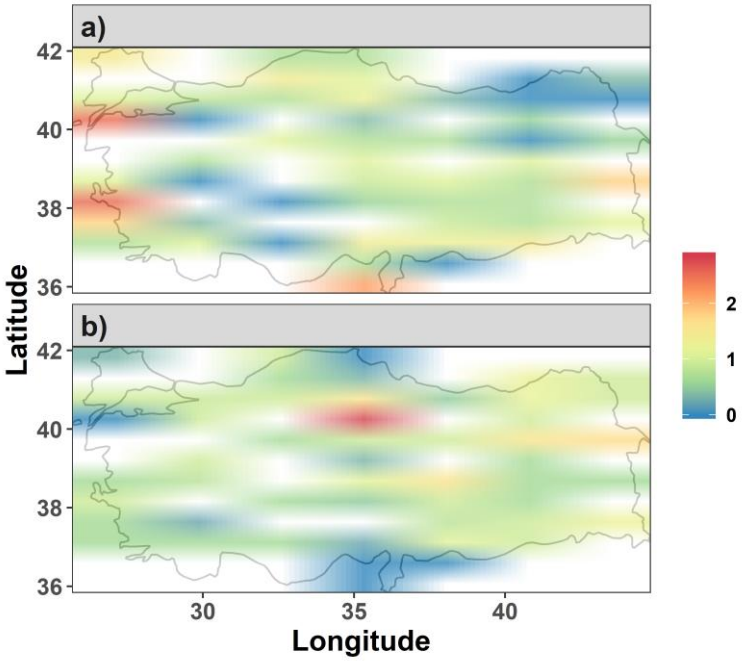

Figure 6.3 : The Tx frequency distribution for (a) weak and (b) moderate BI during blocked days in the summer season.

6.1.1.4 Tx distribution for blocking longitudinal extent

The Tx frequency distribution for different blocking longitudinal extent during the summer is seen in Figure 6.4. The Tx values vary between 0.0% and 3.9% when the blocks have small longitudinal extent. The area in the eastern part of the country has the greatest Tx frequency. The eastern half of the Black Sea coastline, an area in the Marmara Region and an area of the southern Mediterranean have lowest Tx frequencies (Figure 6.4a). When the blocking longitudinal extent is moderate, the minimum of Tx frequency is 0.0 whilst the maximum is 2.8%. The zone from north to the south along the center of the country and an area in the Marmara Region with the maximum around Gaziantep have greatest Tx values. The southernmost part of the country has a minimum Tx value of 0.0% (Figure 6.4b). The Tx frequency has a minimum and maximum of 0.0% and 1.2% respectively, for the blocking events with large longitudinal extent. The eastern Black Sea coastline and part of the East Anatolia Region have the greatest Tx values greater than 1.0%. The rest of the country has values of less than 0.8% of Tx frequency values (Figure 6.4c).

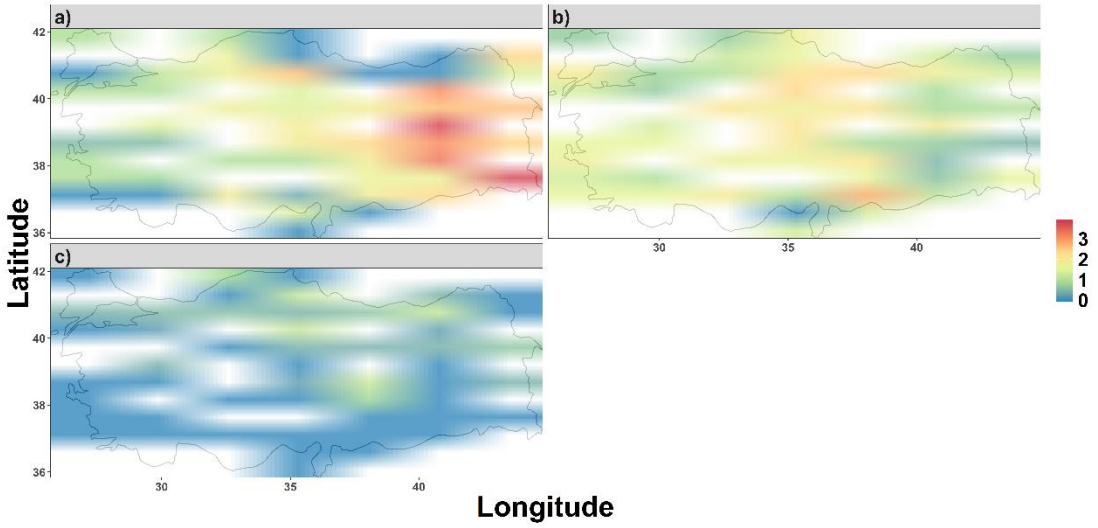

Figure 6.4 : The Tx frequency distribution for (a)small, (b) moderate, and (c) large blocks during blocked days in the summer season stratified by the block size.

6.1.1.5 Tx distribution for blocking duration

The Tx frequency distribution stratified by blocking duration during summer is seen in Figure 6.5. The Tx frequency varies between 0.0% and 2.6% for the short duration blocking events. The vast majority of the country has Tx values around 0.0% for short duration events. An area in the Marmara Region has a maximum Tx frequency of 2.6%. There is a zone from the Black Sea to South East Anatolia passing through Central Anatolia that has a Tx value greater than 1.0%. The Mediterranean Region, the Aegean Region, and a large part of the East Anatolia Region have the Tx value around 0.0% (Figure 6.5a). For the moderate duration blocking events, Tx frequency has a minimum and a maximum of 0.0 and 2.2%, respectively. An area in the northern part of Central Anatolia Region has the maximum Tx frequency values. Areas in the southernmost and northern parts of the country have a minimum Tx of 0.0%. (Figure 6.5b). The minimum Tx frequency is 0.0% and the maximum is 3.5% for the most persistent blocking events. An area in the East Anatolia Region has a maximum of 3.5% whilst the area in the southernmost part of the country has a minimum of 0.0% (Figure 6.5c).

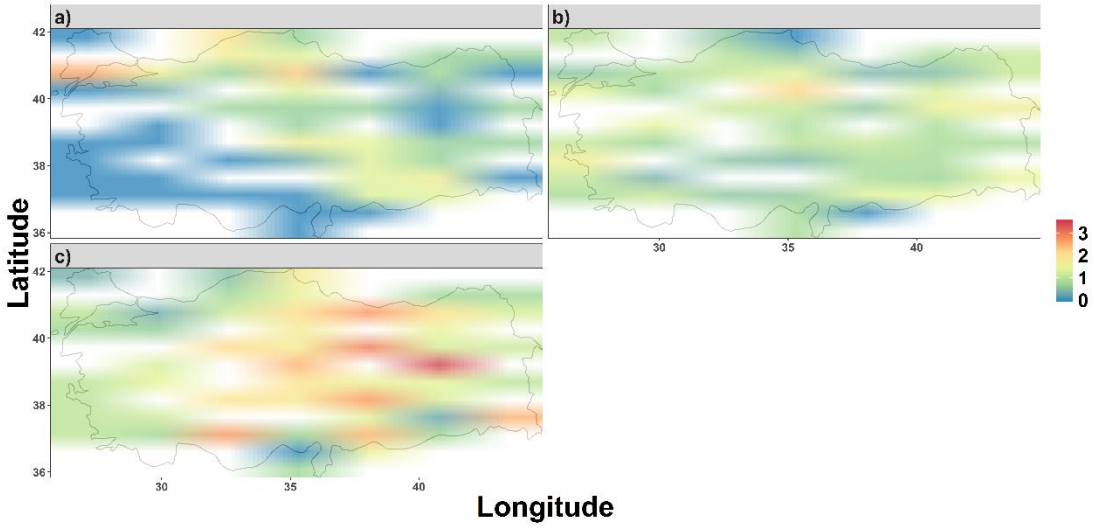

Figure 6.5 : The Tx frequency distribution for (a) short-lived, (b) moderate, and (c) most persistent blocks during blocked days in the summer season.

6.1.2 Extreme minimum temperature

6.1.2.1 Tn distribution for all data

The mean Tn distribution during summer is seen in Figure 6.6. The Tn values fluctuate between 0.4% and 2.0% across the country. The area in the Marmara Region, an area in the Central Anatolia Region and an area in the northwest of the country have Tn values lower than 0.7%. The Center Anatolia, Black Sea Region and the inner parts of all regions have Tn values fluctuates between 0.9% and 1.7%. The Southeast Anatolia Region and areas in the Aegean Region have Tn values greater than 1.5%. Blocking has an increasing impact on Tn frequency in the summer. The outer regions have greater Tn distributions during blocking events.

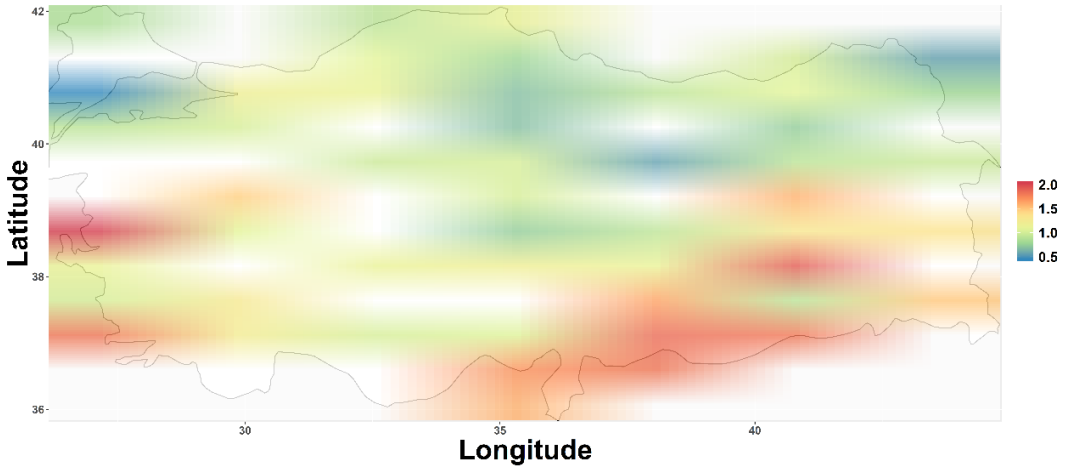

Figure 6.6 : The Tn frequency distribution during blocked days in summer.

6.1.2.2 Tn distribution for blocking center

In this section, the Tn frequency distribution for the block center location during summer is examined. The Tn distribution is seen in Figure 6.7. During the summer season, only one blocking event is located in S1. So, S1 was removed for the summer season results. When the block center is located in S2, the Tn frequency values have a minimum and maximum of 0.0% and 3.3%. The Aegean Region and the Southeast Anatolia Region have the greatest Tn frequency values while an area includes some parts of Black Sea, Marmara, and Aegean Region and the rest of the country have values around 2.0% and below 1.0%, respectively (Figure 6.7a). The Tn frequency values have a range of 0.3% and 2.4% when the block center is located in S3. The belt around 38^{o} N latitude bounded between 37 and 40^{o} E longitudes has the greatest Tn frequency. Minimum Tn frequency values are observed over the area in the northeast Anatolia and an area in the south East Anatolia Region (Figure 6.7b). For S4, several areas (yellow shaded) across the country have the greatest mean Tn frequency; approximately 2.7% with the maximum value of 6.4% over the inner part of the Aegean Region. Several areas (green shaded) across the country have a Tn frequency value around 2.0% while the rest of the country has a Tn frequency below 0.5% (Figure 6.7c).

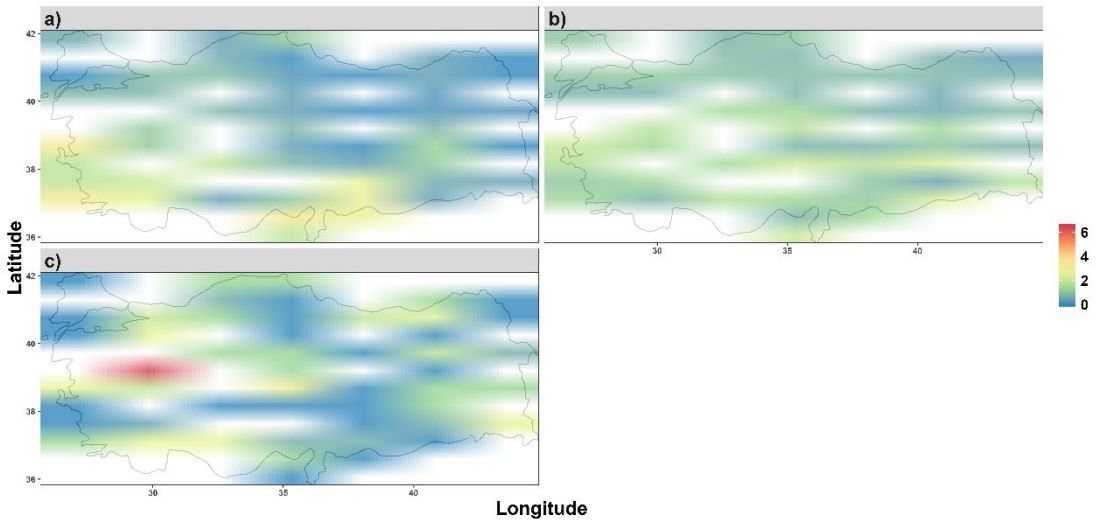

Figure 6.7 : The Tn frequency distribution for (a) S2, (b) S3 and (c) S4 during summer season blocked days.

6.1.2.3 Tn distribution for blocking intensity

The mean Tn frequency distribution stratified by BI during summer is seen in Figure 6.8. The BI is divided into three categories as stated in Chapter 2. However, there was no summer season blocking events classified as strong. The Tn frequency fluctuates between 0.0% and 1.2% for blocking events classified as weak. Central Anatolia Region has the greatest Tn frequency. The inner parts of the Mediterranean Region and the southeastern part of the country have Tn values below 0.5% (Figure 6.8ab). The minimum mean Tn frequency is 0.0% and the maximum is 5.0% when the BI is moderate. Southwestern part of the country has the greatest Tn frequency while the rest of the country has the lowest frequencies (Figure 6.8b).

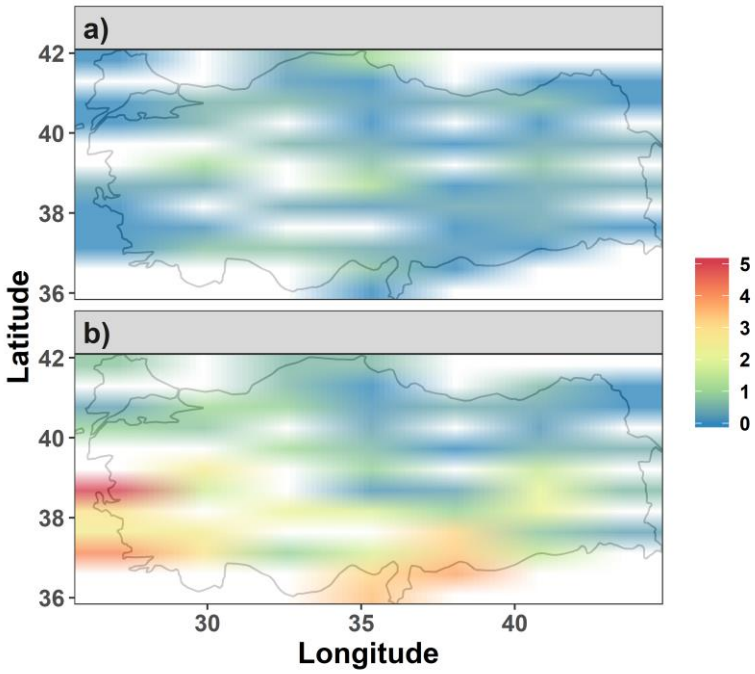

Figure 6.8 : The Tn frequency distribution for (a) weak and (b) moderate BI during blocked days in the summer season.

6.1.2.4 Tn distribution for blocking longitudinal extent

The Tn frequency distribution for different blocking longitudinal extent during the summer is seen in Figure 6.9. The Tn values vary between 0.0% and 2.4% when the blocks have small longitudinal extent. The most southeastern part of the country has

the greatest Tn frequency. The greater part of the East Anatolia Region, the South Anatolia Region, the vast majority of the Mediterranean Region and a large fraction of the Aegean Region have lowest Tn frequencies (Figure 6.9a). When the longitudinal extent is moderate, the minimum of Tn frequency is 0.2% whilst the maximum is 2.0%. The continental part of the Aegean Region has greatest Tn values. The northwestern part of the Marmara Region, a great area in the Central Anatolia Region and part of the East Anatolia Region have the minimum Tn value of 0.2% (Figure 6.9b). The Tn frequency has a minimum and maximum of 0.0% and 5.6% respectively, for the large longitudinal extended events. The South Anatolia Region, an area over the East Anatolia Region and areas over the Aegean Region have the greatest Tn values greater than 4.0%. Blue shaded areas over the northern part of the country have values less than 1.0% of Tn frequency values (Figure 6.9c).

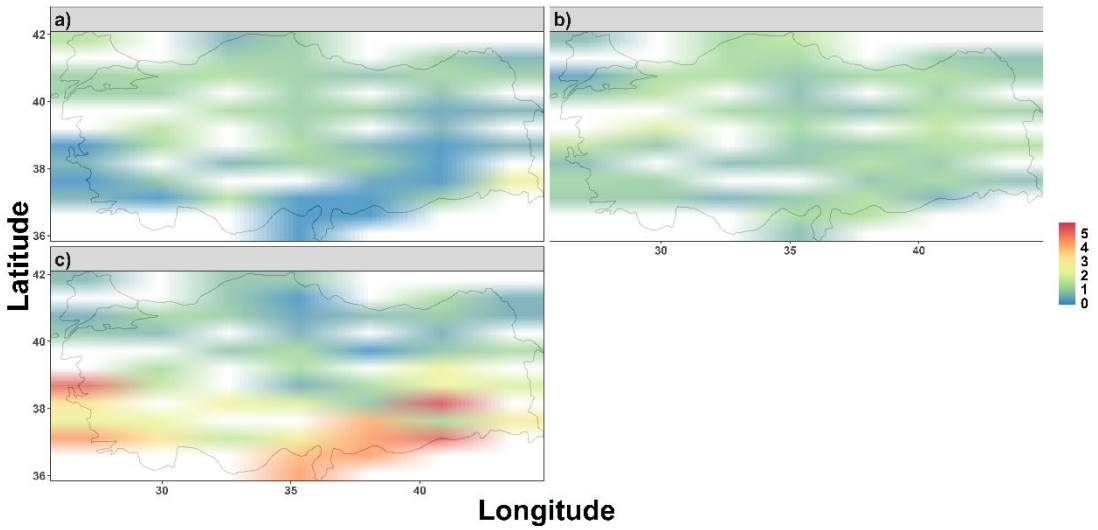

Figure 6.9 : The Tn frequency distribution for (a) small, (b) moderate, and large extend blocking events in the summer season.

6.1.2.5 Tn distribution for blocking duration

The Tn frequency distribution stratified by block duration during summer is seen in Figure 6.9. The Tn frequency varies between 0.6% and 6.0% for the short duration blocking events. Only the northeast part of the country has Tn values below 0.5% for short duration events. Areas in the southeastern and southernmost parts of the country have a maximum Tn frequency over 5.8%. The outer areas of the country have a Tn value greater than 3.0%. The rest of the country have Tn value of less than 2.0% (Figure 6.10a). For the moderate duration blocking events, Tn frequency has a

minimum and a maximum of 0.0% and 2.2%, respectively. An area in the southwestern part of the country has the maximum Tn frequency values. The northern part of the country, Central Anatolia Region and East Anatolia Region have a minimum Tn of 0.0%. (Figure 6.10b). The minimum Tn frequency is 0.5% and the maximum is 2.7% for the most persistent blocking events. An area in the southeast Anatolia Region (yellow shaded) has a maximum of 2.7% whilst several areas (blue shaded) has a minimum of 0.5% (Figure 6.10c).

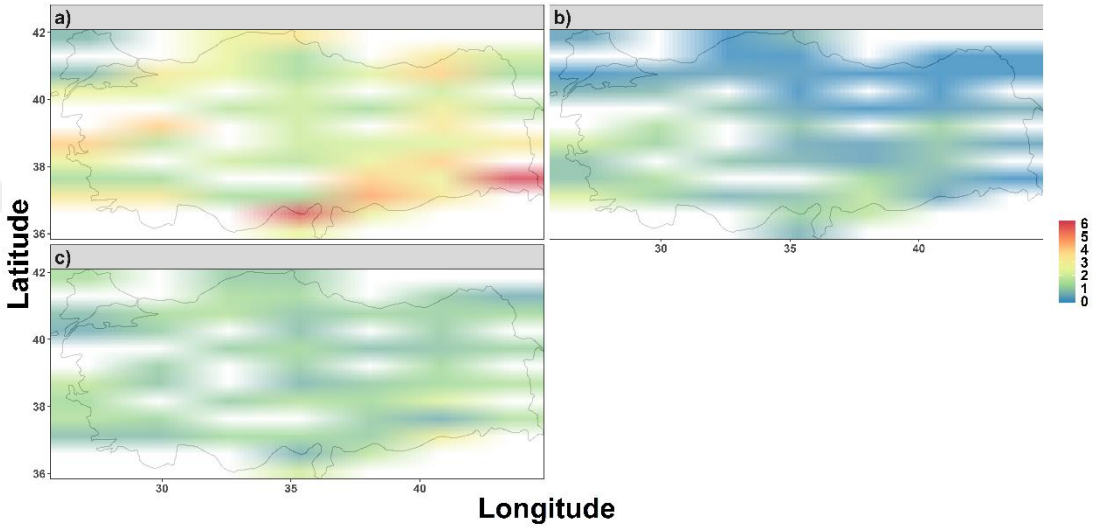

Figure 6.10 : The Tn frequency distribution for (a) short-lived, (b) moderate, and (c) most persistent blocking events during the summer season.

6.2 Winter Season

6.2.1 Extreme maximum temperature

6.2.1.1 Tx distribution for all data

The mean Tx distribution during the winter season is seen in Figure 6.11. The Tx values fluctuate between 0.0% and 1.0% across the country. The central Black Sea Region, areas in the Central Anatolia Region, areas in the Aegean Region and an area at the northeastern part of the country have the minimum mean Tx values lower than 0.2%. Almost all East Anatolia Region has Tx values of less than 0.7%. A small portion of southeast Anatolia, East Anatolia, and Mediterranean Region have Tx values greater than 0.7%. Thus, blocking has a larger impact on Tn distribution although it has a lesser impact on Tx during the winter season overall.

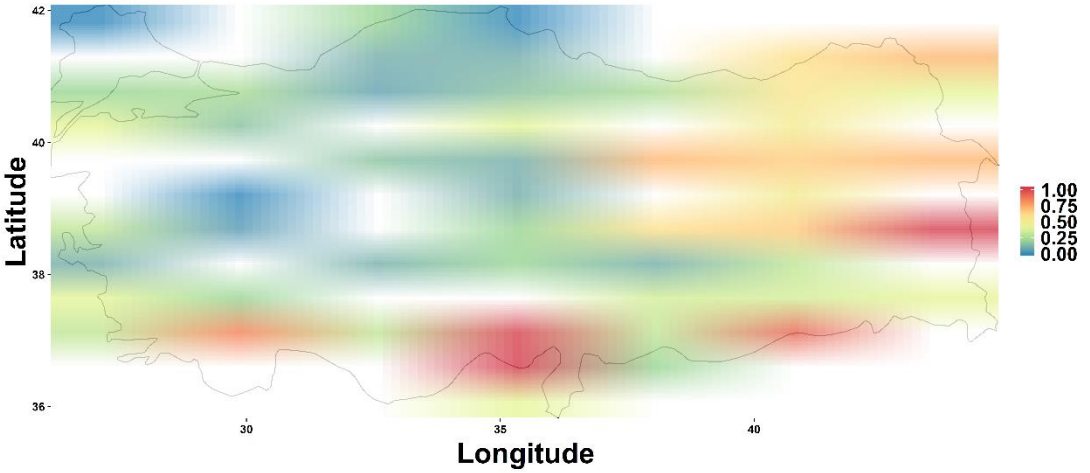

Figure 6.11 : The Tx frequency distribution during blocked days in winter.

6.2.1.2 Tx distribution for blocking center

In this section, the Tx frequency distribution for different sectors of blocking activity during winter is examined. The Tx frequency distribution is seen in Figure 6.12. The Tx values fluctuate between 0.0% and 5.3% when the block center is located in S1. Areas in the South East Anatolia Region and the Mediterranean Region have the maximum Tx frequency with the value of greater than 5.0%. The western part and some areas across the country have minimum Tx values around 0.0% (Figure 6.12a). When the block center is located in S2, Tx frequency values have a minimum and maximum of 0.0% and 1.0% respectively. An area in the East Anatolia Region has the greatest Tx frequency values whilst the rest of the country has values below 0.7% (Figure 6.12b). The Tx frequency values have a range of 0.0% and 1.8% when the block center is located is S3. An area over the eastern part of the country has the greatest Tx frequency. Minimum Tx frequency values, smaller than 0.5% are observed over the rest of the country (Figure 6.12c). In S4, a small area in the east of the Black Sea Region has the greatest mean Tx frequency around 0.8%. The rest of the country has a minimum Tx frequency value of exactly 0.0% (Figure 6.12d).

6.2.1.3 Tx distribution for blocking intensity

Mean Tx frequency distribution stratified to the block intensity during winter is seen in Figure 6.13. The Tx frequency fluctuates between 0.0% and 4.9% during the weak blocking events. Areas in the southwestern part of the country and around Hatay have the greatest Tx frequency. The rest of the country except southern parts has Tx values below 1.5% (Figure 6.13a). The minimum mean Tx frequency is 0.0% and the

maximum is 1.5% when the BI is moderate, respectively. The area over the northeastern part of the country has the greatest Tx frequency whilst the rest of the country has lower frequencies. (Figure 6.13b). The Tx frequency distribution during strong blocking events can be seen in Figure 6.13c. The entire country has a value of 0.0%.

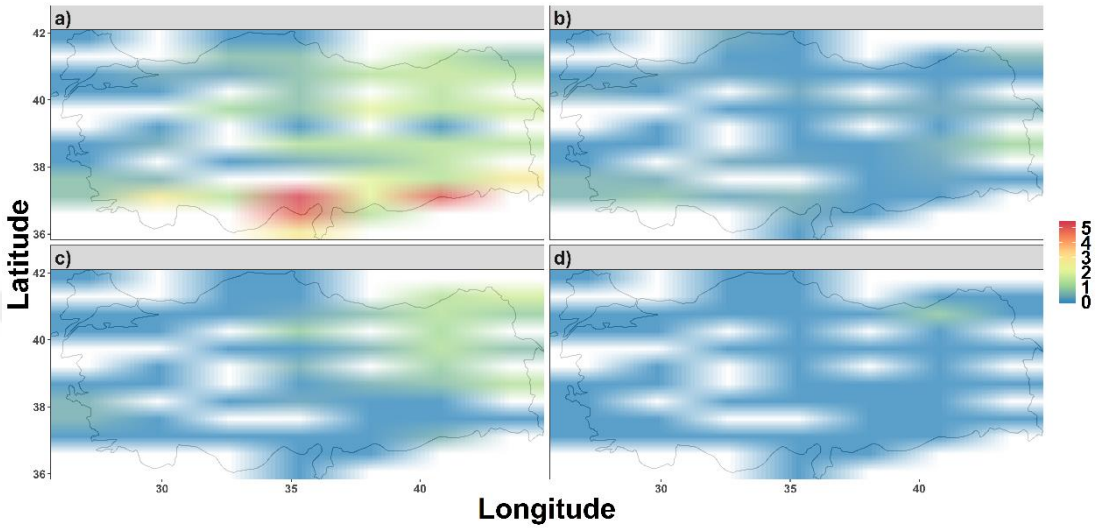

Figure 6.12 : The Tx frequency distribution for (a) S1, (b) S2, (c) S3 and (d) S4 during winter season blocked days.

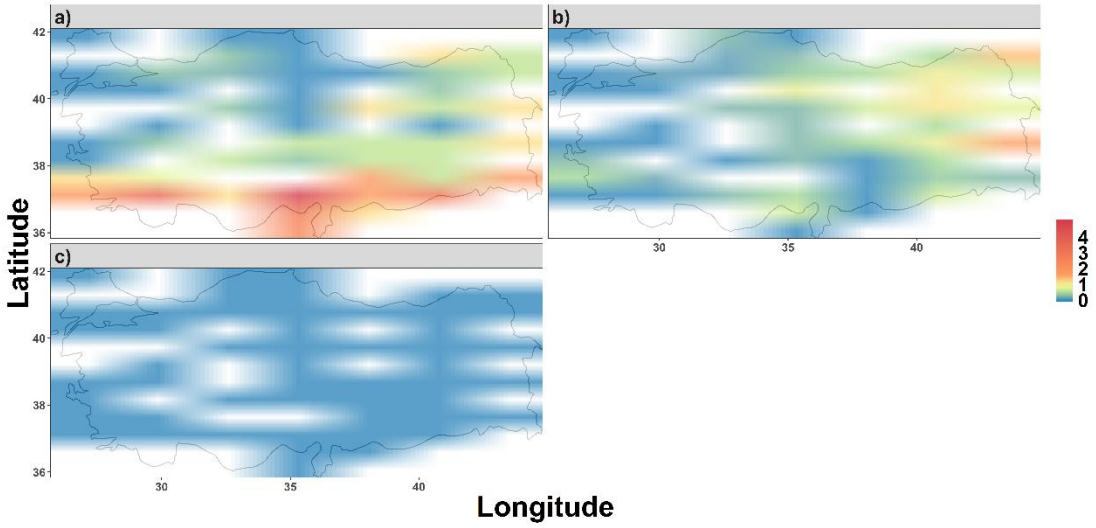

Figure 6.13 : The Tx frequency distribution for (a) weak (b) moderate and (c) strong BI during blocked days in the winter season.

6.2.1.4 Tx distribution for blocking longitudinal extent

The Tx frequency distribution for different blocking longitudinal extent for winter is seen in Figure 6.14. The Tx values changes between 0.0% and 3.4% when the blocks have small longitudinal extent. Areas in the eastern and southern parts of the country have greatest Tx frequencies. The central part of the Black Sea coastline, the Central Anatolia Region and the Aegean Region have lowest Tx frequencies (Figure 6.14a). When the blocking longitudinal extent is moderate, the minimum of Tx frequency is 0.0% whilst the maximum is 1.1%. Areas in the East Anatolia Region and in the southwestern part of the country have greatest Tx values. The rest of the country has a minimum Tx value of 0.0% (Figure 6.14b). The Tx frequency has the minimum and maximum of 0.0% and 1.0%, respectively for the large longitudinally extended blocking events. Several areas in the southern part of the country have the greatest Tx values greater than 0.8%. The rest of the country has values of less than 0.5% of Tx distribution (Figure 6.14c).

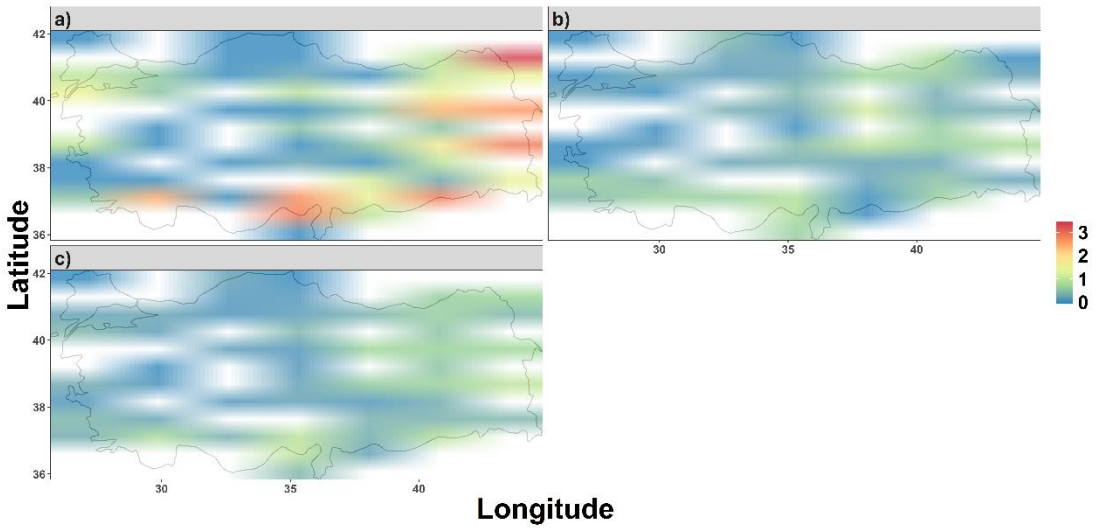

Figure 6.14 : The Tx frequency distribution for (a) small, (b) moderate, and (c) large blocks during blocked days in the winter season stratified by the block size.

6.2.1.5 Tx distribution for blocking duration

The Tx frequency distribution stratified by block duration during winter is seen in Figure 6.15. The Tx frequency fluctuates between 0.0% and 4.0% for the short lasting blocking events. An area in East Anatolia Region has a maximum Tx frequency of 4.0%. The rest of the East Anatolia Region and the Mediterranean Region have Tx values greater than 1.3%. The Aegean Region, the Black Sea Coastline and the vast

majority of the Marmara Region have the Tx values around 0.0% (Figure 6.15a). For the moderate lasting blocking events, Tx frequencies have a minimum and a maximum of 0.0% and 1.4%, respectively. An area in the southernmost part of the Mediterranean Region has the maximum Tx frequency values. The western part of the country, the Central Anatolia Region, the Black Sea coastline and an area from southeast Anatolia Region have a minimum of 0.0%. (Figure 6.15b). The minimum Tx frequency is 0.0% and the maximum is 0.8% for long-lasting blocking events. Areas in the Aegean and Marmara Regions have a maximum of 0.8% whilst the rest of the country except several small areas has a frequency of 0.0% (Figure 6.15c).

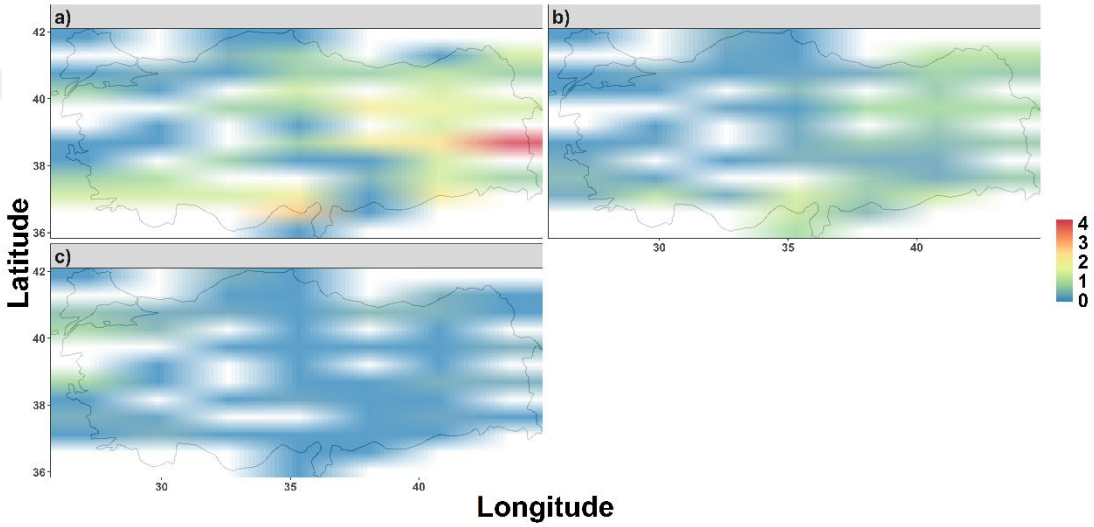

Figure 6.15 : The Tx frequency distribution for (a) short-lived, (b) moderate, and (c) most persistent blocks during blocked days in the winter season.

6.2.2 Extreme minimum temperature

6.2.2.1 Tn distribution for all data

The mean Tn distribution during the winter season is seen in Figure 6.16. The Tn values fluctuate between 0.8% and 2.4% across the country. Areas in the most southern and southeast part of the country have the minimum mean Tn values lower than 1.0%. Almost all Anatolia has Tn values that fluctuate between 1.0% and 1.8%. The Trace Region, east Black Sea coastline and a small part of the Central Anatolia have Tn values greater than 1.8%. Thus, blocking has a larger impact on Tn distribution.

6.2.2.2 Tn distribution for blocking center

In this section, the Tn frequency distribution for different sectors of blocking activity during winter is examined. The Tn frequency distribution is seen in Figure 6.17. The Tn values fluctuate between 0.0% and 1.4% when the block center is located in S1. An area in the southwest part of the country has a maximum Tn frequency with the value of around 1.4%. The rest of the country have minimum Tn values smaller than 0.6% (Figure 6.17a).

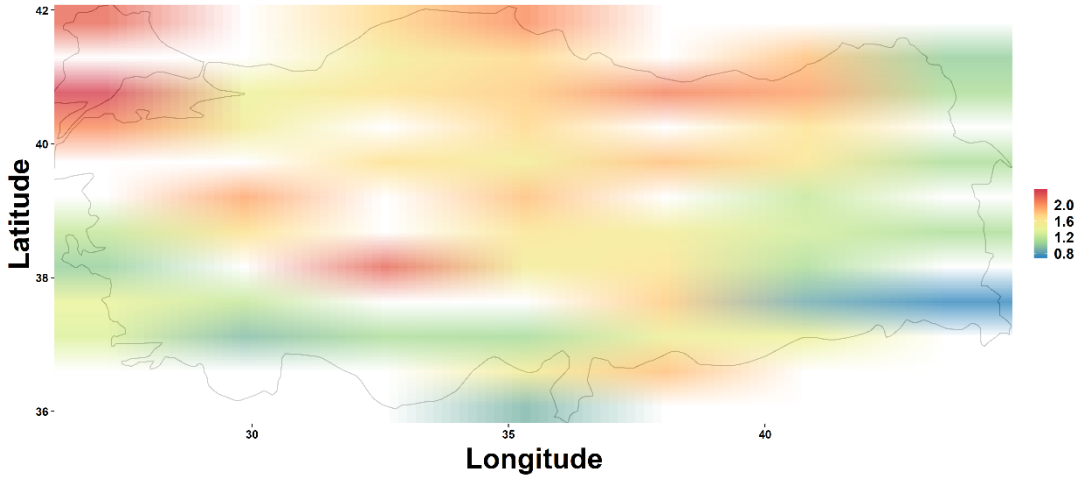

Figure 6.16 : The Tn frequency distribution during blocked days in winter.

When the block center is located in S2, Tn frequency values have a minimum and maximum of 0.1% and 2.5% respectively. The southern and northern parts of the country except the Marmara Region has the greatest Tn frequency values whilst the inner parts of the country have values below 1.0% (Figure 6.17b). The Tn frequency values have a range of 0.4% and 5.9% when the block center is located is S3. Areas in the Marmara Region and around Sinop has the greatest Tn frequency. Minimum Tn frequency values, around 0.0% are observed over a small area in the northeast Anatolia and the Mediterranean Region (Figure 6.17c). In S4, the area in the East Anatolia Region has the greatest mean Tx frequency around 6.0%. The western part of the country, an area in the East Anatolia Region and several areas in the Central Anatolia has the minimum Tn frequency value below 0.5% (Figure 6.17d).

6.2.2.3 Tn distribution for blocking intensity

Mean Tn frequency distribution stratified to the block intensity during winter is seen in Figure 6.18. The Tn frequency fluctuates between 0.0% and 6.1% during the weak blocking events. Northern part and several areas across the country have the greatest

Tn frequency. The inner parts of the Mediterranean Region and an area in the southeastern part of the country have Tn values below 1.0% (Figure 6.18a).

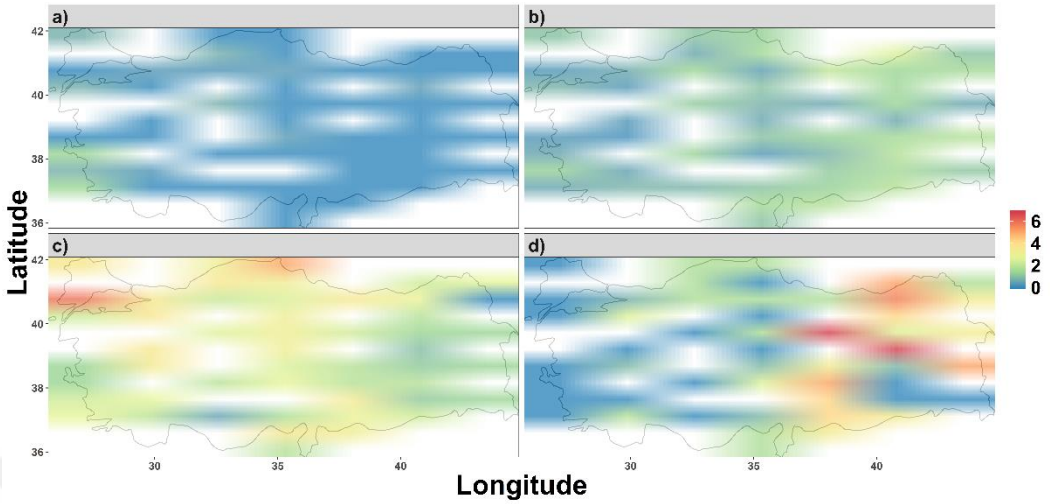

Figure 6.17 : The Tn frequency distribution for (a) S1, (b) S2, (c) S3 and (d) S4 during winter season blocked days.

The minimum mean Tn frequency is 0.0% and the maximum is 1.8% when the BI is moderate, respectively. The southern part of the country has the greatest Tn frequency whilst the rest of the country has lower frequencies. (Figure 6.18b).The Tn frequency distribution during strong blocking events can be seen in Fig. 6.18c. Almost the entire country with a few exceptions has a value of 0.0%. An area around Aydın has a Tn value of 12.5% and areas in Black Sea coastline and around Çanakkale has Tn frequency value of 6.25%.

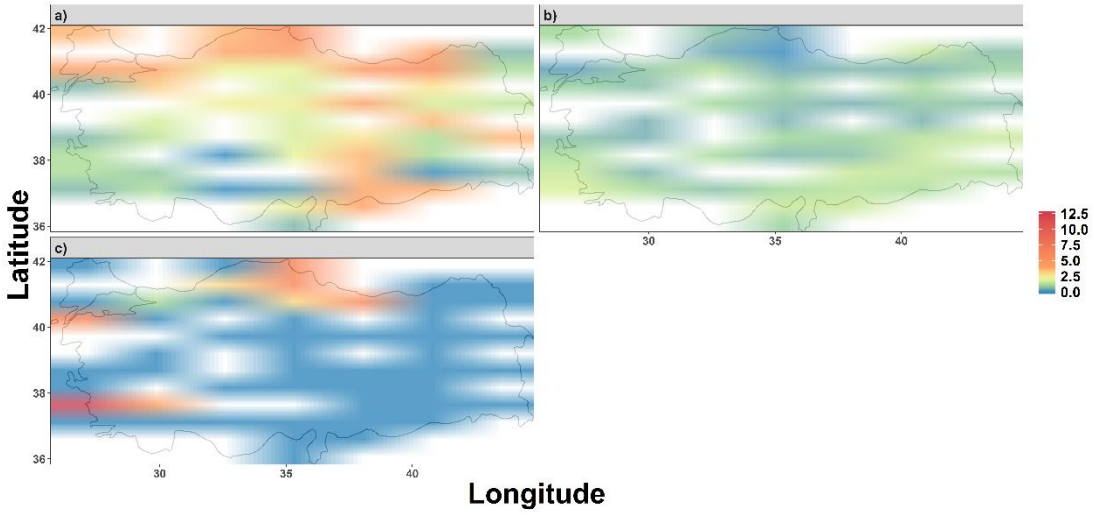

Figure 6.18 : The Tn frequency distribution for (a) weak, (b) moderate, and (c)strong BI during blocked days in the winter season.

6.2.2.4 Tn distribution for blocking longitudinal extent

The Tn frequency distribution for different blocking longitudinal extent for winter is seen in Figure 6.19. The Tn values changes between 0.0% and 2.9% when the blocks have small longitudinal extent. The eastern part of the country and the Southeast Anatolia Region have greatest Tn frequencies. The area in the Marmara Region and the zone from Black Sea Region to the Mediterranean Region have lowest Tn frequencies (Figure 6.19a). When the longitudinal extent is moderate, the minimum of Tn frequency is 0.2% whilst the maximum is 3.2%. The area at the intersection of the Central Anatolia and Mediterranean Region have greatest Tn values. Areas in the southeastern and southwestern part of the country have the minimum Tn value below 0.5% (Figure 6.19b). The Tn frequency has the minimum and maximum of 0.7% and 2.2%, respectively for the large longitudinally extended block events. The Trace part of the Marmara Region and part of the continental Mediterranean Region have the greatest Tn values greater than 2.0%. The southwest part of the Aegean Region, the south part of the Mediterranean Region and area in the southeast part of the country have values less than 1.0% of Tn distribution (Figure 6.19c).

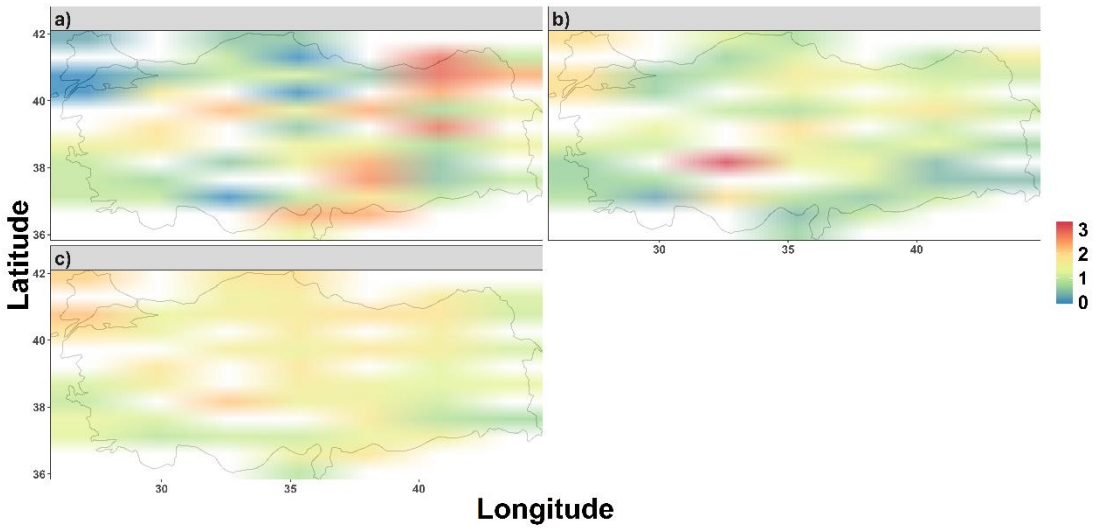

Figure 6.19 : The Tn frequency distribution for (a) small (b) moderate, and c. large blocks in the summer season.

6.2.2.5 Tn distribution for blocking duration

The Tn frequency distribution stratified by block duration during winter is seen in Figure 6.19. The Tn frequency fluctuates between 0.0 and 2.0% for the short lasting blocking events. The area in southeast Anatolia Region has a maximum Tn frequency

of 2.0%. Several areas across the country have Tn values smaller than 1.0%. The rest of the country have the Tx value of around 0.0% (Figure 6.20a). For the moderate lasting blocking events, Tn frequencies have a minimum and a maximum of 0.5% and 2.8%, respectively. Areas in the Marmara Region, in the northern part of the Black Sea Region and in the Central Anatolia has the maximum Tn frequency values. Areas in the southern part of East Anatolia Region and the northern part of the Central Anatolia Region have a minimum of 0.5% (Figure 6.20b). The minimum Tn frequency is 0.5% and the maximum is 3.8% for long-lasting blocking events. An area in the intersection of the East Anatolia and Central Anatolia Region has a maximum of 3.8% whilst the area in the southernmost part of the country has a frequency of 0.0% (Figure 6.20c).

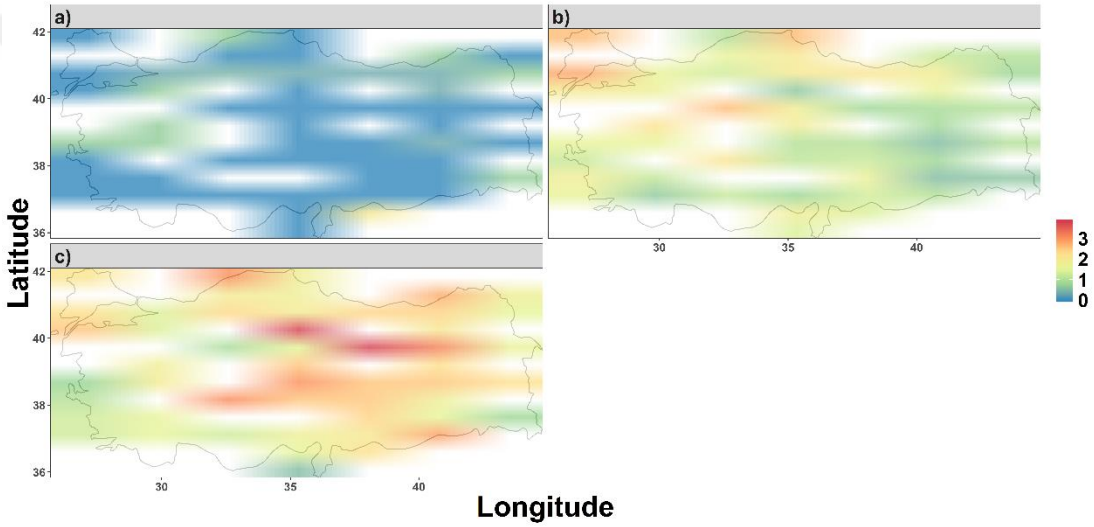

Figure 6.20 : The Tn frequency distribution for a. short-lived, b. moderate, and c. most persistent blocks in the winter season.

7. CONCLUSIONS AND RECOMMENDATIONS

Using the NCEP - NCAR re-analyses and data acquired from the Turkish State Meteorological Service, the effects of atmospheric blocking on meteorological parameters investigated for Turkey from 1977 to 2016. An investigation of the impact of blocking on any meteorological parameter of Turkey has not been done previously. Thus, the following results are new and will provide an operational community with forecast guidance under blocking situations.

7.1 Blocking

The main characteristics of blocking in the study region during the study period can be explained briefly as follows. The mean duration of blocking events impacting Turkey is 8.8 days, with a maximum of 9.2 days in both winter and spring and the minimum of 8.1 days in summer. The mean occurrence of blocking is 11.7 events per year with a maximum of 3.9 events in spring and 2.5 events in summer. This is consistent with Lupo et al. (2019) for the Atlantic Region and Northern Hemisphere in recent years. The mean annual value for atmospheric blocking occurrences within the study region is 11.7. The most intense blocking events are observed in winter (2.50) and weakest events are observed in summer (1.91). These results including the seasonal variability are consistent with WI02 or Barriopedro et al. (2006) for their Atlantic region climatologies. The mean longitudinal extent is 28 degrees longitude with the maximum in winter (29 degrees longitude) and minimum in summer (25 degrees longitude). Block size and duration, as well as block size and intensity, were positively correlated here with the statistically significance at 95% confidence level except for block size and duration in summer, and these results are consistent with LS95, especially for the winter season. LS95 showed these relationships were strongest in the Atlantic sector as well.

7.2 Temperature

Blocking events play a crucial role on the temporal distribution of the mean seasonal temperature anomaly of all stations even though blocking frequency is around 30% during the year. There were four main patterns are observed for temperature anomalies during blocked days, non-blocked days, and the differences between these two situations. The definition of patterns with respect to blocking events is as follows; P1b can be described as minimum temperature anomaly in winter, increasing towards 0^{o} C in the spring season, small increasing or decreasing in the summer and decreasing during fall. P2b can be characterized as the same magnitudes of negative anomalies in cold seasons, and anomalies around 0^{o} C during the warm seasons. P3b is associated with negative anomalies during winter, increasing toward $+0.5^{o}$ C in spring and then decreasing during both the summer and fall seasons. The last pattern (P4b) is associated with warmest temperature anomalies approximately 0^{o} C during the spring and nearly same the negative anomalies in other seasons. The northwest part of Turkey experiences negative temperature anomalies during all seasons in association with blocking. This is compatible with the results of Sousa et al. (2017) who showed that southeast Europe (includes the northwestern part of Turkey) has a negative maximum temperature anomaly during winter regardless of the domain that blocking occurs.

The spatial distribution of temperature anomalies associated with blocking was examined as well. The northwest part of Turkey experiences strong or very strong negative temperature anomalies during blocked days for all seasons. This region is located on the downstream flank of a ridge during blocking events and is the most affected by cold air advection. The west part of the country experiences very strong, strong or moderate negative temperature anomalies; the central part experiences moderate negative anomalies at most stations. The eastern part of the country has moderate temperature anomalies which is consistent with the location of blocking. This situation is not inconsistent with Sillmann et al. (2011), and they noted that the Baltic Sea coastline is a major region that is influenced by atmospheric blocking. However, their study focuses on only the North Atlantic Blocking during the winter months.

Additionally, blocking events that impact Turkey are largest, strongest, and most persistent during the winter season and there is a statistical relationship between the

strength of the cold anomalies and block size, duration, and persistence as in LS95. During the other seasons, these relationships were not as clear.

Lastly, the composite plot of 500 hPa geopotential height shows that both coldest (March 1985) and warmest temperature anomalies (September 2015) are associated with a Rex – type block. As seen here, the tilt of the blocking axis plays an important role as mentioned in Luo et al. (2015) and Yao et al. (2016). March 1985 was one of the most memorable winter periods in Turkey because of heavy snow that influenced all of the Istanbul Region as well as the greater northwestern part of the country. All schools and government institutions were closed because transportation was halted due to the extreme snow depth. Also, a second atmospheric blocking event associated with very cold temperature anomalies was observed during March 1987 (not shown). Again, during that period the schools and government institutions were closed. It was mentioned in a previous study that the cause of the 1987 cold wave was a blocking event (see Tayanç et al., 1998). The warmest event has no memorable effects due to the short duration of the event.

Additionally, Nunes et al. (2017) demonstrated that during ten extremely cold months for the Belgorod Region of Southwest Russia (1944-2015), atmospheric blocking was observed over Europe, while for extremely warm months, blocking was located over the region or east of the region. This is true for Turkey as well based on the case studies here.

7.3 Precipitation

During blocked days, the highest MPF in Turkey were observed in general along the Black Sea Coastline and the northeastern part of the Marmara Region. The lowest MPF were observed within southern Turkey especially along the Mediterranean coastline and in several cities located in the South Anatolia Region. Rize, Giresun, and Ordu are the cities that observed the highest MPF with values of 0.43, 0.39 and 0.36, respectively. For non – blocked days, MPF ranges between 0.12 and 0.38 nationwide. Similar to the blocked days, the Black Sea coastline and northeast part of the Marmara Region have the highest MPF. Rize, Giresun, and Ordu are the cities that observed the highest MPF with the values 0.38, 0.32 and 0.29, respectively. These results here demonstrated that blocking increases the MPF across the country. The change in MPF

ranges from 12% to 42% in Turkey. The inner part of Anatolia had greater increases in MPF as opposed to the western Black Sea region that observed the lowest values.

The MPF distribution with respect to season showed that winter had the highest values across the country and the mean was 0.31 during blocked days. The average MPF during blocked days was 0.29, 0.13 and 0.21 in spring, summer and fall, respectively. The Black Sea Region observed the highest MPF values for all seasons, particularly the city of Rize, which always observed one of the top three MPF values in any category. During non-blocked days, the mean MPF values show a similar pattern to the blocked days MPF values, but with lower values. The winter and spring seasons had similar MPF values, 0.26 and 0.24, respectively. The summer season observed the minimum MPF value of 0.09. For the fall season, the mean MPF was 0.16. The ratio of MPF for blocked days to non-blocked days in the entire data set and across Turkey explicitly showed that MPF increased during the blocked days. The average MPF change across Turkey was 19%, 19%, 60% and 28% during the winter, spring, summer, and fall season, respectively. The higher summer season MPF ratios were due to smaller values of MPF for both blocked and non-blocked days.

S1 and S2 observed the greatest MPF values at 0.25 and 0.27, respectively while the mean MPF values for the overall country for S3 and S4 are 0.22 and 0.21, respectively. When blocking was located in the first and second sector, Turkey was located on the downstream flank of blocking events, whereas it is located on the upstream flank when blocking was centered in the remaining sectors. Rimbu et al. (2015) found that extreme precipitation events were related to blocking activity within the $0^o – 70^o$ E sector, which covers the second, third and part of the fourth sector defined here. Huang et al. (2019) indicated that 77% of extreme precipitation events over China are preceded by European blocking events.

In Turkey, there was no relationship between blocking duration and MPF or blocking extent and MPF for the entire data set in any season. Also, there was no relationship between BI and MPF during the winter and spring seasons for the entire data set. However, for the summer season, the CC between BI and MPF is 0.35 for the entire data set. Additionally, for the fall season, BI was correlated (CC = 0.43 – significant at the 95% level) with MPF in the data set.

When examining the 10 wettest MPF blocking events during the study period, it was shown that the blocking center was located in S1 and the S2 during all seasons. Their mean BI values were 2.81, 2.23, 2.34 and 2.81 for winter, spring, summer, and fall seasons events, respectively. Omega-type blocking was observed during cold season events whereas no particular type of blocking was observed during warm seasons. The average wind was westerly during 10 wettest events for any season and the wind speed was larger for the wet events than during driest events as inferred using the geostrophic relationship. When the 850 hPa charts were examined, there was specific humidity advection out of the Mediterranean during wet events for all seasons.

The blocking event associated with the greatest MPF was also examined. The event took place between 31 October 2009 and 5 November 2009. This event was associated with a nationwide MPF of 0.73 and mean total precipitation of 63.4 mm. The BI was 2.52 and longitudinal extent was 20 degrees. During this event, heavy rainfall and flash flood events were observed in some cities located in Turkey. In order to understand the influence of blocking as related to extreme precipitation events, a detailed study similar to Nunes et al. (2017) should be performed in the future. Finally, operational forecasters or policymakers should use the results gained here as guidance when blocking is anticipated in short-range or long-range forecasts.

7.4 Extreme Temperature

First, the Tx and Tn frequency distribution for whole data were examined. During the summer season, the distribution for both extremes fluctuates between 0.5 – 1.8 percent for Tx and 0.4 – 2.0 percent for Tn. Thus, there is a slightly greater spread for the frequency of Tn than for Tx. However, lower frequency values are observed over larger areas for Tn when compared to Tx. During the winter, the cooling effect of blocking is quite evident. The Tx distribution fluctuates between 0 and 1 percent, that means most of the country observes less Tx events during blocking than normal conditions. There is a latitudinal pattern, higher the latitude, lower the Tx frequency. On the other hand, the minimum Tn frequency is 0.8 and the maximum is 2.4. There is a counter latitudinal pattern in the Tn distribution. The northern part of the country has greater Tn values whilst the southern part has lower.

Secondly, the impact of blocking center location on Tx and Tn were examined. The lower and upper boundaries of Tx frequency increases when the mean block center

moves from west to east. In S4, the maximum value reaches 6.4 percent. However, large areas with small Tx frequency values in S2 and S4 need to be taken into consideration. Lower boundaries of Tn frequency also increase with the movement of the blocking center location, similar to the Tx. However, the maximum Tn value in S1 is greater than that in S2. Similar to Tx distribution, the spatial distribution of low frequencies is obvious in S2 and S4. For summer, if the block center moves to the east the Tx frequency values decreases and the area covered by lower values increases. When the block center is located on the S1, the maximum Tx value is 5.3 and only less than half of the country is covered by lower Tx frequencies. However, when the block center is located in the other three sectors, the maximum Tx value is 1.8 and almost all of the country is covered with lower values. Even, for the S4, all the country except a small area over the northeast part of the country has the Tx value of 0 percent. The eastward-moving of the block center has an almost opposite effect on Tn frequency distribution. When the blocking center moves eastward, the maximum Tn value increases. The area covered by the lower Tn values decreases from S1 to S3. However, it increases in the S4. For S1 almost all the country is covered by the values lower than 0.5 percent. In S3 small areas are covered by lower values.

Thirdly, Tx and Tn were examined when considering the BI. The Tx frequency change with respect to BI is not clear during the summer. The Tx frequency boundaries, as well as area coverage of values, are very similar for blockings with weak and moderate intensities. However, the impact of BI is clearer for Tn frequency across the country. The spatial coverage of the lower Tn frequency values decreases with the BI increases from weak to moderate. The maximum frequency reaches 5.0 percent during moderate intensities. During the winter, the maximum Tx frequency decreases with the class of BI. The maximum Tx frequency is almost five percent for weak blockings whilst it is negligible for strong blocking events. The spatial coverage of lower Tx frequency values is increasing with increasing BI. For Tn frequency distribution, the spatial coverage of lower values is similar to the Tx. The spatial coverage of lower Tn values increases with an increase in BI. The maximum Tn frequency decreases in S2 with respect to S1 and then increases in S3 reaching 12.5 percent.

Then, the effects of the blocking longitudinal extent were investigated for Tx and Tn for summer. The longitudinal extent has a different impact on Tx and Tn. An increase in blocking longitudinal extent decreases the maximum frequency of Tx values and

increases in the area covered by the lower values. However, increasing longitudinal extent increases the maximum Tn values without a precise influence on the area covered by the lower values. The observed distribution of Tn during large blocking events is opposite to that in small events, and this is the noteworthy result from this section. During the winter, the maximum Tx frequency is around 3.3% and almost half of the country is covered by the lower Tx frequency values for the blocking events with small longitudinal extent. When the blocking longitudinal extent becomes moderate, the maximum Tx frequency reduces to 1.39% and the covered area increases. For the events with large longitudinal extent, decreasing in frequency continues and reaches to 0.96% although the area coverage remains the same. For the Tn frequency, the maximum value increases for the events with moderate longitudinal extent according to the events with small longitudinal extent but, it covers a smaller area. For large events, it decreases to 2.2%. The area covered by the lower Tn frequency values decreases with the increase in blocking longitudinal extent.

Lastly, the impact of the block duration is analyzed. For summer, block duration has an increasing effect on maximum Tx frequencies and decreasing effect on the spatial coverage of lower Tx values. The spatial coverage of lower Tn frequencies is minimum during short-lived events and maximum for moderate duration events. The maximum Tn frequency value is greatest during short duration events and smallest during moderate duration events. For winter, block duration has also the same effect as intensity. The maximum Tx frequency decreases and the area covered by the lower values increase with the increase of block duration. On the other hand, block duration has an enhancing effect on Tn frequency values. The area covered by the lower values decreases and the maximum Tn values increases with the block duration such that there is almost no area with the lower values during moderate and large blocking events.

REFERENCES

Antokhina, O. Y., Antokhin, P. N., Devyatova, E. V., and Martynova, Y. V. (2018). Wintertime atmospheric blocking events over Western Siberia in the period 2004-2016 and their influence on the surface temperature anomalies. *The 2nd International Electronic Conference on Atmospheric Sciences (ECAS 2017)*, 16-31 July 2017: Sciforum Electronic Conference Series, Vol *2*, 1-9.

Baltacı, H., Akkoyunlu, B.O., and Tayanç, M. (2017). Relationship Between Teleconnection Patterns and Turkish Climatic Extremes, *Theor Appl Climatol*, https://doi.org/10.1007/s00704-017-2350-z

Barriopedro, D., García-Herrera, R., Lupo, A. R., and Hernández, E. (2006). A Climatology of Northern Hemisphere Blocking. *Journal of Climate 19*(6): 1042-63. https://doi.org/10.1175/JCLI3678.1

Berggren, R., Bolin, B. ve Rossby, C.G. (1949). "An aerological study of zonal motion, its perturbations and break-down", *Tellus*, *1* (2), 14–37.

Brunner, L., Hegerl, G. C. and Steiner, A. K. (2017). Connecting Atmospheric Blocking to European Temperature Extremes in Spring. *Journal of Climate 30*, 585-594. https://doi.org/10.1175/JCLI-D-16-0518.1

Demirtaş, M. (2017). The Large-Scale Environment of the European 2012 High-Impact Cold Wave: Prolonged Upstream and Downstream Atmospheric Blocking. *Weather 72*: 297 -301. https://doi.org/10.1002/wea.3020

Deniz, A., and Gönençgil, B. (2015) Trends of summer daily maximum temperature extremes in Turkey. *Physical Geography*, *36*(4), 268–281.

Diao, Y., Xie, S. P., and Luo, D. (2015). Asymmetry of Winter European Surface Air Temperature Extremes and the North Atlantic Oscillation. *Journal of Climate 28*: 517-30. http://dx.doi.org/10.1175/JCLI-D-13-00642.1

Efe, B., Lupo, A. R. and Deniz, A. (2019) The Relationship Between Atmospheric Blocking and Precipitation Changes in Turkey between 1977 – 2016. *Theoretical and Applied Climatology*, DOI: https://doi.org/10.1007/s00704-019-02902-z

Elliott, R. D. and Smith, T. B. (1949). "A study of the effects of large blocking highs on the general circulation in the Northern-Hemisphere westerlies*", J. Meteor*, *6*, 67–85.

Gazete Vatan (2009) Yağış nedeniyle bazı seferler iptal!. (Turkish) Accessed 21 December 2018, http://www.gazetevatan.com/yagis-nedeniyle-bazi-seferler-iptal--268162-yasam/.

Huang, W., Yang, Z., He, X. et al. (2019). A possible mechanism for the occurrence of wintertime extreme precipitation events over South China. *Clim Dyn 52*: 2367. https://doi.org/10.1007/s00382-018-4262-8

Kalnay, E. et al. (1996). The NCEP/NCAR 40-Year Reanalysis Project. *Bulletin of the American Meteorological Society*, *77*, 437-471.

Kömüşcü, A.Ü. and Çelik, S. (2013). Analysis of the Marmara flood in Turkey, 7–10 September 2009: an assessment from hydrometeorological perspective. *Nat Hazards 66: 781*. https://doi.org/10.1007/s11069-012-0521-x

Lejenäs, H. and Økland, H. (1983). Characteristics of Northern Hemisphere Blocking as Determined from a Long Time Series of Observational Data. *Tellus A 35*(5): 350-362. https://doi.org/10.3402/ tellusa.v35i5.11446

Luo, D., Yao, Y., Dai, A, and Feldstein, S. B. (2015). The Positive North Atlantic Oscillation with Downstream Blocking and Middle East Snowstorms: The Large-Scale Environment. *Journal of Climate 28*: 6398–6418, https://doi.org/10.1175/JCLI-D-15-0184.1

Lupo, A. R. and Smith, P. J. (1995). Climatological Features of Blocking Anticyclones in the Northern Hemisphere. *Tellus A 47*(4): 439-456. https://doi.org/10.1034/j.1600-0870.1995.t01-3-00004.x

Lupo, A. R., Mokhov, I. I., Chendev, Y. G., Lebedeva, M. G., Akperov, M. and Hubbart, J.A. (2014) Studying Summer Season Drought in Western Russia. *Advances in Meteorology,* Volume *2014*, Article ID 942027. http://dx.doi.org/10.1155/2014/942027

Lupo, A. R., Jensen, A. D., Mokhov, I. I., Timazhev, A. V., Eichler, T. and Efe, B. (2019) Changes in Global Blocking Character During the Most Recent Decades. *Atmosphere*, *10*, 92. Doi:https://doi.org/10.3390/ atmos10020092

Mokhov, I. I., Timazhev, A.V. and Lupo, A. R. (2014). Changes in Atmospheric Blocking Characteristics within Euro-Atlantic Region and Northern Hemisphere as a Whole in the 21st Century from Model Simulations Using RCP Anthropogenic Scenarios. *Global and Planetary Change 122*: 265-270. http://dx.doi.org/10.1016/j.gloplacha.2014.09.004

Nunes, M. J., Lupo, A. R., Lebedeva, M. G., Chendev, Y. G., and Solovyov A. B. (2017). The Occurrence of Extreme Monthly Temperatures and Precipitation in Two Global Regions. *Papers in Applied Geography 3*(2): 143-156. http://dx.doi.org/10.1080/23754931.2017.1286253.

NTV (2009). Yağış, Sel, Soğuk!. (Turkish) Accessed 21 December 2018, https://www.ntv.com.tr/galeri/turkiye/etkili-yagis-sel-soguk, 4Kdy6v3fXkagcL9Iv9BlNg/ Hc1gAa7_102QpS4ONJRTHw.

Pearson, K. (1896). Mathematical Contributions to the Theory of Evolution. XIX . Second Supplement to a Memoir on Skew Variation Author (S): Karl Pearson Source?: *Philosophical Transactions of the Royal Society of London. Series A, Containing Papers of a Mathematical or. Philosophical Transactions of the Royal Society of London 187*: 253-318.

Pelly, J. L., and B. J. Hoskins. (2003). "A new perspective on blocking", *J.Atmos.* Sci., *60*, 743–755.

R Core Team (2019). R: A language and environment for statistical computing. R Foundation for Statistical Computing, Vienna, Austria. Retrieved (https://www.R-project.org/).

Rabinowitz, J. L., Lupo, A. R., Guinan, P. E. (2018). Evaluating Linkages between Atmospheric Blocking Patterns and Heavy Rainfall Events across the North-Central Mississippi River Valley for Different ENSO Phases. *Advances in Meteorology*, Volume *2018*, Article ID 1217830,

Radcliffe, R. A. S. (1985). Review of Spring 1985 over the Northern Hemisphere. *Weather*, *40*: 254-255. https://doi.org/10.1002/j.1477-8696.1985.tb06888.x

Rex, D. P. (1950). "Blocking action in the middle troposphere and its effect upon regional climate I: An aerological study of blocking". *Tellus*, *2*(3), 196-211.

Rimbu, N., Stefan, S. and Necula C. (2014). The Variability of Winter High-Temperature Extremes in Romania and Its Relationship with Large-Scale Atmospheric Circulation. *Theor Appl Climatol 121*: 121-130. https://doi.org/10.1007/s00704-014-1219-7

Rimbu, N., Stefan, S., Busuioc, A., and Georgescu, F. (2015). Links between Blocking Circulation and Precipitation Extremes over Romania in Summer. *International Journal of Climatology*, *36*(1). https://doi.org/10.1002/joc.4353

Scherrer, S. C., Croci-Maspoli, M., Schwierz, C. and Appenzeller, C. (2006). Two-Dimensional Indices of Atmospheric Blocking and Their Statistical Relationship with Winter Climate Patterns in the Euro-Atlantic Region. *International Journal of Climatology 26*(2): 233-249. https://doi.org/10.1002/joc.1250

Shabbar, A., Huang, J. and Higuchi, K. (2001). The Relationship between the Wintertime North Atlantic Oscillation and Blocking Episodes in the North Atlantic. *International Journal of Climatology 21*(3): 355-369. https://doi.org/10.1002/joc.612

Sirdas, S. A., Özdemir, E. T., Sezen, İ., Efe, B., and Kumar, V. (2017) Devastating extreme Mediterranean cyclone's impacts in Turkey. *Nat Hazards*, *87*: 255 - 286. https://doi.org/10.1007/s11069-017-2762-1

Sillmann, J., Croci-Maspoli, M., Kallache, M., and Katz, R. W. (2011). Extreme Cold Winter Temperatures in Europe under the Influence of North Atlantic Atmospheric Blocking. *Journal of Climate 24*(22): 5899-5913. https://doi.org/10.1175/2011JCLI4075.1

Sitnov, S. A., Mokhov, I. I. and Lupo, A. R. (2014). Evolution of the Water Vapor Plume over Eastern Europe during Summer 2010 Atmospheric Blocking. *Advances in Meteorology,* vol. *2014*, Article ID 253953. http://dx.doi.org/10.1155/2014/253953

Sousa, P. M., Trigo R. M., Barriopedro D., Soares P. M. M., Ramos A.M., and Liberato M. L. R. (2016). Responses of European precipitation distributions and regimes to different blocking locations. *Climate Dynamics 48*: 1141-1160. https://doi.org/10.1007/s00382-016-3132-5.

Sousa, P. M., Trigo, R. M., Barriopedro, D., Soares, P. M. M., and Santos., J. A. (2017). European Temperature Responses to Blocking and Ridge Regional Patterns. *Climate Dynamics 50*: 457-477. https://doi.org/10.1007/s00382-017-3620-2

Takvim. (2009) Urfa'nın etrafı sel!. (Turkish) Accessed 21 December 2018, https://www.takvim.com.tr/ yasam/2009/10/31 /urfanin_etrafi_sel.

Tayanç, M., Karaca, M., and Dalfes, H. N. (1998). March 1987 Cyclone (Blizzard) over the Eastern Mediterranean and Balkan Region Associated with Blocking. *Monthly Weather Review 126*(11): 3036-47. https://doi.org/10.1175/1520-0493(1998)126<3036:MCBOTE>2.0.CO;2

Tibaldi, S., and Molteni, F. (1990). On the Operational Predictability of Blocking. *Tellus* A *42*(3): 343-365.

Toros, H. (2012) Spatio-temporal variation of daily extreme temperatures over Turkey. *Int J Climatol.* doi: 10.1002/joc.2325

Treidl, R.A., Birch, E. C., and Sajecki, P. (1981). Blocking Action in the Northern Hemisphere: A Climatological Study. *Atmosphere-Ocean 19*(1): 1-23 https://doi.org/10.1080/07055900.1981.9649096

Türkeş, M., and Erlat, E. (2005) Climatological responses of winter precipitation in Turkey to variability of the North Atlantic Oscillation during the period 1930–2001. *Theor. Appl. Climatol. 81*: 45. https://doi.org/10.1007/s00704-004-0084-1

Türkeş, M., and Erlat, E. (2009). Winter Mean Temperature Variability in Turkey Associated with the North Atlantic Oscillation. *Meteorology and Atmospheric Physics 105*(3-4): 211-25. https://doi.org/10.1007/s00703-009-0046-3

Unal, Y., Tan, E., and Menteş, S. (2013) Summer heat waves over western Turkey between 1965 and 2006. *Theor Appl Climatol 112,* 339–350. doi: https://doi.org/10.1007/s00704-012-0704-0.

de Vries, H., Woollings, T., Anstey, J., Haarsma, R. J., and Hazeleger, W. (2013). Atmospheric Blocking and Its Relation to Jet Changes in a Future Climate. *Climate Dynamics 41*(9-10): 2643-2654. https://doi.org/10.1007/s00382-013-1699-7

Weather Log, (2015). September 2015: Coolest September for 21 years in south-but a vast improvement on summer in Scotland. *Weather, 70*: 1-5.

Whan, K., Zwiers, F., and Sillmann, J. (2016). The Influence of Atmospheric Blocking on Extreme Winter Minimum Temperatures in North America. *Journal of Climate 29*(12): 4361-81. https://doi.org/10.1175/JCLI-D-15-0493.1

Wickham, H. (2019). ggplot2: Elegant Graphics for Data Analysis. New York: Springer-Verlag. Retrieved (http://ggplot2.org).

Wickham, H., Francios, R., Henry, L. and Müller, K. (2019). Dplyr: A Grammar of Data Manipulation. Retrieved (https://cran.r-project.org/package=dplyr).

Wiedenmann, J. M., Lupo, A. R., Mokhov, I. I. and Tikhonova, E.A. (2002). The Climatology of Blocking Anticyclones for the Northern and Southern Hemispheres: Block Intensity as a Diagnostic. *Journal of Climate, 15*(23):3459-3473.https://doi.org/10.1175/1520-0442(2002)015<3459:TCOBAF>2.0.CO;2

Yao, Y., Luo, D., Dai, A., and Feldstein, S. B. (2016). The Positive North Atlantic Oscillation with Downstream Blocking and Middle East Snowstorms: Impacts of the North Atlantic Jet. *Journal of Climate, 29*: 1853–1876, https://doi.org/10.1175/JCLI-D-15-0350.1

Yesilırmak E., and Atatanır, L. (2016) Spatiotemporal variability of precipitation concentration in western Turkey. *Natural Hazards, 81*(1): 687-704. https://doi.org/10.1007/s11069-015-2102-2

CURRICULUM VITAE

Name Surname **:** Bahtiyar EFE

Place and Date of Birth **:** Niğde, 03.01.1984

E-Mail **:** bahtiyarefem@gmail.com

EDUCATION **:**

- **B.Sc.** **:** 2009, İTÜ, Faculty of Aeronautics and Astronautics, Meteorological Engineering Department
- **M.Sc.** **:** 2009, İTÜ, Faculty of Aeronautics and Astronautics, Meteorological Engineering Department

PROFESSIONAL EXPERIENCE AND REWARDS:

- 2018 - 2019 Visiting Research Scholar at the University of Missouri - Columbia, Atmospheric Science Department, Columbia, MO, USA (by TUBITAK – 2214 Fellowship)
- 2017 – 2018: Visiting Research Scholar at the University of Missouri - Columbia, Atmospheric Science Department, Columbia, MO, USA
- 2010 – 2019: Research Assistant, İstanbul Technical University

PUBLICATIONS, PRESENTATIONS AND PATENTS ON THE THESIS:

- **Efe, B.,** Lupo, A. R., and Deniz. A, 2019: The Relationship Between Atmospheric Blocking and Precipitation Changes in Turkey between 1977 – 2016. Theoretical and Applied Climatology. DOI: 10.1007/s00704-019-02902-z
- **Efe, B.,** Lupo, A., Sezen, I. and Deniz, A. 2018: Analysis Of Trends In Atmospheric Blocking Events by Innovative Trend Method. Scientific Congress

of the Turkish National Union of Geodesy and Geophysics, May 30 – June 2, 2018, İzmir, Turkey.

- **Efe, B.,** Sezen, İ., Lupo, A.R. and Deniz, A.2018: The Effects Of Atmospheric Blocking On Temperature Observations In Turkey. The Annual Meeting of the Missouri Academy of Science, April 27 & 28, 2018, Rolla, Missouri, USA.
- **Efe, B.,** Lupo, A., Sezen, I. and Deniz, A. 2017: Investigation of Change in Atmospheric Blocking Events. 4th Turkey Climate Change Congress, July 5 – 7, 2017, Istanbul, Turkey.

OTHER PUBLICATIONS, PRESENTATIONS AND PATENTS:

- Lupo, A. R., Jensen, A. D., Mokhov, I. I., Timazhev, A. V., Eichler, T. and **Efe, B**. (2018) Changes in Global Blocking Character During the Most Recent Decades. Atmosphere 2019, 10, 92.
- Sirdas, S., Özdemir, E. T., Sezen, I., **Efe, B.** and Kumar V., 2017: Devastating extreme Mediterranean cyclone's impacts in Turkey. Natural Hazards, Volume 87, Issue 1, Pages 255- 286.
- Çapraz, Ö., **Efe, B.** and Deniz A., 2016: Study on the association between air pollution and mortality in İstanbul, 2007– 2012. Atmospheric Pollution Research, Volume 7, Issue 1, Pages 147–154.
- **Efe, B.**, Lupo, A.R. and Deniz, A.: The Relationship between Atmospheric Blocking and Precipitation Changes in Turkey between 1977 and 2016. 32nd Conference on Climate Variability and Change, AMS 2019, January 6 – 10, 2019, Phoenix, AR, USA.
- **Efe, B.**, Aslan, E. and Deniz, A. 2018: Analysis Of Pm2.5 Concentration In Istanbul. Scientific Congress of the Turkish National Union of Geodesy and Geophysics, May 30 - June 2, 2018, İzmir, Turkey
- **Efe, B.,** Durna, B., Doğanşahin, K., Deniz, A. and Şahin., A. D. 2016: Installation of Photovoltaic on the Roof of the High School in Sarıyer, Istanbul. National Clean Energy Symposium (UTES 2016), October 24-26, 2016, Istanbul, Turkey.
- **Efe, B.,** Toros, H. and Deniz, A. 2015: Trends in Temperature and Precipitation Data across Turkey, 7th Atmospheric Science Symposium (ATMOS), April 28-30, 2015, İstanbul, Turkey.
- Özgür, E., **Efe, B.,** Koçak, K., Deniz, A. 2014: Trends of Maximum and Minimum Temperatures Around Istanbul. Climate Change and Climate Dynamics Conference, November 8 – 10, 2014, Istanbul, Turkey.
- Özgür, E., **Efe, B.** and Akbayir, İ. 2014: Analysis of Monthly Total and Annual Total Precipitation Data of Southeast Anatolia Project (GAP) Cities, II. International Drought and Desertification Symposium, September 16 – 18, 2014, Konya, Turkey.
- Özgür, E. and **Efe, B**. 2014: Drought Analysis of Konya and Surroundings by Standard Precipitation Index (SPI) and Percent of Normal Index (PNI), II. International Drought and Desertification Symposium, September 16 – 18, 2014, Konya, Turkey.

- Şen, N. Moral, A.C., **Efe, B.,** Lauber, A., Mertol, O. and Aslan, Z**.** 2014: Comparison of three model results for nowcasting in a convective boundary layer, Organization of Scientifique and Technique Vol a Vole (OSTIV) Congress, 30 July – 6 August, 2014, Leszno, Poland.
- **Efe, B.,** Unal, A., Deniz, A., Özdemir, T., Sezen, İ. and İncecik, S. 2014: PM10 Levels In The Kağıthane Valley, Istanbul, Turkey and Meteorological Influences, 9th International Air Quality Conference, March 24 -28, 2014, Garmisch-Partenkirchen, Germany.
- Ağaç, K., Deniz, A., **Efe, B.,** İncecik, S., Özdemir, T. and Sezen, İ**.** 2014: The Assessment of NOx Concentration Values of Kağıthane, İstanbul, 9th International Air Quality Conference, March 24 -28, 2014, Garmisch-Partenkirchen, Germany.
- Özdemir, E. T., Sezen, I., **Efe, B.,** Deniz, A. 2013: Synoptic Analysis of BLSA (Blowing Sand) and Episodic PM10 Concentrations in Istanbul,1st Remote Sensing in Meteorology Workshop, November 5-7, 2013, Antalya, Turkey.
- Öztaner, Y. B., Özdemir, E.T., Sezen, İ. and **Efe, B.** 2013 : An Examination of Atmospheric Transports of Sand and Dust PM10 Profiles at Airports Over Turkey on 18 April 2012 when Southern Storm Has Occurred, Organization of Scientific and Technique Vol a Vole (OSTIV) Met Panel, OSTIV2013, September 20-21, 2013, Alanya, Turkey.
- Özdemir, E.T., Yerli, B., **Efe, B.,** Kaymak, M.K., Sezen, İ. and Şahin, A.D. 2013**:** Feasibility Analysis for the Wind Power Plant near Çatalca Meteorological Radar by using RETScreen and Homer, 6th Atmospheric Science Symposium, April 24 – 26, İstanbul, Turkey.
- Yerli, B., Özdemir, E.T., Kaymak, M.K., Sezen, İ., **Efe, B.,** Eftimiyadis, K. and Şahin, D. 2013: Unlicenced Electricity Generation from Photovoltaics in Turkey and Feasibility Analysis for Istanbul Technical University(ITU), 6th Atmospheric Science Symposium (ATMOS), April 24 – 26, İstanbul, Turkey.
- Ünal, E., Tan, E., Menteş, Ş.S., Ünal, Y., **Efe, B.,** İncecik, S. Önol, B., Barutçu, B., Öner, E., Anbarcı, K. Topçu, S., Göktepe, N., Sayinta, M. and Yilmaz, E. 2013: Assessing the Performance of AES RuzgarSIM and Windsim Models in Short-Term Wind Power Forecasting in Manisa, Turkey, 6th Atmospheric Science Symposium (ATMOS), April 24-26, 2013, İstanbul, Turkey.
- **Efe, B**., Menteş, Ş.S., Ünal, E., Ünal, Y.S., Tan, E., Özdemir, E.T., Barutçu, B., Önol, B. and Topçu, S. 2012: 72hr Forecast of Wind Power in Manisa, Turkey by usıng the Wrf Model Coupled to Windsim, ICRERA,The International Conference on Renewable Energy Research and Applications, November 11 – 14, 2012, Nagasaki, Japan.
- Özdemir, E.T., Mentes, Ş.S., Tan, E., Ünal, E., **Efe, B.,** Unal, Y., Oner, E., Anbarcı, K., Önol, B., Borhan, Y. and İncecik, S. 2012: Short-Term Wind Power Prediction Forecast in Manisa, Turkey by Using the WRF Model Coupled to a CFD Model, EWRES & ECRES The European Conference & Workshop on Renewable Energy Systems, September 17 - 28, 2012, Antalya- Turkey.
- Yesilkoy, S., Aktar, Ç., Inceoglu, Ö., Menteş, Ş.S., **Efe, B.,** Basar, U., Tan, E., Unal, Y. and Unal, E. 2012: Performance Analyses of Windsim and WAsP Models

to Estimate Wind Energy Potential in Soma, EWRES & ECRES The European Conference & Workshop on Renewable Energy Systems, September 17 – 28, 2012, Antalya- Turkey.

- **Efe, B.,** Mentes, Ş. S., Akcan, D., Tan, E., Unal, Y., Onol, B., Tanriover, Ş., Rüstemoğlu, S., Anbarcı, K., Oner, E. and Incecik, S. 2011: Preliminary Results of Short-Term Wind Energy Prediction System(SWEPS) for the Northwestern Region of Turkey. EMS Annual Meeting, September 12-16, 2011, Berlin, Germany.
- Akcan, D., **Efe, B.,** Mentes, Ş. S., Unal, Y., Tan, E., Onol, B., Incecik, S., Tanriover, Ş., Barutcu, B., Anbarcı, K. and Oner, E. 2011: Preliminary Results of Short-Term Wind Energy Prediction System (SWEPS) for Soma, Manisa in Turkey, EGU General Assembly Vol. 13, April 3 -8, 2011, Vienna, Austria.
- Deniz, A., Toros, H. and **Efe, B.** 2009: Investigation of tourism climate Index (TCI) in Turkey. International Conference on Tourism Development and Management, September 2009, Kos Island, Greece.